THE UNIVERSITY OF MICHIGAN

INDUSTRY PROGRAM OF THE COLLEGE OF ENGINEERING

HIGH TEMPERATURE PHASE EQUILIBRIA IN THE SYSTEM CARBON-OXYGEN-URANIUM

John R. Piazza

A dissertation submitted in partial fulfillment
of the requirements for the degree of
Doctor of Philosophy in the
University of Michigan
Department of
Chemical and Metallurgical Engineering
1961

September, 1961

IP-533

Doctoral Committee:

Professor Maurice J. Sinnott, Chairman
Professor Guiseppe Parravano
Associate Professor David V. Ragone
Professor Lars Thomassen
Professor Lawrence H. Van Vlack
Professor Edgar F. Westrum, Jr.

ACKNOWLEDGMENTS

Credit must be given to a number of individuals and organizations who provided important assistance to the author in the accomplishment of this thesis. The author is most indebted to the Chairman of the Doctoral Committee, Professor Maurice J. Sinnott. Throughout the course of the work, Dr. Sinnott made himself available for consultation, provided much encouragement, and made valuable suggestions regarding the technical aspects of the thesis. Also, prompt action on his part in assisting in the procurement of funds, services, equipment, and supplies avoided much delay.

Professor Lars Thomassen offered helpful advice regarding temperature measurement and applications of X-ray diffraction. Associate Professor David V. Ragone provided the germ of the scheme for the experimental studies and made valuable suggestions concerning the thermochemical and thermodynamic aspects of the work. The other members of the Doctoral Committee provided assistance and encouragement through their suggestions and their interest in the work. Professor Lee O. Case, in his course in heterogeneous equilibrium, provided much enlightenment regarding applications of the phase rule. Dr. Edward E. Hucke provided technical advice and furnished high purity graphite felt and batting. Mr. Frank Drogosz assisted in equipment and instrument repairs. He and his assistants analyzed the gas samples. Mr. Gunther Kessler built the Pyrex vacuum system, which performed without fault throughout the experimental investigation. Mr. Cleatis Bolen assisted in the construction of the experimental

system. Miss Jane Norby contributed many hours of her time in assisting with the preparation of the manuscript.

The Phoenix Project of the University of Michigan provided supplementary funds for the execution of the work and a fellowship from the Ford Foundation enabled the author to concentrate his efforts on the completion of the work during the last year.

The Industry Program of the College of Engineering of the University of Michigan reproduced the dissertation.

TABLE OF CONTENTS

TABLE OF CONTENTS CONT'D

LIST OF TABLES

LIST OF TABLES CONT'D

LIST OF TABLES CONT'D

LIST OF FIGURES

LIST OF FIGURES CONT'D

ABSTRACT

Equilibrium relationships among uranium monocarbide, uranium dicarbide, graphite, uranium dioxide, and carbon monoxide have been investigated in the temperature range between 1400 and 1700°C and at pressures below one atmosphere. The two univariant equilibria $UO_2 + 4C = UC_2 + 2CO$ and $UO_2 + 3UC_2 = 4UC + 2CO$ were found to exist over the temperature range studied.

Carbon monoxide equilibrium pressure as a function of temperature has been determined for both equilibria. Carbon monoxide pressures were determined by measuring the total system pressure with a mercury manometer and analyzing a sample of the gaseous phase using a mass spectrometer. Temperature was measured using a disappearing filament type optical pyrometer. The pressure-temperature data were used to formulate analytical expressions for the carbon monoxide equilibrium pressures. These expressions were determined as $\log_{10}P_{CO} = -18{,}000/T + 8.23$ and $\log_{10}P_{CO} = -16{,}600/T + 7.26$ for the first and second mentioned equilibria respectively. In the expressions, temperature is in degrees Kelvin and pressure in atmospheres. The expressions were determined by means of the method of least squares, and statistical analyses were made to assess the random error of the measurements.

Experiments were made to assess the activity of the solid phases involved in the equilibria and to determine the order of magnitude of errors due to the presence of nitrogen in the system. These experiments included precision lattice parameter determinations at room temperature of the monocarbide and dioxide phases in the solid residues. As a result of these

studies the activities of the monocarbide and the dicarbide were estimated as 0.95 ± 0.05 throughout the range of temperatures investigated. It was concluded from the study of the effect of nitrogen that the errors in the carbon monoxide equilibrium pressures for the first equilibria are negligible and that those for the second amount to ten per cent or less.

The equilibrium pressure expressions and estimated activity values were used to determine expressions for standard Gibbs free energies of reaction in calories. For the reactions $UO_2 + 4C \rightarrow UC_2 + 2CO$, $UO_2 + 3UC_2 \rightarrow 4UC + 2CO$, $UO_2 + 3C \longrightarrow UC + 2CO$, and $UC + C \longrightarrow UC_2$, the expressions determined are 164,500-74.23T, 152,200-65.42T, 161,400-72.03T, and 3,100-2.20T respectively.

The results of the study of the effects of nitrogen indicate that, at temperatures in the range studied, uranium mononitride will coform with uranium monocarbide if nitrogen is present in the gas phase. These results also indicate that lowering of the monocarbide activity stabilizes mixtures of the monocarbide and graphite with respect to the dicarbide. The extent to which the monocarbide activity need be lowered to equilibrate graphite, the monocarbide and the dicarbide is indicated by the free energy of reaction for $UC + C \rightarrow UC_2$ given by 3,100-2.20T calories. The results of the studies involving nitrogen are consistent with this expression.

INTRODUCTION

The investigation of high temperature phase equilibria in the carbon-oxygen-uranium system was prompted by several matters of current interest. The carbides and oxides of uranium are being carefully evaluated for use as nuclear fuels. Uranium monocarbide, in particular, has merit in that it is isotropic, relatively tough at elevated temperatures, and contains about 95 weight per cent uranium. From the standpoint of overall energy requirements, the commercial formation of the uranium carbides directly from uranium oxide and carbon would be less costly than formation from uranium and carbon. There is some confusion in the literature with regard to conditions required for formation of the various carbides. The complete determination of phase equilibria involving uranium carbides and oxides would establish the range of possible operating conditions for the formation of each of the various carbides. Furthermore, these determinations would enable the computation of thermodynamic functions for the various chemical reactions involved. These considerations provided the impetus for this study.

An experimental program has been carried out to determine the nature of univariant equilibria that can be achieved involving carbides and oxides in the carbon-oxygen-uranium system at temperatures between 1400°C and 1700°C and pressures below one atmosphere. Two four phase equilibria were found, both involving solid phases and carbon monoxide, and the carbon monoxide equilibrium pressure has been measured as a function of temperature for each of these univariant equilibria.

The composition of the solid phases involved in these univariant equilibria has also been assessed. Finally, the data of gas pressure and solid phase compositions as functions of temperature were used to determine analytical expressions for the standard Gibbs free energies of reaction, applicable in the temperature range studied.

The detailed procedures and results of the experimental program will be enumerated later. In way of introduction to the account of the experimental program, several topics of fundamental importance will first be considered. These include the theoretical bases for the work, relevant aspects of the system carbon-oxygen-uranium, and the technical problems involved in conducting the high temperature phase equilibrium studies.

Phase Equilibria, the Phase Rule, and the Phase Diagram

The determination of equilibrium phase relations in multicomponent systems is a complex problem. The phase rule is a theorem that provides immense simplification and unification in analysis of phase equilibria. This rule was first enunciated by the great American scientist, J. Willard Gibbs in 1876.[1] According to the phase rule, the number of degrees of freedom, F, of a system influenced by X external variables and comprised of C components distributed among P phases in mutual equilibrium with one another is given by:

$$F = C - P + X . \qquad (1)$$

Derivations of the phase rule are presented in numerous works, including those of Case[2] and Darken and Gurry,[3] as well as in Gibbs'

paper.(1) As a basis for considering the ramifications of the rule as they apply to the problem at hand, it will be worthwhile to outline its derivation.

The phase rule is essentially an algebraic theorem. The number of degrees of freedom or the variance of a set of simultaneous equations or relations in a number of variables is the difference between the number of variables and the number of independent equations in those variables. Gibbs showed that the variance of a system in a state of chemical equilibrium is the number of components comprising the system plus the number of external variables influencing the system minus the number of phases present. The phase rule is applicable only to a system in a state of chemical equilibrium because the independent equations in the system variables express the necessary and sufficient conditions for chemical equilibrium, which are that the chemical potential of each component be the same in each phase present. The variables of the system are the external variables and the composition variables of each phase. Hence there are $P(N-1) + X$ independent phase rule variables. The condition that the chemical potential of each component be the same in each phase present involves $(P-1)$ independent equations for each component so that the total number of independent equations in the phase rule variables is $N(P-1)$. Expressing the number of degrees of freedom as the excess of independent variables over independent equations yields Equation (1) directly.

In applying the phase rule, the number of components and the number of external variables must first be assessed. The determination

of the number of components requires careful analysis of the system involved. The number of components, N, is stated by Darken and Gurry to be the smallest number of independently variable constituents by means of which the composition of each phase involved in the equilibrium may be expressed.(3) Case shows(2) that the number of components is the difference between the total number of constituents present in the system and the number of independent chemical equations expressing equilibrium among three or more constituents. It is apparent that alternate descriptions are valid for a given system. However, extreme care must be used in evaluating N in all but the most trivial cases; and a general approach to this problem is presented by Case.(2)

In the problem at hand it is convenient to describe the system as comprised of the elements carbon, oxygen, and uranium. Since no equations can be written expressing chemical equilibrium among elements, the number of components is equal to the number of constituents -- three in this case.

It should be noted, however, that the number of components is not necessarily equal to the number of elements comprising the system. For example, in a system comprised of stoichiometric calcium carbonate, lime, and carbon dioxide in equilibrium, the number of components is two even though the system is comprised of three elements. By subtracting the number (one) of independent equations expressing chemical equilibrium among the three constituents, the number of components is counted as two.

The analysis of phase equilibria in the system carbon-oxygen-uranium can now be undertaken. This analysis will consist of considering possible groups of phases that can exist in mutual equilibrium in

accordance with the phase rule, and the variance and number of independent variables for each combination of phases. Particular attention will be given to the application of the phase rule in fixing requirements for internal consistency among related features of the phase diagram.

Temperature and pressure will be considered as the only external variables of importance in this study so that Equation (1) becomes

$$F = C - P + 2 . \qquad (2)$$

Using Equation (2), Table I has been prepared to show the dependence of the degrees of freedom and number of phase rule variables involved in the general case for a three component system. In this case there are two composition variables per phase in addition to temperature and pressure.

TABLE I

DEGREES OF FREEDOM (F) AND NUMBER OF PHASE RULE VARIABLES (V) AS A FUNCTION OF THE NUMBER OF PHASES PRESENT (P) AT EQUILIBRIUM FOR THE GENERAL CASE OF A THREE COMPONENT SYSTEM INFLUENCED ONLY BY TEMPERATURE AND PRESSURE

P	F	V
1	4	2 + 2
2	3	4 + 2
3	2	6 + 2
4	1	8 + 2
5	0	10 + 2

It should be noted that for special or degenerate cases, the number of phase rule variables will be less than that shown for the general case. For example, if one of the phases involved in an equilibrium is essentially

a pure component, the number of phase rule variables is diminished by two. Of course, the variance is unaffected by degeneracies because each loss of a phase rule variable is accompanied by a loss of one independent equation.

The relation between the phase rule, the variance, and the phase diagram is effectively treated by Case,[2] and the following analysis of the three component system is based on his treatment. The phase diagram is a device for effectively showing the equilibrium state of a system as a function of its overall composition and the external variables influencing it. For the case of a three component system acted upon only by temperature and pressure, the phase diagram has four dimensions: namely, temperature, pressure, and the concentrations of two of the three components expressed in any convenient units. If such a system can be comprised of a particular set of five phases in equilibrium, the system is invariant. This means that there is a unique set of values for all the phase rule variables, and that this equilibrium is represented on the phase diagram by five points in $p\text{-}t\text{-}x_1\text{-}x_2$ space, each point denoting the composition of one of the five phases making up the system. Furthermore, if such an invariant equilibrium exists, then five univariant equilibria must be found representing the five possible combinations of the five phases taken four at a time. Consequently, these univariant equilibria are represented by five sets of four curves in $p\text{-}t\text{-}x_1\text{-}x_2$ spaces.

Since four dimensional space is inconvenient to use, let the analysis now be limited to the three dimensional $p\text{-}x_1\text{-}x_2$ space with t as a parameter. Consider any four phase equilibria existing over a range

of temperatures and pressures. Since this equilibria is univariant, it is theoretically possible to express all but one of the phase rule variables as a function of the remaining one. Hence at a specified temperature within the range of stability of the equilibria, the system will be at a unique pressure and each phase will have a particular composition. At the specified temperature, the four phase equilibrium will appear on the phase diagram as four points, each having as co-ordinates the composition of one of the phases and the equilibrium pressure. Emanating from these points will be four groups of three space curves representing three phase equilibria among each possible combination of the four phases of the univariant equilibrium. These curves pierce planes of constant pressure in sets of three points constituting the so-called tie triangles, and this is a direct consequence of the divariance of three phase equilibria. Furthermore, each curve in $p\text{-}x_1\text{-}x_2$ space represents the intersection of two surfaces, which are loci of compositions of the phase in question in equilibrium with one of the other two phases. These surfaces pierce constant pressure planes in curves, and the line in such planes connecting the compositions of two phases in equilibrium are the so-called tie lines.

It is apparent at this point that a great deal of internal consistency must exist between the related phase equilibria of a system. More can be said in this regard. The curves in $p\text{-}x_1\text{-}x_2$ space representing three phase equilibria must terminate in one of two ways. First, they may terminate at points representing four phase equilibrium among the three phases in question and a fourth phase. Second, they may terminate at a binary face of the diagram. In the latter case the loss of a component is accompanied by loss of a degree of freedom. Thus information about

phase relations in a binary system can be utilized in analyzing phase relations in a related ternary system.

Although application of the phase rule will not quantitatively locate the points, curves, and surfaces of the phase diagram, it can be of great value in deducing relative locations of these features. This can be done by collecting all the known data on the system in question and utilizing the phase rule ramifications that have been outlined above to deduce possible configurations; then a few critical equilibrations can be made to test hypotheses made. After the general configuration is established, the features of the diagram can be determined in a systematic manner to the extent desired.

The application of the phase rule to carbide-oxide equilibria in the carbon-oxygen-uranium system will be taken up after summarizing relevant aspects of that system.

Aspects of the Carbon-Oxygen-Uranium System

It is of fundamental importance to ascertain what phases may be present in the temperature and pressure range of interest in this study and the nature of these phases. By the nature of a phase is meant its state and its range of compositions within the region of interest.

A fairly complete picture of the condensed phases involved can be obtained by examining the binary systems carbon-uranium and oxygen-uranium. Phases in these binary systems expected to be involved in carbide-oxide equilibria are listed in Table II with their melting points and states. Crystal systems are indicated for each phase expected to be in the crystalline state. The table was compiled from data presented by Rough and Bauer[4] and by Hansen.[5]

TABLE II

CONDENSED PHASES INVOLVED IN CARBIDE-OXIDE EQUILIBRIA BETWEEN 1200° AND 1800°C

Phase	Melting Point, °C	State
C (gr)	about 5000 (sublimes)	Hexagonal
UC_2	about 2500	Tetragonal (CaC_2 type)
U_2C_3	1775 (decomposes)	Cubic
UC	2590 ± 50	Cubic (NaCl type)
U	1128.9	Liquid
UO_2	about 2875	Cubic (CaF_2 type)

Much work has been done in investigating the carbon-uranium system. This has been summarized by Rough and Bauer,[4] who present a phase diagram of the binary system based on their assessment of the available evidence. This diagram has several features relevant to this study. First, the solubility of uranium in carbon is negligible. Second, the solubility of carbon in the monocarbide phase and uranium in the dicarbide phase is small but significant above 1600°C so that at 1800°C the saturated composition of these phases reaches 52 and 65 atom percent carbon respectively. Third, the carbon content of the uranium rich liquid phase in equilibrium with uranium monocarbide, while very low near the melting point of uranium, increases to about 15 atom per cent carbon at 1800°C. Fourth, the range of compositions of the sesquicarbide phase is negligible at all temperatures at which it is stable.

A number of oxides of uranium have been discovered, and these are enumerated in a summary of the oxygen-uranium system made by Rough and Bauer.[4] However, most of the uranium oxides decompose at relatively low temperatures. Moreover, since uranium dioxide is the lowest oxide of

uranium, it, rather than a higher oxide, would be expected to be found in equilibrium with carbon and a carbide of uranium. The dioxide phase has been shown by Hering and Perio[6] to exist over a range of oxygen concentrations from 30 to slightly over 33-1/3 atomic per cent uranium.

Uranium monoxide (UO) has been reported by several investigators including Rundle[7] and Vaughn.[8] In no case has this compound been isolated, but it has been reported as being in solid solution with uranium monocarbide. The monoxide has a sodium chloride type cubic structure, isomorphous with the monocarbide, and unlimited solubility is believed to exist between these compounds. Hence, it is possible that equilibrium monocarbide phases may contain an appreciable amount of monoxide in solid solution.

With regard to the gas phase composition it is pertinent to note that the vapor pressures of both liquid uranium and graphite are less than 10^{-5} atmospheres at 1800°C.[9] Furthermore, for the equilibria

$$2CO = CO_2 + C \qquad (3)$$

and

$$CO = C + 1/2\ O_2 \qquad (4)$$

at temperatures above 1200°C and CO partial pressures below one atmosphere, the calculated volume fractions of CO_2 and O_2 are very small. Consequently, the gas phase present in equilibrium with carbon would be essentially carbon monoxide throughout the temperature range of interest in this study.

Except for possible ternary compounds of carbon, oxygen, and uranium, the phases expected to be encountered in this study are as listed

in Table III. Phase rule variables are also listed for each phase. The variables a, b, c, and d remain very near zero in magnitude.

TABLE III

EXPECTED PHASES (EXCLUDING TERNARY COMPOUNDS) IN HIGH TEMPERATURE PHASE EQUILIBRIA INVOLVING CARBIDES AND OXIDES OF URANIUM

Phase	State	Composition Variables
CO	gas	0
C	crystalline	0
$UC_{1+a}O_b$	crystalline	2 (a,b)
UC_{2+c}	crystalline	1 (c)
U_2C_3	crystalline	0
UO_{2+d}	crystalline	1 (d)
U rich solution	liquid	2 (%C, %O)

The phase rule analysis of a system of phases in equilibrium will now be illustrated by means of an example. Suppose that the following five phases are in equilibrium: CO, $UC_{1+a}O_b$, C, U rich solution, and UO_{2+d}. Let the constituents be taken as CO, $UC_{1+a}O_b$, C, O [in U (l)], U, and UO_{2+d}. Three independent equations can be written in these six selected constituents as follows:

$$C + O = CO \tag{5}$$

$$U + (2+d)\ O = UO_{2+d} \tag{6}$$

$$U + (1+a)\ C + bO = UC_{1+a}O_b \tag{7}$$

Hence the system consists of three components, which may be taken as any three of the six entities selected as constituting the system. Alternatively, the system could be described by the four constituents, CO, U, C, and O. Then only one equation could be written in

these constituents (Equation 5) so that the system would consist of three components. Thus the system described is invariant; that is, if an equilibrium existed among these five phases it could exist only for one combination of values of pressure, temperature, a, b, c, and d.

Rather than attempt to consider whether or not the existence of the described equilibria would be consistent with the known features of the three binary systems, it is desirable at this time to mention two additional relevant facts regarding the system carbon-oxygen-uranium. First, all the uranium carbides have been synthesized in open systems from mixtures of uranium dioxide and graphite at temperatures within and above the range of interest.[10] The overall chemical reaction involved in these syntheses are essentially as follows:

$$UO_2 + 4C \longrightarrow UC_2 + 2CO \quad , \tag{8}$$

$$UO_2 + 3C \longrightarrow UC + 2CO \quad , \tag{9}$$

and

$$2UO_2 + 7C \longrightarrow U_2C_3 + 4CO \quad . \tag{10}$$

Moreover, Heusler has discovered the existence of equilibria among the reactants of Equation (8) and has measured the CO equilibrium pressure as a function of temperature over a temperature range of 1480° to 1801°C.[11] The corresponding range of values of CO pressures measured by Heusler is 18 to 738 millimeters of mercury.

Ramifications of the phase rule can now be used to reconcile Heusler's results with the reactions represented in Equations (8), (9), and (10). To be consistent with Heusler's results, isothermic and isobaric planes of the carbon-oxygen-uranium phase diagram must have the

features shown in Figure 1. (Phases expected to have variable compositions are shown as such in this and following figures.) These diagrams are consistent with the experimental results of Heusler and the principle of Le Chatelier, showing that if the carbon monoxide pressure is maintained below the equilibrium pressure p_1 at t_o, carbon tends to react with uranium dioxide forming uranium dicarbide and carbon monoxide.

However, these diagrams do not indicate that a mixture containing seven gram atoms of carbon per two gram moles of uranium dioxide would react to form uranium sesquicarbide as indicated by Equation (10). Furthermore, the diagrams do not indicate that a mixture containing three gram atoms of carbon per gram mole of uranium dioxide would react to form uranium monocarbide as indicated by Equation (9). Indeed, if both of these cited mixtures were reacted at t_o and the carbon monoxide pressure maintained at p_2, all the graphite would eventually react with UO_2 resulting in a mixture of uranium dicarbide and unreacted uranium dioxide in equilibrium with carbon monoxide at p_2. The simplest explanation consistent both with the phase rule and Equations (9) and (10) is that four phase equilibria exist as follows:

$$UO_2 + 7UC_2 = 4U_2C_3 + 2CO \qquad (11)$$

and

$$UO_2 + 3U_2C_3 = 7UC + 2CO \qquad (12)$$

At temperature t_o, the CO equilibrium pressures p_3 and p_5 for Equations (11) and (12) respectively would be such that $p_2 > p_3 > p_5$. The corresponding characteristics of the phase diagram at t_o over the range of CO pressures from p_2 to below p_5 are sketched in Figure 2.

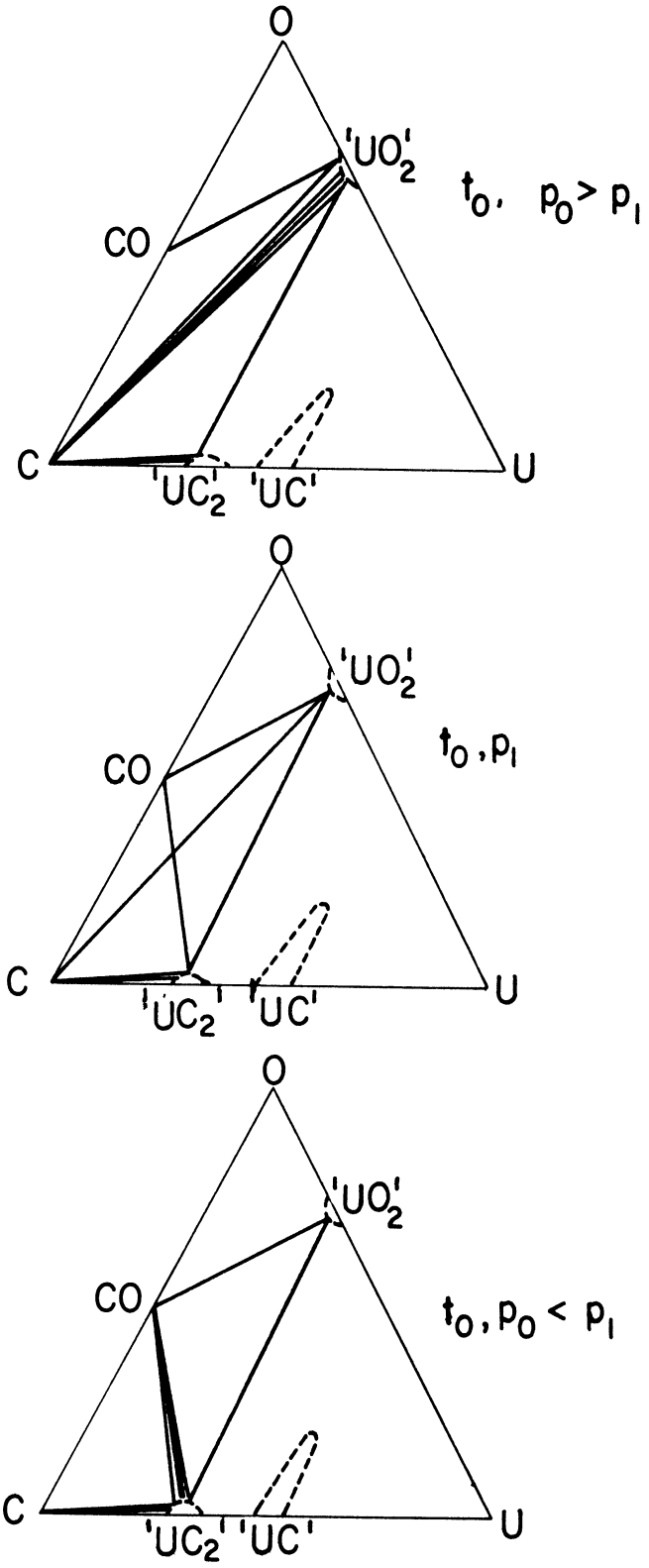

Figure 1. Constant Temperature - Constant Pressure Sections of the C-O-U Phase Diagram at, above, and below the CO Equilibrium Pressure for the Equilibrium, $UO_2 + 4C = {}'UC_2' + 2CO$, at Temperature t_o.

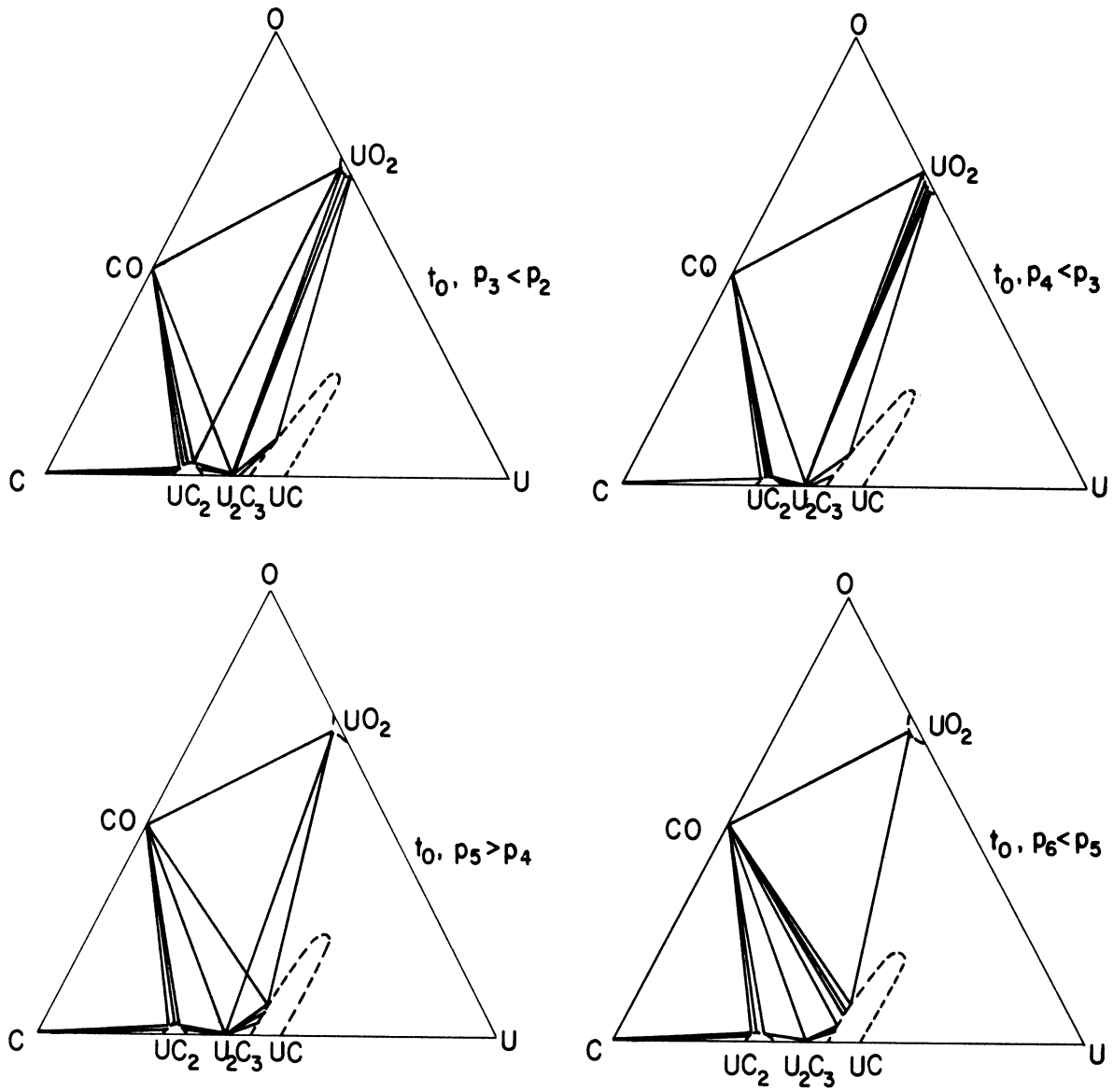

Figure 2. Predicted Constant Temperature - Constant Pressure Sections of the C-O-U Phase Diagram at, above, and below the CO Equilibrium Pressures for the Equilibria $UO_2 + 7UC_2 = 4U_2C_3 + 2CO$ and $UO_2 + 3U_2C_3 = 7UC + 2CO$ at Temperature t_o.

The consistency with the phase rule of the portion of the phase diagram characterized by the isothermic and isobaric sections of Figures 1 and 2 is readily demonstrated. For the equilibria represented by Equations (11), (12), and by

$$UO_2 + 4C = UC_2 + 2CO \,, \qquad (13)$$

lowering the CO pressure would favor the formation of the compounds on the right of the equality sign from those on the left. Consequently, the two loci of tie triangles representing the three phase equilibria between the phases on the left of an equal sign and one of the phases on the right would extend in the direction of higher pressure. Similarly, the other two loci of tie triangles associated with the four phase equilibria in question would extend in the direction of lower pressure. Consider now the three space curves representing the compositions of the uranium sesquicarbide and uranium dioxide phases, and carbon monoxide in mutual equilibrium. These curves must move in the direction of higher pressure from p_5 and in the direction of lower pressure from p_3. Consequently p_5 must be less than p_3 and these three phase equilibria can occur only at pressures between p_3 and p_5 as shown. By applying the same reasoning with regard to the three phase equilibria between the uranium dicarbide and uranium dioxide phases and carbon monoxide, it similarly follows that p_3 must be less than p_1 and that these three phase equilibria can occur only at pressures between p_1 and p_3.

It also can be pointed out that if the equilibria of Equations (11), (12), and (13) exist as postulated, then an equilibrium such as

$$UO_2 + 3C = UC + 2CO \qquad (14)$$

would not be a stable equilibrium unless it occurred at the same temperature, t_o, and pressure, p_5, of Equation (12). This is because the space curves representing the three phase equilibria between UC, UC_2, and CO would be required to extend upward from the equilibrium pressure of Equation (14) at t_o as well as from p_5.

In this section the phase rule has been applied to demonstrate that certain hypotheses regarding the nature of a portion of the carbon-oxygen-uranium phase diagram are consistent with related observations and the phase rule. Although the phase rule cannot be used to quantitatively determine analytic expressions in the phase rule variables, it certainly can be used to advantage in a priori analysis of complex systems. Once plausible hypotheses have been formulated, they can then be tested by means of experiments. After hypotheses are shown to be valid, the phase diagram then can be systematically determined in any degree of detail considered desirable or necessary.

Experimental Considerations in the High Temperature Equilibrium Studies

The overall goal of this study is to identify existing univariant phase equilibria involving carbides and the dioxide of uranium, and to determine equilibrium pressure and phase compositions as a function of temperature for these equilibria. The study was to be made at temperatures from about 1200° to 1800°C and pressures between one millimeter and one atmosphere. From the measured data of the phase rule variables as a function of temperature, the free energy, enthalpy and entropy of reaction then can be determined for the reactions involved. General considerations for the design of experiments to accomplish the desired investigation will be considered in this section.

The general subject of experimental phase equilibrium and thermochemical investigations is treated systematically and thoroughly by Kubaschewski and Evans[12] and by Bockris, White, and MacKenzie.[13] The subject of heterogeneous equilibria as it applies to carbide-oxide equilibria will be considered in this section. The important requirements of an experimental system to determine high temperature carbide-oxide equilibria will first be considered. Then a critical account of previous investigations of this type is presented.

A closed system for experimental determination of high temperature phase equilibria between carbides, oxides, carbon, and a gas phase at high temperatures and low pressures should meet a number of requirements. Contamination of the reactants must be avoided or taken into account. Side reactions must be avoided. The equipment must be gas tight and mechanically stable. The reactants must be heated to and held at a uniform and constant temperature. The system must be brought to equilibrium. The temperature and pressure of the system at equilibrium must be accurately measured. To the extent that these requirements are imperfectly fulfilled, systematic errors will be incurred. All of these requirements will now be considered in detail.

The use of pure reactants is a necessary but not a sufficient condition for avoiding contamination. Neither the container nor the gas phase should be a source of contamination, and the gas phase ideally should be uncontaminated itself. Gas phase contaminants can be of two types. One type is gas that appreciably interacts with the condensed phases; the other type is gas that is inert in this respect. Argon and hydrogen would fall in the class of inert gases in this case. Nitrogen, on the other hand, was

suspected to be a gas that would interact with the solid phases. In their studies of the carbon-nitrogen-uranium system, Austin and Gerds found that the solubility of nitrogen in uranium dicarbide and uranium sesquicarbide was negligible.(14) However, these authors showed that the isomorphs, uranium mononitride (UN) and uranium monocarbide, are soluble in all proportions. Consequently, the presence of nitrogen in the gas phase might result in appreciable errors in measured carbon monoxide pressures in equilibrium with the monocarbide and other phases. This error would result from the monocarbide activity being lowered due to the presence of the mononitride in solid solution with it.

It was found necessary in these studies to sample and analyze the gas phase and make corrections for the presence of gases other than CO. The principal impurity was hydrogen. Consequently, it was also necessary to make an additional correction for thermal diffusion of hydrogen since the gas samples were taken from a cool portion of the closed system used. The thermal diffusion corrections and gas sampling and analyses procedures are described in Appendixes C and B respectively. Small amounts, usually less than two per cent, of nitrogen were also found in the gas phase, and experiments were made to assess the effect of this nitrogen on the composition of the monocarbide phase. These experiments are described in the sections on procedure and results.

The requirements that side reactions be avoided and that the system be gas tight and mechanically stable are interrelated. An inert reaction vessel that leaks or frequently fails during the equilibration is, of course, inadequate. From the standpoint of resistance to thermal shock, graphite and vitreous silica are excellent vessel materials. However,

graphite-silica interfaces in a vessel should not be allowed to become hot enough to react to form silicon carbide and carbon monoxide. Also, vitreous silica tends to devitrify fairly rapidly above 1000°C.[15]

Ideally, it would be desirable to maintain the entire closed system at the constant temperature of equilibration. However, for the temperatures in question, this was considered technically unfeasible. Consequently, the equipment was designed with the reaction vessel communicating with the remainder of the reduced pressure space, which operated at ambient temperature. This facilitated the problem of vacuum seals, which could then be made by means of greased O rings and tapered glass joints. Because of the nature of the gas phase, there was no problem of deposition on cold surfaces. Furthermore, by using single small tablets of the condensed phases and a large hot zone in the vessel, and by not circulating the gas phase, thermal gradients in the sample would be minimized.

Temperatures up to 1800°C can be attained electrically by utilizing either impressed or induced current in a heating element. Graphite seems to be an ideal material for such an element. The use of induction heating would offer the advantage of simplicity of technology as compared to electrical resistance heating; this would eliminate the need for terminal blocks and sealed and insulated electrical leads communicating with the exterior of the vacuum system.

The problem of maintaining a constant temperature is not easy in studies of this type because of the high temperatures involved. The difficulty lies in the provision of a suitable sensing device. If a

thermocouple is used, avoiding deterioration of the couple is a big problem. If a total radiation pyrometer is used, the system design is complicated. However, Kubaschewski and Evans contend that with a suitable generator for induction heating, temperature can be maintained within $\pm$ 5°C of a desired value. This was confirmed in this work and is considered adequate control for the study in question.

It is of vital importance to assure that the system is at or very near a state of equilibrium. This can be directly accomplished in a study of this type by approaching the equilibrium in both the directions of increasing and decreasing carbon monoxide pressure at constant temperature.

The last consideration to be made in the design of a system for the experimental program is the means to be used for measuring the phase rule variables. Temperatures can be measured using a thermocouple, radiation pyrometer, or an optical pyrometer. The use of a thermocouple would require rather elaborate precautions to locate the couple near the sample, to avoid deterioration of the couple and to communicate through the system enclosure. The use of a pyrometer avoids these problems. Since a radiation pyrometer requires a larger source of uniform temperature than is considered feasible to provide and since it is difficult to calibrate such a pyrometer accurately,[15] it was decided to measure temperature by means of a disappearing filament type optical pyrometer. The question of accurate temperature measurement with such a pyrometer involves a number of factors, and these will be taken up in the next section.

The measurement of the total gas pressure at equilibrium is not difficult. For pressures above one millimeter this can be accomplished using a simple mercury manometer. However, it is necessary to establish

whether the gas phase is contaminated as was discussed earlier in this section.

Finally, it is important to establish the identity and composition of the condensed phases in equilibrium at the temperature investigated. Depending on the nature of the solid phases and the degree of accuracy desired in the determination of their composition, quenching techniques may or may not be necessary. In the assessment of the phases that had been present at equilibria by examination of the cooled residue it is important to determine for each phase involved, whether freezing, solid state transformation, chemical reaction, or precipitation occurs on cooling. Such an assessment can be made in many cases by means of X-ray diffraction supplemented by examination of microstructure.

The problem of the determination of compositions of intermixed solid phases is difficult and discussion of this will be deferred until later when it can be directed to specific phase mixtures resulting after equilibration.

Results of investigation of carbide-oxide phase equlibria have been reported by a number of investigators. The methods and equipment used in some of these investigations will now be considered.

All of these investigations utilized closed systems in which equilibria were approached in the directions of increasing and decreasing CO pressure while the reactants were held at constant temperature. In some of the studies, the reactants were actually brought to equilibrium. In the others, the rate of change of pressure at constant temperature was measured as a function of pressure. Then the equilibrium pressure at the temperature in question was determined by graphical interpolation.

The latter method was used by Prescott in investigating the equilibria

$$ZrO_2 + 3C = ZrC + 2CO \qquad (15)$$

over the temperature range of 1880 to 2015°K,[16] by Prescott and Hincke for the equilibria

$$2Al_2O_3 + 9C = Al_4C_3 + 6CO \qquad (16)$$

from 1900° to 2300°K,[17] by Prescott and Hincke for

$$ThO_2 + 4C = ThC_2 + 2CO \qquad (17)$$

from 2057° to 2494°K,[18] and by Brantley and Beckman for

$$TiO_2 + 3C = TiC + 2CO \qquad (18)$$

from 1278 to 1428°K.[19]

All of these investigations were conducted using apparatus originally designed by Prescott.[16] In this apparatus, a small pellet of compressed oxide and graphite was heated by an electric current passing through a very small graphite furnace tube. The tube, at its central region, was 2.54 cm. in length and 0.34 cm. in diameter with a wall thickness of 0.04 cm, and its total length was 5.7 cm. It was supported by tungsten rods pressed into its ends. The charge was retained in the center of the central section by graphite plugs resting loosely against the tungsten rods. The rods were welded to flexible copper wire through a nickel intermediary, and the cord was welded to a 0.635 cm. copper rod, which was silver soldered through a copper disc seal in the end of a 1.9 cm. Pyrex tube.

The furnace was connected through a small trap to a manometer, and the entire gas space that was enclosed during measurements was immersed in a thermostatically controlled water bath. Temperature was measured by means of an optical pyrometer sighted on the outside of the furnace. Corrections were made for the emissivity of graphite, and for absorption of radiation by glass and water between the furnace and the instrument. Temperature was controlled by manual adjustment of direct current supplied by an array of storage batteries.

Attainment of equilibrium was judged to take place too slowly to attempt to equilibrate the phases. Instead the change in pressure was measured over a period of 15 to 40 minutes, during which reasonably constant rates were observed.

One drawback considered inherent in this technique of measuring rate of change of pressure is that it is possible to overlook systematic errors, such as side reactions, which result in the consumption or generation of carbon monoxide. Furthermore, desorption of foreign gases from the solid phases or other surfaces in the system would cause apparent equilibrium pressures to be found which would be higher than the true equilibrium pressures. Errors due to such effects would tend to be aggravated if rates of the reaction under investigation were relatively low.

Sources of systematic error due to competing reactions can be found by holding the system for a long time at the assumed equilibrium pressure. If the reactants are changing with time, one or more phases eventually will disappear; and the system pressure will begin changing with time due to the spurious reaction or reactions. Furthermore, subsequent examination of the solid phases will verify the disappearace of

phases. In other words, necessary and sufficient conditions for chemical equilibrium are that the system remain at constant pressure and the amounts of each reactant remain constant with time.

The particular system of Prescott is apparently invulnerable to side reactions. However, desorption of foreign gases may have been a source of error in this system. Various procedures for baking out the furnace and charges were employed in the several investigations made using the Prescott system, but in no case was it established conclusively that spurious sources of gas were insignificant.

There are other shortcomings inherent in this method of indirect determination of the equilibrium pressure. It is assumed in using such methods that the rate of change of pressure is a function only of the difference between the instantaneous pressure and the equilibrium pressure. Actually, this rate depends on the interfacial area between phases, the nature of the distribution of phases in the aggregate and the amount of each phase present, and perhaps on other factors. There is some question that all these factors can be rendered immaterial by duplication of aggregates used for each run, especially when a very small sample is used, as would be necessary in Prescott's system. Moreover, in the investigations of Prescott(16) and Prescott and Hincke(17) the same charge was used for a number of measurements so that sintering and varying relative amounts of phases present may have influenced rates of change of pressure.

Another shortcoming of this technique seems to be manifested by the fact that varying degrees of uncertainty were encountered in establishing the equilibrium pressure by interpolation of the experimental data.

It is considered desirable whenever possible to actually bring the system to equilibrium. It seems reasonable to expect that at the high temperatures involved in most carbide-oxide equilibrium studies, fairly high rates of reaction should be attainable, even near equilibrium. The rate can be maximized by using finely divided and well-mixed reactants and a reasonably large sample size. Boericke found it feasible to approach equilibria in his investigations of carbide-oxide phase equilibria in the system carbon-oxygen-chromium.(20) Heusler also was able to achieve equilibrium in investigating the equilibria between uranium dioxide, graphite, uranium dicarbide, and carbon monoxide cited earlier.(11) These two studies will now be considered in some detail with regard to the specifications for equilibrium studies set forth earlier in this section.

Two criticisms of Heusler's study seem appropriate. First, his system apparently was not air-tight. Second, he failed to establish conclusively the identity of the phases present at equilibrium. Examination of Heusler's data, reproduced in Table IV reveals that the equilibrium gas phase contained over 10% nitrogen in half of his equilibrations. However, it was established in this work (see page 74) that nitrogen is not an inert gas in this case. These results indicate that univariant equibria near 1600°C involve a solid solution of uranium monocarbide and uranium mononitride when the gas phase contains more than 10% nitrogen. Moreover, Heusler, not being aware of the existence of uranium monocarbide, apparently did not establish that uranium dicarbide had been present at equilibrium. Indeed, in another portion of his investigation, in which he qualitatively studied the formation of uranium nitrides from uranium dicarbide, he made erroneous conclusions about the compositions of the nitride compounds

involved. All the nitrides he reported are presently considered nonexistent. The reason for this appears to be that his conclusions were based on the results of the overall elemental analysis of the solid residues resulting and on the assumption that all combined carbide is present in the dicarbide.

Boericke measured CO equilibrium pressure as a function of temperature for the following univariant equilibria.

$$3Cr_2O_3 + 13C = 2Cr_3C_2 + 9CO \quad , \tag{19}$$

$$5Cr_2O_3 + 27Cr_3C_2 = 13Cr_7C_3 + 15CO \quad , \tag{20}$$

$$5Cr_2O_3 + 14Cr_7C_3 = 27Cr_4C + 15CO \quad , \tag{21}$$

$$Cr_2O_3 + 3Cr_4C = 14Cr + 3CO \quad . \tag{22}$$

These equilibria were found to exist in a temperature range from 970 to 1500°C and at pressures between 42 millimeters of mercury and one atmosphere. Boericke's data of pressure vs temperature have been plotted in Figure 3. Examination of Figure 3 reveals that these equilibria are completely analogous to those represented by Equations (11), (12), and (13), which were hypothesized to exist among uranium carbides and oxides.

Boericke utilized a gas tight porcelain reaction tube in communication with manometers, a vacuum pump, and gas sampling apparatus. A 'Globar' furnace was employed, and two platinum against 10% rhodium in platinum thermocouples were used, one for temperature measurement, the other as a sensing element for a temperature controller. The reaction mixture was contained in a porous alundum thimble.

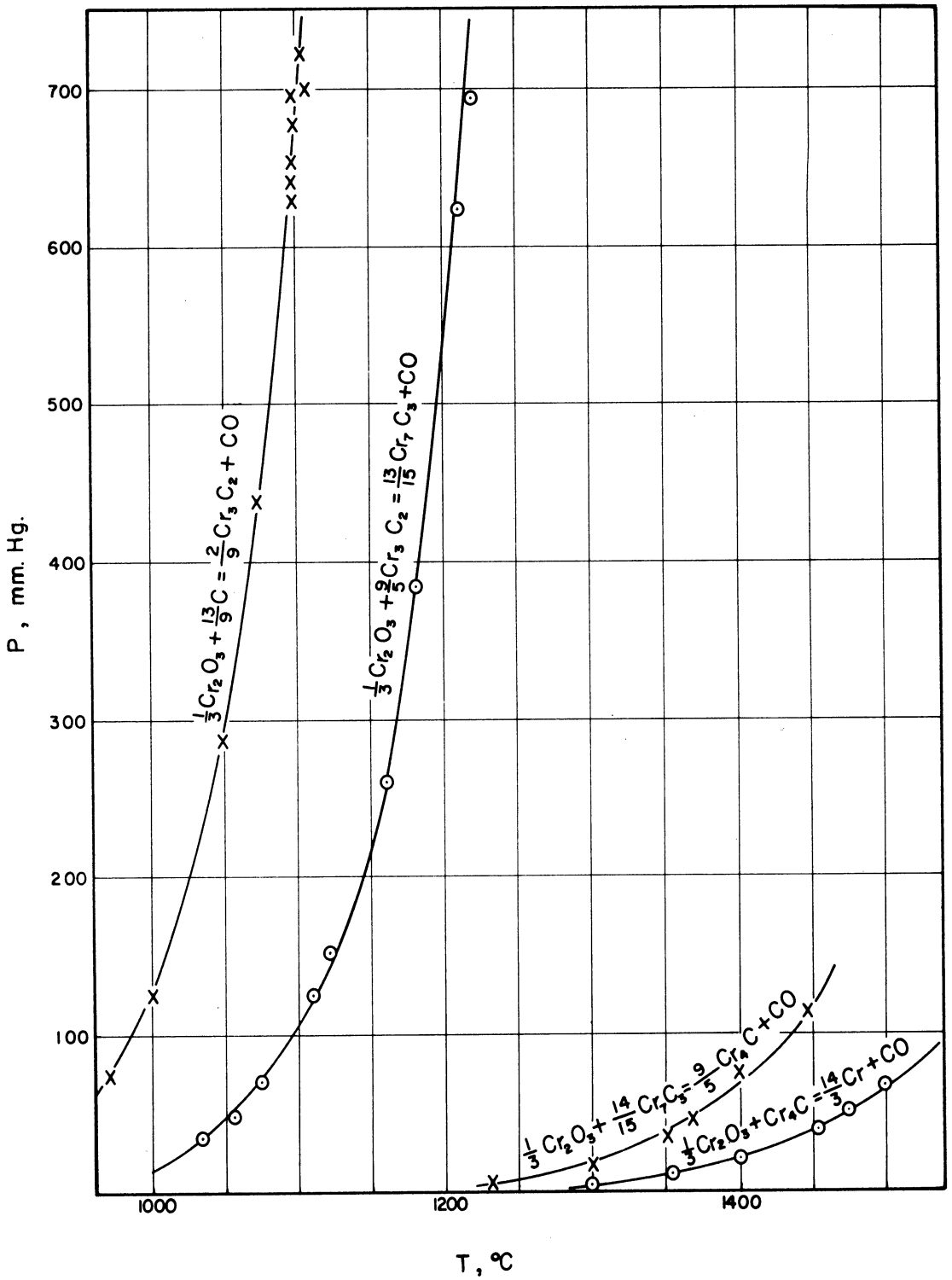

Figure 3. Carbon Monoxide Equilibrium Pressure in Millimeters of Mercury versus Temperature in Degrees Centigrade for Phase Equilibria Involving Chromium Oxide, Chromium Carbides, Carbon, and Carbon Monoxide.(20)

TABLE IV

SUMMARY OF DATA OF EQUILIBRIUM GAS PRESSURE VS. TEMPERATURE REPORTED BY HEUSLER[11] FOR THE EQUILIBRIA $UO_2 + 4C = UC_2 + 2CO$

Run	Direction	Total Pressure, mm Hg	$\%N_2$	Nitrogen Pressure, mm Hg	Carbon Monoxide Pressure, mm Hg	Temp., °C
1	forward	841	12.2	102.5	738.5	1801
2	forward	795	3.77	30	765	1793
3	reverse	787	7.85	62	725	1793
4	forward	623	10.2	63	560	1782
5	forward	623	2.92	18	605	1780
6	forward	571	8.58	49	522	1768
7	reverse	487	6.25	30.5	456.5	1754
8	reverse	345	4.88	17	328	1732
9	forward	327	3.81	12.5	314.5	1732
10	reverse	197	13.2	24	173	1684
11	forward	162	18.4	30	132	1660
12	reverse	123.5	1.6	2.5	121	1650
13	reverse	72	42.7	31	41	1561
14	reverse	57	22.0	12.5	44.5	1558
15	forward	52	23.0	12.0	40	1554
16	reverse	56.5	50.5	28.5	28	1516
17	forward	26.0	33.0	8.0	18	1480

The carbon monoxide content of the gas was determined by means of absorption in acid cuprous chloride. The major impurity was found to be hydrogen, and it was believed to have been contained on carbon in the initial charge. Some nitrogen also was found to be present because of slow leakage of air through the porcelain tube walls during equilibration at the higher temperatures.

Boericke did not measure the hydrogen contents of the gas phase. Consequently, small errors resulted in the measured CO pressure due to thermal diffusion of hydrogen. The hydrogen molecules, being much smaller

and lighter than those of carbon monoxide, would tend to diffuse toward the hot zone of the system, so that a concentration gradient would exist at steady state. Richardson points out[23] that whereas Boericke found 1/2 to 5 per cent hydrogen to be present in the gas samples, the hydrogen concentration in the hot zone may have ranged from 1 to 15 per cent. Of course, the magnitude of this error would be small relative to that error resulting in studies involving two gaseous reactants when thermal diffusion effects are neglected. Nevertheless, the error in Boericke's work due to neglect of thermal diffusion of hydrogen is significant though small. This example illustrates the importance of assessing the nature and extent of impurities in the gas phase.

In all of the studies that have been mentioned in this section, the compounds involved have been assumed to be stoichiometric and invariant. While this assumption is quite valid for the chromium and aluminum oxides and carbides, it may not be valid in regard to some of the others. As a matter of fact, Meerson and Lipkes[21] have contended that the findings of Brantley and Beckman[19] regarding the equilibria of Equation (18) are in error because the latter authors failed to take into consideration the formation of solid solutions of titanium monocarbide and titanium monoxide. Meerson[22] has demonstrated by chemical analysis and lattice parameter measurements that the reaction of titanium dioxide with carbon proceeds in steps, the last of which is the reduction of titanium monoxide by carbon according to

$$TiO + 2C = TiC + CO \qquad (23)$$

whereby the monocarbide and the monoxide form a complete series of solid

solutions. Thus the univariant equilibria represented by Equation (18) probably involve a titanium monocarbide rich phase rather than pure titanium monocarbide in equilibrium with graphite, titanium dioxide and carbon monoxide.

In many cases, compound-like phases display a considerable range of compositions at high temperatures. This is especially common in compounds of transition elements of the fourth, fifth and sixth groups. Wherever such characteristics exist, the composition of the phases involved must be determined in order to completely describe the phase equilibria in question.

Accurate Temperature Measurement Using a Disappearing Filament Optical Pyrometer

Accurate determination of the temperature of a glowing object can be accomplished using a disappearing filament optical pyrometer if three requirements are satisfied. These are that the instrument be properly calibrated to measure the temperature of a source with a certain emissivity, that the fraction of radiation from the source absorbed on the way to the pyrometer be known, and that the effective emissivity of the source be known. These requirements and their achievement will be considered in detail in this section.

It is also possible to perform accurate temperature measurement by correcting for the combined effect of instrument, media, and source errors; this constitutes calibration of the entire system. This type of calibration will be considered in Appendix A with reference to the system designed for the equilibrium studies.

In order to emphasize the factors involved in accurate temperature measurement, relevant aspects of the instrument, source, and media will be considered separately. Pertinent concepts of the physics of light and radiation will be cited to the extent necessary to form a coherent treatment.

The basis for temperature measurement with an optical pyrometer is that the intensity of light of a specified wavelength emanating from an object increases in a definite manner with temperature. The problem is complicated, however, by the fact that different objects at the same temperature emit spectral radiation of varying intensity depending upon the nature of the emitter. The measure of the proclivity of an object to emit radiation of a specified wavelength is the spectral emissivity, which is

defined as the ratio of the intensity of radiation of the specified wavelength emitted by the body to that emitted by a perfect radiator at the same temperature. (A perfect radiator is defined as a radiator which, at any specified temperature, emits radiation in each part of the spectrum of maximum attainable intensity as a result of temperature alone. Such a radiator is more commonly referred to as a "black body.") The relation between the intensity of spectral radiation from a perfect radiator, wavelength and temperature was first formulated by Wien[24] as follows:

$$J_\lambda = c_1 \lambda^{-5} \exp [-c_2 \lambda T] \tag{24}$$

where λ and T denote wavelength and absolute temperature, respectively, c_1 is a constant depending upon geometry, and c_2 is a universal constant of proportionality. It was later established that at high values of temperature and wavelength, Wien's law inadequately relates the involved variables. The desired relation in accord with experiment is Planck's law,[25] which postulates the following relation:

$$J_\lambda = c_1 \lambda^{-5} [\exp (c_2/\lambda T) - 1]^{-1}. \tag{25}$$

Before considering pyrometer calibration it will be necessary to establish what is meant by temperature. The International Temperature Scale of 1948[26] defines 1063.0°C as the normal freezing point of gold. From 630.5 to 1063.0°C, the Scale is defined by means of a 10% rhodium-platinum against pure platinum thermocouple using the quadratic equation, to express the emf. vs temperature relationship as

$$E = a + bt + ct^2. \tag{26}$$

The constants are determined by measurements at the freezing points of antimony (630.5°C), silver, and gold. Since the antimony point is not one of the primary fixed points and in order to ensure a measure of continuity with the resistance thermometer scale, it is specified that the freezing point of the actual sample of antimony which is used shall be determined by means of the standard platinum resistance thermometer, which defines the scale from -182.97 to 630.5°C. The value so determined is to be used in the calculation of the thermocouple calibration. Alternately the thermocouple may be compared directly with the resistance thermometer at a temperature close to 630.5°C.

Temperatures above the gold point are defined in the International Scale of 1948 by the following relation:

$$\frac{J_t}{J_{Au}} = \frac{\exp[c_2/1336.15\lambda] - 1}{\exp[c_2/(t+273.15)\lambda] - 1} \qquad (27)$$

This relation expresses the ratio of intensities J_t and J_{Au} of radiation of wavelength λ emanating from perfect radiators at temperatures t and 1063.0°C, respectively, and obeying Planck's law. The value for c_2 is assigned as 1.438 cm-°C.

Calibration of a pyrometer consists essentially of determining its filament current as a function of temperature. A primary calibration involves the use of a perfect radiator immersed in each of several metals whose melting points are accurately known. To illustrate the procedure for a primary standardization, an account given by Foote and associates[27] will be described. Each of several metals, which melt below 1400°C is caused to melt or freeze over a time period of about 20

minutes. During this period, 30 to 40 observations are made of the filament current when the filament is matched with the image of the perfect radiator immersed in the molten metal. The mean values of the currents are substituted in the equation,

$$i = a + bt + ct^2 + dt^3, \tag{28}$$

to determine the values of the constants. This relation is the basis for calibration of the instrument from about 650 to 1400°C.

It should be noted that Foote's work was written even before the creation of the International Temperature Scale of 1927. In conformity with scale of 1948, melting points which were not primary standards would be established based on the standard rhodium-platinum against platinum thermocouple.

Also, observations should be made on a source maintained at several temperatures within the range of 1063 to 1400°C. By employing rotating sector discs precisely constructed to permit a specified fraction of light to pass them, additional data can be obtained so that the calibration constants can be determined using least squares techniques. This is done by adjusting the source temperature so that the intensity of light passing the sector disc is very near that corresponding to the gold point. Thus the source provides radiation equivalent to that from a perfect radiator at a temperature determined by utilizing Planck's radiation law, which defines the temperature scale in the range in question. The current corresponding to this temperature is determined by matching the source image and filament after removing the disc from the light path.

Use of optical pyrometers above 1400°C requires the use of absorbing screens or sectored discs. These are required to avoid the excessive brightness associated with the higher temperatures. Each screen or set of discs corresponds to another scale range of the pyrometer which must also be calibrated. If enough melting points are available in the range in question, the same procedure can be used as for below 1400°C. Otherwise, the absorbing power of the screens or the reduction in intensity resulting from use of the disc must be established. Precise calibration of these devices is a complicated and laborious process[27] and will not be considered in detail. It will suffice to mention that the complications are caused by the fact that the effective wavelength of the red light transmitted by the red glass ocular of the pyrometer varies with source temperature.

According to Foote, a secondary calibration of a properly designed disappearing filament pyrometer may easily be made with an accuracy of 5°C and, if necessary, 2°C.[27] Hence, for the work of this thesis the accuracy of a secondary calibration would be sufficient. Such a calibration involves a comparison method, whereby radiation from a constant and uniform light source is detected by both the pyrometer and a standard pyrometer. The light source may be a specially designed furnace or a carbon or tungsten strip lamp and need not be a perfect radiator as long as the pyrometers are designed to detect nearly the same wavelengths. This calibration can be effected over all ranges of the pyrometer, or the percent transmission of light through the screens or discs can be determined separately.

It should be noted that although pyrometers are usually calibrated to read the temperature of a perfect radiator, it is not necessary

that the source in question have an effective emissivity of unity. It is, however necessary that the emissivity of the source be established. Then the actual temperature can be determined from the apparent temperature utilizing Planck's law. Curves have been prepared to facilitate these determinations and are readily accessible.

In most cases it is best to design the system in such a manner that a close approach to a perfect source is achieved. For example, in this work the emissivity of the charge will vary somewhat with composition. The 0.65 micron spectral emissivity of graphite powder is greater than 0.9.[27] A value of 0.9 has been reported for uranium monocarbide and the value for the dicarbide is expected to be of the same order of magnitude. A value of 0.51 has been reported for uranium dioxide powder.[29] The spectral emissivity of a finely divided mixture should be amenable to approximation by assuming it to be an additive property based on volume fraction.

It is well known that a close approach to a perfect radiator is achieved by using an enclosure maintained at constant temperature and with a small opening from which radiation is emitted. The basis for this can be illustrated utilizing Figure 4. This figure illustrates the arrangement, with respect to the pyrometer line of sight of sample tablets and crucibles employed in this study. The pyrometer is sighted on the upper surface of the tablet itself, which is placed so that the line of sight is inclined about 20° from the normal to the sample surface. The radiation detected by the pyrometer is that emitted by region A on the tablet plus radiation emitted from region B and reflected at A plus radiation emitted from C and reflected from B and A and so on.

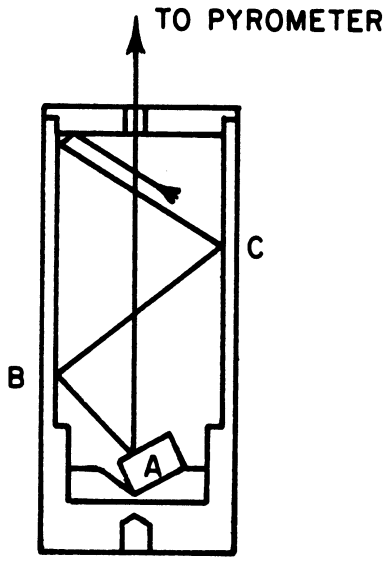

Figure 4. Cross Section of Crucible and Sample Tablet Showing Radiation Geometry.

Radiation incident on a surface is either refracted or reflected and the reflecting power, p_λ, defined as the fraction of incident radiation of wavelength λ that is reflected, is a measure of the reflecting tendency of the surface. Radiation that is refracted is either transmitted or absorbed. Since opaque bodies are involved, no transmission will occur. Hence, the spectral absorptivity, a_λ, defined as the fraction of incident radiation of wavelength λ absorbed, is a measure of the ability of the body to absorb radiation. Furthermore, for a body in thermal equilibrium with its surroundings, the spectral absorptivity is equal to the spectral emissivity.[30] For this case ϵ_λ, a_λ, and p_λ are related by,

$$\epsilon_\lambda = a_\lambda = 1 - p_\lambda \tag{29}$$

Returning to the source shown in Figure 4, if as few as two reflections contribute to the total radiation directed at the pyrometer, the effective emissivity of the source is given by,

$$(\epsilon_\lambda)_{eff} = (\epsilon_\lambda)_A + (\rho_\lambda)_A(\epsilon_\lambda)_B + (\rho_\lambda)_A(\rho_\lambda)_B(\epsilon_\lambda)_C. \tag{30}$$

Using $(\epsilon_\lambda)_A = 0.8$ and $(\epsilon_\lambda)_B = (\epsilon_\lambda)_C = 0.9$, $(\epsilon_\lambda)_{eff}$ is calculated to be 0.998.

This treatment is exactly analogous to that of Wood and Cork[31] for the optical wedge, another common source of near perfect radiation which is especially useful when the spectral emissivity of the source is inherently low.

The next question that must be resolved is linked with the fact that it is impossible to maintain the enclosure at a perfectly uniform temperature, and the degree of departure from this state will result in

a proportionate amount of systematic error. The size of this error that can be reasonably expected in the experimental system for equilibrium studies will now be assessed.

Two extreme cases will be assumed, which are considered to exceed the degree of departure from uniform temperature experienced in the experimental system of this study. These assumptions are based on observations of system temperatures reported on page 57. The first of these is the case where the crucible walls are 30°C below that of the specimen, and where only two reflections contribute to the radiation detected. The second case is that where the crucible walls are 30°C higher than the sample and an infinite number of reflections are involved. Of course, both of these situations are physically impossible at a steady state since the sample is heated mainly by the radiation from the walls of the crucible, each point of which is exchanging radiation with all other points seen, including those on the sample. With the aid of the reflection concept developed earlier, and using Planck's radiation law, the apparent temperatures of the tablet were calculated for the two cases, with a sample temperature of 1773°K being used. The value used for the emissivity of the sample was 0.8. Apparent sample temperatures of 1768 and 1781°K were calculated for cases one and two, respectively. Consequently, any errors due to lack of uniform temperature in the enclosure used are expected to be very small.

Even with a perfect source and a properly calibrated detector, error will result if absorption of radiation occurs on the way to the detector. This absorption can be classified as to whether it is determinable or indeterminable, and indeterminable absorption must be eliminated.

Two common types of indeterminable absorption are caused by the presence of smoke and by the deposition of a solid film on transparent media in the system. In systems where appreciable smoke or other dust can not be avoided, the use of an optical pyrometer is generally not satisfactory. The deposition of a film can normally be eliminated by using a shutter between the source and the transparent media.

A magnetically actuated shutter was employed in this investigation. It is considered to have been completely effective because no sign of deposit was observed on the sight glass during the experimental studies.

No medium is completely transparent, and the glass window and totally reflecting prism were found to absorb an appreciable fraction of radiation incident upon them. However the absorbing power u of a material can be determined experimentally using the relation,

$$(I)_\lambda = (I_o)_\lambda e^{-ut} \qquad (31)$$

where $(I_o)_\lambda$ and $(I)_\lambda$ are the intensities of incident and transmitted radiation of wavelength λ, respectively, t is the thickness and the u is the coefficient of absorption. This coefficient is numerically equal to the reciprocal of that thickness of material that would reduce the emergent $(I)_\lambda$ to 1/2.718 of the incident radiation intensity $(I_o)_\lambda$ (32).

Having shown that a crucible enclosure can constitute a source of nearly perfect radiation and having taken into account absorption effects, a secondary calibration of the pyrometer itself would seem to complete the fulfillment of requirements set forth for accurate temperature measurement with the pyrometer. Such a calibration was carried out, and

the results of this and the calibrations for absorption are described in Appendix A.

Determination of Thermodynamic Functions from the Results of the Phase Equilibrium Studies

The standard Gibbs free energy of a chemical reaction can be indirectly measured as a function of temperature by equilibrating the reactants and measuring the phase rule variables. The standard Gibbs free energy is related to the phase rule variables through the equation

$$\Delta G_T^\circ = - RT \ln K_T \tag{32}$$

where K_T is the thermodynamic equilibrium constant, T is the absolute temperature, and R is the gas constant. The equilibrium constant for the general chemical reaction at constant temperature and pressure

$$lL + mM + \ldots = qQ + rR + \ldots \tag{33}$$

is related to the activities of the reactants in mutual equilibrium by

$$K = \left(\frac{a_Q^q \, a_R^r}{a_L^l \, a_M^m} \cdots\cdots \right) \tag{34}$$

The derivation of Equation 32 follows from the definitions of the Gibbs free energy and the activity of a substance and can be found in any textbook of chemical thermodynamics, for example that of Lewis and Randall[32] or Guggenheim.[33] Consequently, the standard Gibbs free energy of reaction can be determined from the values of the activities of the reactants when these reactants are in equilibrium with one another. The general problem of the determination of the activity of a substance from its composition at a certain temperature and pressure is the subject of the

thermodynamics of solutions. This topic will be taken up here only as it directly relates to the problem at hand. For a treatment of the thermodynamics of solutions the reader is referred again to the works of Guggenheim[33] and of Darken and Gurry.[3]

For convenience, the standard state will be taken as the pure components at atmospheric pressure. The small change of free energy with pressure at constant temperature between one atmosphere and a few millimeters of mercury will be neglected. The solubility of oxygen and uranium in graphite will be considered to be negligible so that the activity of graphite can be considered as invariant and equal to unity. The carbon monoxide will behave as an ideal gas so that its activity is equal to its pressure in atmospheres. The activity of the uranium dioxide and carbide phases will be determined in a manner to be decided after the composition of these phases is assessed. It was expected that each of these phases would be comprised of over 90% of the related stoichiometric compound. Consequently, the activity of each reactant involved in a univariant equilibrium can be measured at various temperatures and values of ΔG_T° calculated using Equations (32) and (34).

Values of ΔH_T° and ΔS_T°, the standard enthalpy and standard entropy of reaction respectively, can then be evaluated by one of the two procedures. Which of these procedures can or should be used depends on whether or not specific heats of the reactants are known as functions of temperature over the range of interest and the relative reliability of these data and the experimentally determined values of ΔG_T°.

In the absence of specific heat data, curve fitting techniques can be used to find an analytical expression for ΔG_T° as a function of

temperature that best fits the data. Then expressions for ΔH_T° and ΔS_T° are obtained utilizing the relations

$$\frac{d}{dT}\left(\frac{\Delta G_T^\circ}{T}\right) = \frac{\Delta H_T^\circ}{T^2} \tag{35}$$

and

$$\Delta G_T^\circ = \Delta H_T^\circ - T\Delta S_T^\circ. \tag{36}$$

The curve fitting procedure can be systematized by taking into account a few basic facts of applied thermochemistry. For limited ranges of temperature above room temperature the heat capacity of a substance can be adequately represented by the first two or three terms of a power series of the type,

$$C_p = a + bT + cT^2. \tag{37}$$

Consequently,

$$\Delta C_p = \Delta a + \Delta bT\ \Delta cT^2 \tag{38}$$

so that

$$d\Delta H_T^\circ = \Delta C_p dT = \Delta a dT + \Delta bTdT + \Delta cT^2 dT. \tag{39}$$

Integration of Equation 39 yields

$$\Delta H_T = \Delta H_o^\circ + \Delta aT + \frac{\Delta b}{2} T^2 + \frac{\Delta cT^3}{3}, \tag{40}$$

where ΔH_o° is an integration constant having the significance that it is the value that the standard enthalpy of reaction would have at absolute zero if the truncated power series for Δ Cp was valid near absolute zero. Now utilizing Equation (35),

$$d\left(\frac{\Delta G_T^\circ}{T}\right) = \left(\frac{-\Delta H_o^\circ}{T^2} - \frac{\Delta a}{T} - \frac{\Delta b}{2} - \frac{\Delta c}{3}T\right)dT. \tag{41}$$

Integrating Equation (41) results in

$$\frac{\Delta G_T^\circ}{T} = I + \frac{\Delta H_o^\circ}{T} - \Delta a \ln T - \frac{\Delta b t}{2} - \frac{\Delta c}{6} T^2, \qquad (42)$$

where I is another integration constant. Consequently, if in a temperature range, the heat capacities of the reactants can be expressed in the form of Equation (37), the free energy of reaction can be expressed in the form

$$\Delta G_T^\circ = \Delta H_o^\circ + IT - \Delta a T \ln T - \frac{\Delta b}{2} T^2 - \frac{\Delta c}{6} T^3. \qquad (43)$$

Thus the experimentally determined values of ΔG_T° versus T are first plotted. If the data are linearly related, then the slope and intercept of the best straight line representing the data can be determined applying the method of least squares. (The use of least squares analyses here is desirable because additional errors due to curve fitting are precluded and also because the magnitude of the random error can be assessed. The application of least squares methods in thermochemistry will be discussed in this section.) Cases where ΔG_T° and T are linearly related are those where ΔC_p is small. The significance of the slope and intercept in such cases is that they represent mean values of the negative of the standard entropy of reaction and the standard enthalpy of reaction for the temperature range investigated. This can be verified by inspection of Equation (36).

In cases where the temperature range investigated is fairly large, where the value of ΔC_p is appreciable, and where the precision and accuracy of the values of ΔG_T° versus T is good, these data will

depart from linearity. In these cases it is desirable to fit the data to an expression of the form

$$\Delta G_T^\circ = A + BT \log T + CT. \qquad (44)$$

This is the form of the expression for ΔG_T° that would be obtained by using an average value of ΔC_p for the temperature range in question and then proceeding in the manner used to derive Equation (43). However, if a least squares analysis were performed to obtain values of the parameters A, B, and C of Equation (44), the value 2.3B can not be expected to approximate ΔC_p. As a matter of fact, the evaluation of specific heat data from free energy data is an inherently poor procedure. The only valid point to be noted here is that there is some physical justification for fitting data by the form of Equation (44). Kubaschewski and Evans point out that free energy expressions of the form of Equation (44) are adequate over fairly large temperatures and that it is unnecessarily cumbersome to use more complicated expressions[12]. Therefore the subject of fitting analytical expressions to free energy data need not be pursued further.

After an analytical expression for the standard free energy of a reaction is formulated, expressions for the standard enthalpy and entropy changes can be readily obtained by using Equations (35) and (36).

In cases where good data on the enthalpy of the reactants are available, more accurate expressions for the standard enthalpy and entropy of reaction may be formulated. The procedure depends on whether the data are tabulated utilizing the free energy function, $(G^\circ - H^\circ)/T$, or in the form of empirical expressions of heat capacity. In the latter case, use can be made of the Sigma function.

The Sigma function was originally conceived on the basis that specific heat can be empirically expressed by

$$C_p = a + bT - \frac{c}{T^2} \tag{45}$$

even beyond the range of temperatures for which the constants were experimentally determined. Kelley first employed this type of empirical representation[34] because of the lack of experimental data and because it was found to be applicable over a larger temperature range than a representation of the type of Equation (37). If specific heats are expressed in the form of Equation (45), then it follows that

$$\Delta G^\circ_T = IT + \Delta H_o - \Delta a T \ln T - \frac{\Delta b}{2} T^2 + \frac{\Delta c}{2T} \tag{46}$$

gives the Gibbs free energy of reaction in terms of Δa, Δb, and Δc. This expression can be derived in the same fashion as Equation (43) was derived, and the constants I and ΔH_o have the same significance. Let ΔG°_T now be replaced by $-RT\ln K$ and Equation (46) arranged to give

$$-R\ln K + \Delta a \ln T + \frac{\Delta b}{2} T - \frac{\Delta c}{2T^2} = I + \frac{\Delta H_o}{T}. \tag{47}$$

The left side of Equation (47) is designated as Σ and called the Sigma function. Values of this function can be calculated from experimentally determined values of K, Δa, Δb, and Δc, and these values of Σ can in turn be used to determine values of ΔH_o and I, utilizing the fact that the relation in Σ and I/T must be linear.

In the application of the Sigma function the question of propagation of error should not be ignored. Scatter of points in a graph of Σ versus I/T is indicative of accumulated random errors in the Σ values.

It is advisable to make a least squares analysis to find the best values of ΔH_o and I and then to calculate the standard deviations of these values using techniques based on the theory of statistics. Methods for determining such standard deviations are presented by Beers[35] and Deming[36]. The general subject of least squares methods is treated by these authors and also by Scarborough[37].

After ΔH_o is evaluated, it can be substituted into

$$\Delta H_T^\circ = \Delta H_o + \Delta aT + \frac{\Delta b}{2} T^2 + \frac{\Delta c}{T} \qquad (48)$$

to obtain an expression for the standard enthalpy of reaction based on the heat capacity data.

The procedure of substituting the values determined for ΔH_o and I into Equation (46) to obtain an expression for ΔG_T° is generally considered inadvisable for two reasons. First, the error in such an expression is propagated from the error in ΔG_T° measured from -RTlnK plus the error in the terms for Δa, Δb, and Δc. Second, the resulting expression is unnecessarily cumbersome as indicated on page 46. It is considered superior in light of these above reasons to use an expression for ΔG_T° in the form of Equation (44). Apparently some investigators find it more expedient to make use of Equation (46). If the heat capacity data are of good quality, the additional error propagated in the value of G_T° will be small.

The use of tabulated values of the free energy function, $(F^\circ - H_0^\circ)/T$, has merit in that errors in fitting and extending specific heat data are avoided. Of course, the existence of the tabulated values of the free

energy function means that the heat capacity has been determined from absolute zero to the temperature in question.

Use of the free energy function is based on the relation

$$\Delta\left(\frac{G_T^\circ - H_0^\circ}{T}\right) = \frac{\Delta G_T^\circ - \Delta H_0^\circ}{T} \qquad (49)$$

Where $G^\circ - H^\circ$ is the difference between the standard free energy and the enthalpy of a reactant, ΔG_T° is the standard Gibbs free energy of reaction, ΔH_0° is the standard enthalpy of reaction at absolute zero, and T is the absolute temperature. The derivation of Equation 49 is presented by Darken and Gurry (3). The use of the free energy function and Equation (49) to evaluate values of ΔG_T° depends on knowledge of the free energy function for all the reactants and of the value of ΔH_0°.

The evaluation of ΔH_0° can be made in one of two ways. First, it can be evaluated if the enthalpy of reaction, ΔH_T°, is known at any temperature within the range of tabulated values of the free energy function. Second, it can be evaluated from data of free energy of reaction. It is the latter method that is of concern here.

Equation (49) can be written explicitly in terms of ΔH_0°. Then values of ΔH_0° can be calculated for each experimental value of ΔG_T°. The average of these values can then be taken as ΔH_0° and the precision of the value easily evaluated. The value of ΔH_0° obtained can then be used in conjunction with the enthalpy data for the reactants to evaluate ΔH_T° at any temperature within the range of the tabulated values. The value of ΔH_0° can also be used in Equation (49) to determine ΔG_T° at any temperature within the range of the tabulated values. However, it should be kept in mind that the error in the free energy function data as well as that of

the experimental error in ΔG_T° is propagated in calculations of this type. From a theoretical standpoint it is superior to fit the experimental free energy to an analytical expression if values of free energy are desired in the temperature range that was investigated. From a practical standpoint, there would be little difference in the procedures if the precision and accuracy of the free energy function data is considerably better than that for the free energy of reaction data.

EXPERIMENTAL PROCEDURE

Equipment

The closed system designed and used for carrying out the carbide-oxide equilibrium studies will be described in this section. Included in this description is an account of the provisions made for determining temperatures and carbon monoxide equilibrium pressures. All the auxiliary equipment used in this study will be mentioned in the description of experimental methods.

The three main components of the equilibration system are an electron tube generator, a high temperature reaction vessel, and a Pyrex vacuum system. These components are shown in Figure 5. The generator served as a source for radio frequency current, which was employed in heating the vessel by induction. It is a modified Model 1070 Generator manufactured by the Induction Heating Corporation. It operates on 220 volts, 60 cycle single phase alternating current. The nominal operating frequency is 375,000 cycles per second, and the maximum output is about 20 kilowatts.

The electronic circuit of the generator is characterized by full wave bridge type rectification and a modified Hartley oscillator circuit capable of use with a voltage reducing output transformer or a direct connected work coil. The tube complement consists of four mercury vapor rectifier tubes and two water cooled, parallel connected oscillator tubes. Feedback to the grid circuit is accomplished by means of an adjustable tickler coil inductively coupled to an induction coil in the tank circuit. Regulation of output power is accomplished by means of a rheostat in the grid circuit; this varies output current while the output voltage remains constant.

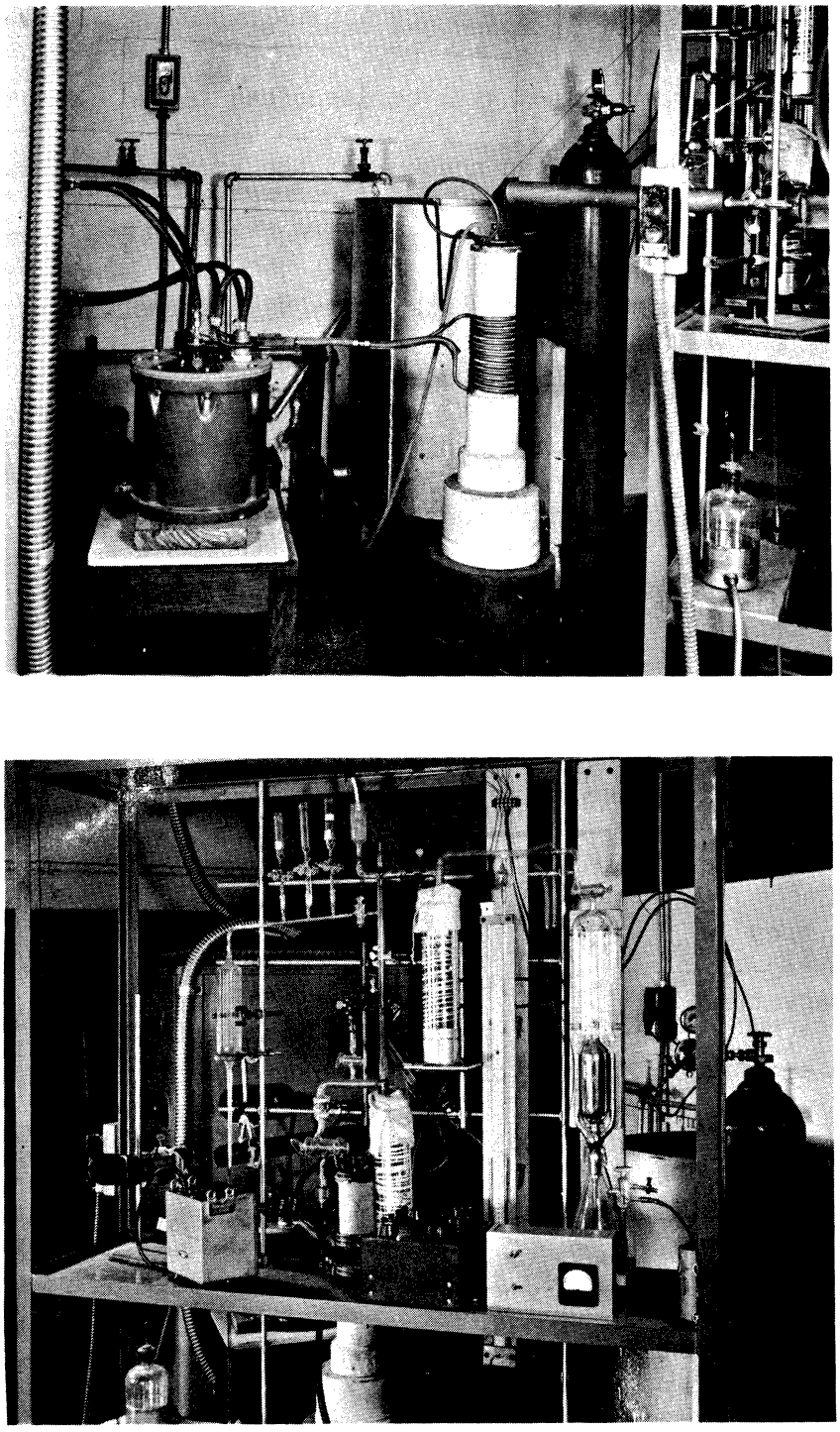

Figure 5. Equipment for the Equilibrium Studies.

The peak voltage across the generator output terminals is approximately 17,000 volts. In preliminary work with the system, a high inductance work coil was connected directly across the generator terminals. Considerable ionization of gases in the vacuum system occurred at low gas pressures, resulting in undesirable arcing to mercury in the system. This was attributed to the high energy of the magnetic field of the coil due to the high coil voltage. Consequently, it was decided to use a voltage reducing radio frequency output transformer between the generator and the work coil.

The transformer used was also manufactured by the Induction Heating Corporation. It consists of an oil filled porcelain case in which are suspended the primary and secondary windings, electrically insulated from each other by the oil. The primary winding was connected across the generator output terminals. It is a coil consisting of 22 turns of $\frac{1}{4}$ inch diameter water cooled copper tubing. The secondary is magnetically coupled to the primary. It is a five turn water cooled copper coil, and the work coil is connected across it.

The work coil used consists of 13 equally spaced turns of 3/8 inch water cooled copper tubing. The inside diameter of this coil is about four inches, and its length is about seven inches. It was necessary to test several coils before one with proper inductance was found. Since the length and the diameter of the coils were fixed by the design of the reaction vessel, the number of coil turns was varied in order to optimize the inductance. With too many turns the current in the coil was inadequate in inducing sufficient current in the susceptor. With too few turns, the generator current at zero load was excessive. Good performance was obtained with the 13 turn coil described above, and it was used in all experimental runs.

The function of the reaction vessel was to enable holding the reactants at temperatures as high as 1700° C with the reactants isolated from the atmosphere. In order to avoid side reactions, as discussed in the introduction, the entire hot region of the vessel was constructed of carbon materials. In order to isolate the system and minimize the possibility of mechanical failure due to thermal shock, vitreous silica was employed in the outer regions of the vessel.

A cross-section of the vessel used for most of the equilibrations is shown in Figure 6. Most of the eddy current was induced in the graphite susceptor tube, which is two inches in diameter, and six inches long, and 1/16 inch thick. The charge was contained near the bottom of a one inch diameter, two inches high graphite crucible that was centered in the vessel by the carbon support and centering pieces as shown in Figure 6. The crucible was heated principally by radiation from the susceptor tube. Sized graphite particles (20 - 100 mesh), placed in the annulus between the graphite tube and the inner silica tube, served as insulation. The assembly above the susceptor, containing the sight tube, is removable. It has a graphite base, which was also heated by induced currents to minimize the vertical temperature gradient in the crucible.

Support and centering pieces made of carbon pipe and rod maintained the crucible and the susceptor axes near the center line of the vessel. The concentric arrangement was provided in order to obtain axial symmetry of radial heat flux and thus minimize circumferential temperature variation. Since the electrical conductivity of the noncrystalline carbon is only about 20 per cent that of the graphite used for the

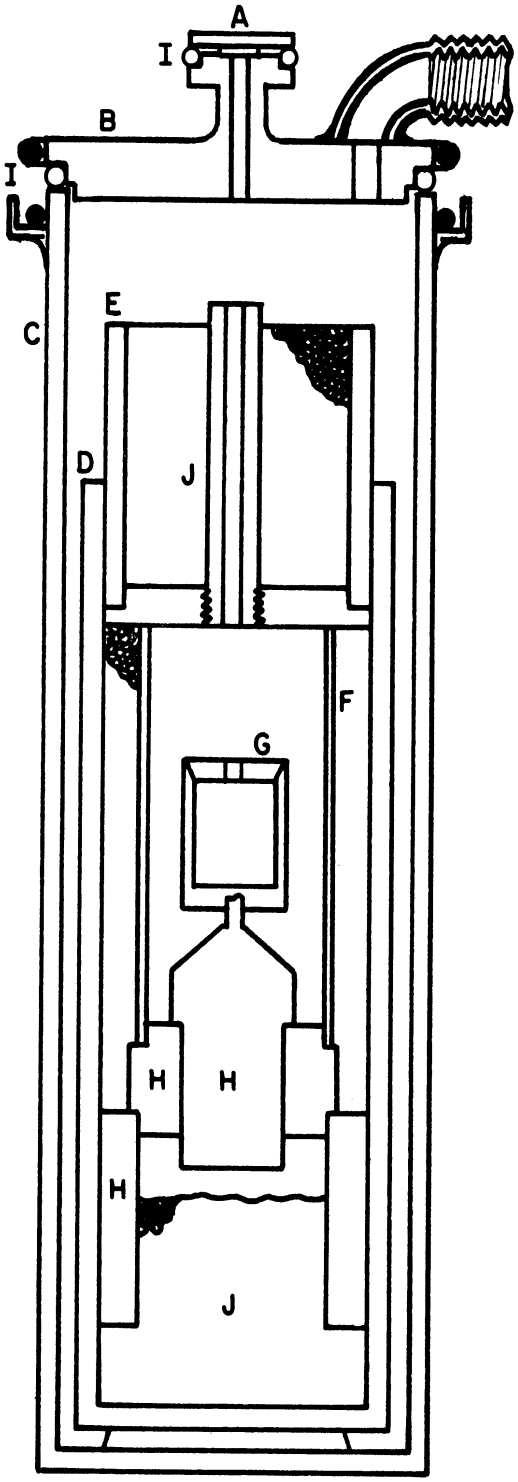

KEY

A. Sight glass and Iron Shutter
B. Brass lid
C. Outer silica tube
D. Inner silica tube
E. Insulating plug with sight tube
F. Graphite susceptor
G. Graphite crucible
H. Carbon support and centering pieces
I. O rings
J. Graphite particles

Figure 6. Cross Section of Reaction Vessel. (Not to scale)

susceptor tube, practically no eddy current heating of these components occurred. Moreover, the thermal conductivity of noncrystalline carbon is only about 5 per cent of that of the graphite so that relatively good thermal insulation was achieved.

A fairly thin annulus was provided for insulating powder between the susceptor and the inner silica tube. This was done in order to promote a heat flux from the susceptor that was nearly radial so that vertical temperature gradients in the central region would be minimized. No quantitative assessments were made of the effectiveness of this practice, but the red light emanating from through the coil turns was observed to be quite uniform over the length of the coil.

Using the vessel shown in Figure 5, it was possible to operate at temperatures in excess of 1700°C. However, it developed that interference was causing systematic errors in the carbon monoxide equilibrium pressures measured for equilibria of the type

$$UO_2 + 4C = UC_2 + 2CO$$

at temperatures above 1600°C. The errors were attributed to the occurrence of a side reaction which can be written as

$$SiC + 2CO \rightarrow SiO_2 + 3C. \qquad (50)$$

The silicon carbide had formed at the interface between the annular graphite insulating powder and the inner silica tube of the reaction vessel. This formation occurred during out-gassing of the vessel at temperatures above 1700°C and at low pressures. Under these conditions the reverse reaction of that of Equation (50) tends to occur.

In order to eliminate the side reaction and to enable completion of the experimental program, the reaction vessel was modified in such a way that the temperature difference between the susceptor and the inner surface of the inner silica tube was substantially increased. This was accomplished by installing a susceptor with a smaller diameter of 1 1/2 inches. Also, the graphite insulating powder was replaced with high purity graphite batting and felt.

The modified vessel was found suitable for use in studying equilibria of the type of Equation (13) above 1600°C without the occurrence of the side reactions previously encountered. Another improvement was attained by use of the modified vessel. This was that the temperature gradients in the crucible were reduced as evidenced by the fact that the crucible lid was observed to be within 5°C of the crucible interior at steady state. With the original vessel, the steady state temperature of the lid was about 30°C below that of the crucible interior.

A brass lid was provided in order to facilitate installation and removal of changes. A rubber O-ring was used in obtaining the vacuum seal between this lid and the top of the outer silica tube, which comprised the outer wall of the reaction vessel. The top of this tube was ground using a slurry of fine silicon carbide abrasive powder on a flat glass plate. The O-ring seating against this surface and the machined surfaces of the lid provided an effective seal. High vacuum silicone grease was applied to the O-ring, and the surfaces it contacted. The sight glass was sealed to the sight glass tube atop the lid by means of a smaller greased O-ring.

A cooling ring was provided to keep the top of the silica tube cool during equilibration. The ring was of copper and contained a single turn of $\frac{1}{4}$ inch copper tubing. Wood's metal was cast into the ring in order to improve heat transfer from the silica. The lid was cooled by water flowing through a single turn of $\frac{1}{4}$ inch copper tubing soft-soldered around the periphery of the lid and in series with the cooling ring for the silica tube.

To prevent clouding of the sight glass, a magnetically actuated shutter was employed. The shutter consisted of a small, thin piece of iron foil lying atop the brass sight tube. By means of a magnet, the shutter was moved to uncover the sight hole so that the vessel interior was exposed to view.

The temperature of the system was measured using a disappearing filament type optical pyrometer. This instrument is a direct reading type manufactured by the Leeds and Northrup Company. Radiation from the crucible interior after passing through the sight glass was directed to the pyrometer by means of a totally reflecting prism mounted in a thin-walled copper tube. It was necessary to make corrections to the observed temperatures, and these calibration procedures are described in Appendix A.

In addition to the reaction vessel, the vacuum system consisted of an open-end mercury manometer, a thermocouple gauge, a McLeod gauge, cold traps, a mechanical vacuum pump, and a system of glass sample tubes.

All the equilibrations made involved carbon monoxide equilibration pressures of greater than one millimeter of mercury. Consequently, all equilibrium gas pressure measurements were made with the mercury manometer. Upon reaching equilibrium, the pressure of the system relative to

the atmosphere was measured. About ten minutes after stopping the power input and pumping from the system, the system pressure was below 100 microns so that the manometer served as a barometer. The absolute carbon monoxide equilibrium pressure was then determined by subtracting the relative pressure from the barometric pressure. Measured absolute pressures were corrected to account for the fact that the mercury was at room temperature rather than 0°C. This correction mounted to $\frac{1}{4}$ millimeter or less.

The thermocouple gauge was useful in detecting small leaks and measuring leak rates in the vacuum system. This was done by pumping the system down to a pressure of a few microns and then isolating it. The leak rate was then determined by measuring the change of system pressure with time. The system was considered suited for operation if the leak rate was less than ten microns per hour. In many cases the rates decreased with increasing pressure, suggesting that the pressure rise was at least partly due to internal evaporation or desorption.

The McLeod gauge was used to calibrate the thermocouple gauge. One of the cold traps was used to minimize escape of mercury from the portion of the system containing the manometer and the McLeod gauge. The other trap was used to freeze out condensible vapors before they reached the pump. Dry ice in n-propanol was used in the cold traps.

A mechanical vacuum pump was used for removing gas from the system. This pump was a CENCO HYVAC 7 type, manufactured by the Central Scientific Company.

Sampling tubes ranging from about 15 to 150 millimeters in capacity were used for taking samples of the gas mixtures at equilibrium. Isolation of the sample was accomplished by closing a vacuum stopcock.

The tubes were fitted to the system with tapered joints so that they could be removed for gas analysis. The tapered joints and stopcocks were greased with Apiezon N high vacuum grease. An additional stopcock was provided for isolating the sampling branch from the rest of the system.

Methods

The experimental procedures described in this section include charge preparations, equilibration techniques, and analyses of gas samples and solid residues.

The initial runs were made with four objectives in mind. These were to test the performance of the equilibration system, to develop techniques for carrying out the equilibrations, to verify the equilibria of Equation (13) reported by Huesler[11], and to test the existence of the equilibria of Equations (11) and (12). The third objective mentioned was attacked by carrying out equilibrations of the type described on the following pages for approaching the equilibria of Equation (13). The last of these objectives was attacked by equilibrating selected graphite-uranium dioxide mixtures at a temperature of 1886°K and a pressure well below the carbon monoxide equilibrium pressure tentatively established for that temperature. The mixtures used in this equilibration, which constituted run 19, are listed in Table VII on page 70. The experimental methods described in the remainder of this section were formulated based on findings of the initial runs.

Four different types of charges were employed. The first type was of uranium dioxide and graphite for approaching the equilibria

$$UO_2 + 4C = UC_2 + 2CO \qquad (13)$$

by the evolution of carbon monoxide. The second type consisted of a mixture rich in uranium dicarbide for approaching the equilibria of Equation (13) by the consumption of carbon monoxide. The third type consisted of a mixture of uranium dioxide and uranium dicarbide for approaching the equilibria

$$UO_2 + 3\ UC_2 = 4UC + 2CO \qquad (51)$$

by the evolution of carbon monoxide. The fourth type consisted of a uranium monocarbide rich mixture for approaching the equilibria of Equation (51) by consumption of carbon monoxide.

The dicarbide and monocarbide rich mixtures used as charges the the equilibration runs were synthesised from uranium dioxide and graphite. The uranium dioxide used was supplied by the Mackay Co., and it was certified to contain less than 0.5 weight per cent of impurities. The graphite used was Ceylon graphite having an ash content measured as 0.2 ± 0.1 per cent. The dioxide powder was very fine and was used in its original form. The graphite was filed into powder, sized, and then outgassed at temperatures in the order of 2000°K. The sizing operation consisted in rejecting powder that would not pass through a 100 mesh screen. The carbide rich mixtures were not sized, but they were carefully ground under carbon tetrachloride to obtain a fine particle size.

Powders were weighed and then mixed by placing them in a polyethylene bottle, which was then rotated on mixing rolls. This practice was later modified to provide better mixing. This was done by placing the bottle in a short length of pipe so that the bottle axis was along a diameter of the pipe. Then the pipe was placed on the rolls. This procedure

caused powder to be tumbled and well mixed as the bottle turned end over end.

Charges for equilibration runs consisted of single tablets compacted from mixed powder. The die for pressing tablets was of hardened steel and was in three pieces. The piece containing the bore was in the shape of a cylinder, about four inches high and two inches in diameter. The bore was 3/8 inches in diameter, concentric, and the length of the die. The tablet was pressed between two 3/8 inch diameter rods. A Buehler metallurgical mounting press was used for pressing, and a pressure of about 50,000 pounds per square inch was applied. A binder of paraffin in tolulene was used for some of the tablets, but it was later found that tablets could be compacted without binder. The tablet thicknesses varied from about 1/16 to 3/16 inch, depending on the amount of powder desired for each equilibration.

The arrangement of the tablet in the crucible is shown in Figure 4. The tablets were placed on a graphite tray, at the bottom of the graphite crucible and then the crucible lid was installed. Then the lid was fitted in place, and the vessel was evacuated to a pressure of about one millimeter of mercury. Next the work coil was energized and the charge heated at fairly low power input, to a red color. Then the coil was de-energized and visual inspection made to verify that the crucible was adequately aligned with the line of sight through the sight tubes. Alignment was considered adequate if all or nearly all of the hole in the crucible lid was in the field of view.

After alignment was achieved, the crucible was heated slowly to the equilibration temperature. During the heating, periodic pumping

from the system was carried out in order to maintain the system at a low pressure and to remove desorbed gases. When the system temperature reached the desired temperature of equilibration, the pump was isolated, a sample tube was opened to the system, and the system was allowed to equilibrate. In cases where equilibration involved consumption of carbon monoxide, this was added to the system until the pressure was in excess of the equilibrium pressure expected. Readings of pressure were taken at fifteen or twenty minute intervals, and the equilibration was allowed to proceed until the rate of change of pressure with time became less than $\frac{1}{4}$ millimeter per hour. During equilibration the system temperature was checked periodically, and appropriate adjustments of the power were made to keep the system temperature at the desired value.

Rather than attempt to hold the system at predetermined temperatures, it was decided to adjust the power input to achieve convenient values of the generator plate current indicated on the plate current ammeter. It was found that maintaining the plate current at a fixed value resulted in maintaining constant temperature in most cases.

It was observed that at temperatures in excess of about 1825°K, the rate of reaction was sufficiently high that small temperature fluctuations caused fluctuations in the system pressure. This behavior was shown by the results of run 62 to be indicative of the reversibility of the system. The equilibria of Equation (13) was approached in both directions during run 62.

The variation of the system pressure with time during the equilibrations carried out in this run is shown in Figure 7. First the original charge of graphite plus uranium dioxide was allowed to react

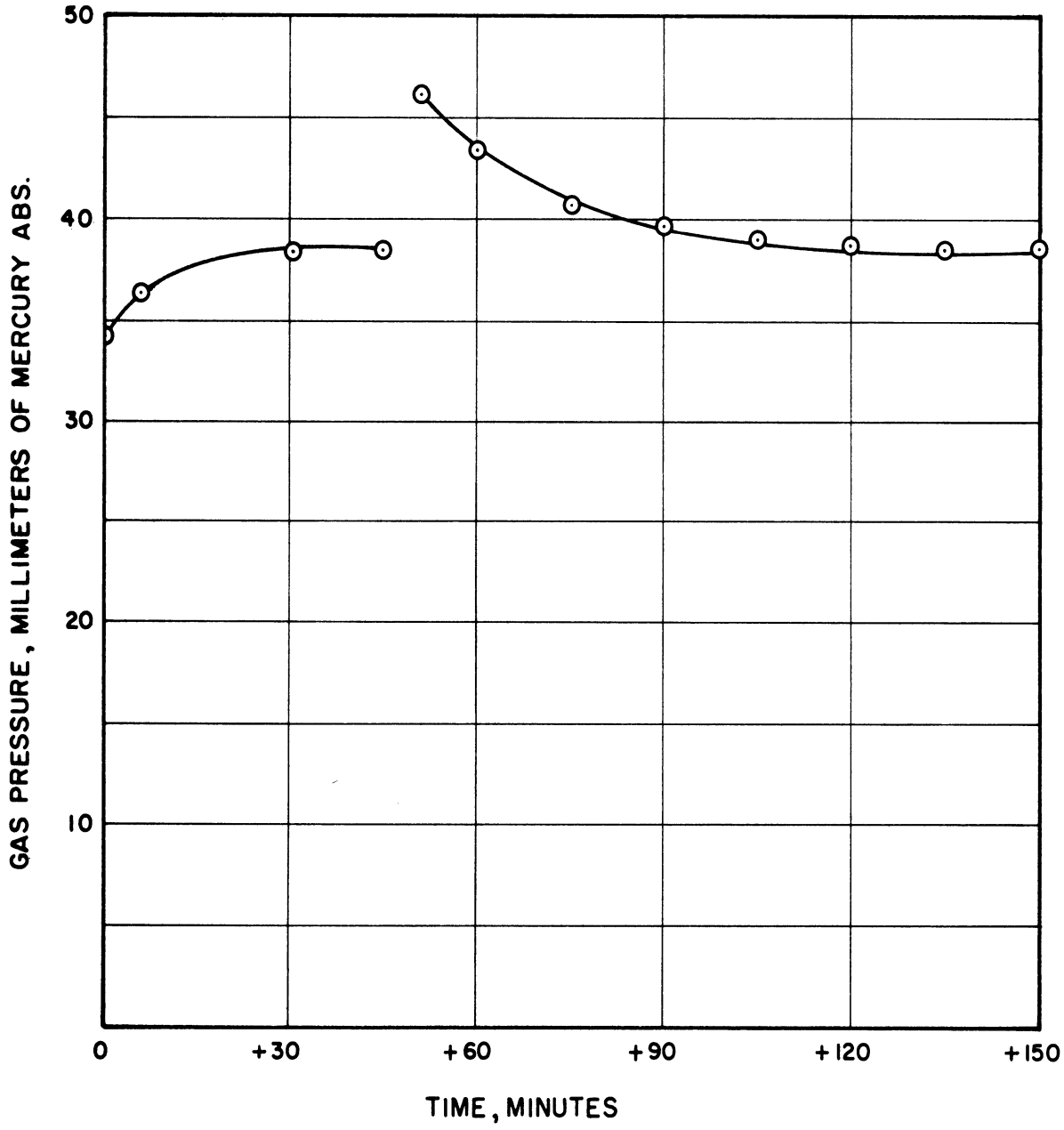

Figure 7. Total Gas Pressure as a Function of Time for the Equilibrations Carried Out in Run 62.

until the total gas pressure became nearly constant at $38\frac{1}{2}$ millimeters of mercury. Then carbon monoxide was added to raise the gas pressure to 46 3/4 millimeters. Finally the system was allowed to approach equilibrium by the consumption of carbon monoxide. When the carbon monoxide pressure again became nearly constant at $38\frac{1}{2}$ millimeters, another gas sample was taken, and the run was considered finished. Because of the ready reversibility demonstrated to exist at temperatures of about 1550°C and above, it was not considered necessary to approach equilibria in both directions at such temperatures.

Upon completion of an equilibration the gas sample was closed off, the power was shut off, and the pump cracked to the system. After about ten minutes, the system pressure was less than 100 microns so that barometric pressure could be read from the open end manometer. The system was then allowed to cool thoroughly. This took about four to five hours, although the crucible temperature fell to less than 650°C in about a half hour. After the system had cooled, it was opened, the solid residue was removed, and a new charge was added. Then the system was pumped out to minimize absorption of gas by the reaction vessel components.

The solid residue was visually inspected and any unusual features noted. Then a portion of the residue was crushed and mounted in a powder holder to enable the obtaining of part of the diffraction pattern of the sample. The holder consisted of a piece of plastic about 5/8 inch by 5/8 inch by 1/4 inch with a 3/8 inch diameter hole in its center. The powder was loaded as follows: A piece of scotch tape was pasted across

the top, covering the hole. Then the powder was poured into the open side of the hole. Finally, a cork was inserted to hold the powder in place. The loaded powder holder was mounted in a cylindrical aluminum tube in such a way that its upper surface was flush with the top of the tube. Modeling clay was used to fix the position of the holder in the aluminum tube.

A North American Philips Water Cooled Diffraction Unit with a Wide Range Goniometer and an Electronic Circuit Panel was used for all the X-ray diffraction work carried out in the study. This equipment was used to obtain part of the diffraction pattern of samples from the solid residue of each run. The assembly of the powder holder in the aluminum tube was placed in the rotating specimen holder of the goniometer. A chart record of intensity versus twice the angle of diffraction, 2 Theta, was obtained using the ratemeter and recording circuits of the electronic control panel. Diffracted radiation was detected by a Geiger counter mounted on the goniometer and driven at an angular velocity of one degree per minute. Either copper or cobalt radiation was used to obtain the diffraction pattern. Enough of the pattern was traced out to verify the presence or absence of all phases involved in this study. The peaks used to identify the various solid phases are listed in Table V.

In some cases precision lattice parameter determinations were made of uranium dioxide or monocarbide phases in the residue. The procedure used for these determinations is described in detail in Appendix D.

The gas samples were analyzed by means of mass spectrometry. The equipment and methods employed for these analyses is described in Appendix B. Because of the presence of hydrogen in the gas samples, it

TABLE V

APPROXIMATE VALUES OF TWICE THE ANGLE OF DIFFRACTION, 2 THETA OBSERVED USING THE WIDE RANGE GONIOMETER FOR PHASE IDENTIFICATION IN THE EQUILIBRIUM STUDIES

Phase	Miller Indices of Diffracting Planes	2 Theta, degrees	
		Cu K_α	Co K_α
C(gr)	{00·2}	27.3	31.7
UO_2	{111}	28.9	33.7
UC_2	{101}	30.1	35.0
UC_2	{002}	30.4	35.4
UC	{111}	32.0	37.0
UO_2	{200}	33.4	39.0
UC	{200}	37.0	42.9

TABLE VI

DETAILS OF NITROGEN ADDITIONS MADE IN RUNS 101 to 105

Run	Gas Pressures, mm. Hg. Abs.	
	Before Addition of Nitrogen	After Addition of Nitrogen
101	24 1/2	54 1/2
102	19 1/4	81 1/4
103	18 3/4	34 1/4
104	21	26
105	-	-

was necessary to make further corrections taking thermal diffusion into account. The derivation of the formula used for determining the correction is described in Appendix C.

A final series of five equilibrations was made at 1878°K with varying amounts of nitrogen in the system. The equilibrations were designated as runs 101 to 105. The charges for the runs 101 to 103 were mixtures of graphite and uranium dioxide. The charges for runs 104 and 105 were mixtures of uranium dioxide and uranium dicarbide rich powder. After the system temperature was brought to a value near 1870°K, nitrogen additions were made as specified in Table VI. No nitrogen was added in run 105.

X-ray powder photographs were made of samples from the crushed residues of the last five runs. Two Debye-Scherrer powder cameras both having diameters of 114.6 mm were used for the photographs. The detailed procedure employed in making the photographs is described in Appendix D.

RESULTS

Univariant Equilibria

Two univariant equilibria were found to exist in the temperature range investigated. These equilibria can be expressed as

$$UO_2 + 4C = 'UC_2' + 2CO \qquad (52)$$

$$\text{and } UO_2 + 3'UC_2' = 4'UC' + 2CO \qquad (53)$$

The use of quotation marks here is to signify that the compositions of designated phases differ slightly from the stoichiometric composition of the compound in question. At a given temperature in the range investigated, the equilibrium pressure for the equilibrium of Equation 53 is lower than that for the equilibrium of Equation 52.

The existence of these equilibria throughout the temperature range investigated was verified by approaching them in the directions of increasing and decreasing carbon monoxide pressure.

The existence of the equilibria of Equation 53 was initially deduced by equilibrations at 1886 and 1878°K, during which the total gas pressures were maintained at 8 3/4 and 24 millimeters of mercury respectively. The results of these equilibrations are summarized in Table VII.

TABLE VII

SUMMARY OF EQUILIBRATIONS AT CONSTANT TEMPERATURE AND CONSTANT PRESSURE TO VERIFY THE EXISTENCE OF THE EQUILIBRIUM $UO_2 + 3'UC_2' = 4'UC' + 2CO$ Near 1880°K

Run	Initial Charge Moles C: Moles UO_2	Temperature °K	Total Gas Pressure, mm.Hg.	CO Pressure mm. Hg.	Phases in Residue
19	2:1	1886 ± 8	8 3/4	$6\frac{1}{2}$	UO_2, 'UC'
19	3.75:1	1886 ± 8	8 3/4	$6\frac{1}{2}$	'UC', 'UC_2'
22	2:1	1878 ± 5	24	$21\frac{1}{2}$	UO_2, 'UC_2'

Carbon Monoxide Equilibrium Pressures for the Univariant Equilibria

The results of the determinations of carbon monoxide equilibrium pressures for the equilibria of Equation (52) are summarized in Table VIII. Listed under the heading of reactants are the phases that were consumed as the equilibrium was approached. Total gas pressures and the gas analysis of gas phase samples from each equilibration are listed. The corrected values of per cent carbon monoxide represent the calculated amounts of carbon monoxide in the hot gas in equilibrium with the solid phases. These values were calculated in the manner described in Appendixes B and C. Finally the values determined for the carbon monoxide equilibrium pressures are listed.

Similar results for the equilibria

$$UO_2 + 3'UC_2' = 4'UC' + 2CO \qquad (53)$$

are listed in Table IX.

Several divariant equilibria were achieved due to the intentional or unintentional loss of a solid phase. All of these results were

TABLE VIII

RESULTS OF CARBON MONOXIDE EQUILIBRIUM PRESSURE DETERMINATIONS FOR THE EQUILIBRIA $UO_2 + 4C = 'UC_2' + 2CO$

Run	Reactants	Temperature °K	Pressure mm. Hg.	Gas Phase Composition							CO Equilibrium Pressure, mm. Hg.
				%CO	$\%H_2$	%N	$\%O_2$	%A	$\%CO_2$	%CO corr.	
30	UO_2, C	1714	3 3/4	83.48	15.03	1.02	0.04	0.00	0.42	77.9	3
42	UO_2, C	1780	10 1/2	84.91	13.65	0.84	0.07	0.04	0.48	79.7	8 1/2
41	$'UC_2'$,CO	1786	11 3/4	93.89	4.80	1.00	0.10	0.01	0.20	92.1	10 3/4
12	UO_2, C	1817	18	90.89	8.46	0.39	0.10	0.01	0.15	86.0	15 1/2
49	UO_2, C	1845	22	89.43	7.87	2.49	0.00	0.00	0.20	86.4	19
39	$'UC_2'$, CO	1839	26 3/4	94.64	3.55	1.36	0.20	0.02	0.23	93.3	25
11	UO_2, C	1853	25	91.83	5.57	1.85	0.33	0.06	0.36	89.9	22 1/2
62	UO_2, C	1869	38 1/2	89.57	9.16	1.04	0.10	0.02	0.10	86.0	33
62	$'UC_2'$, CO	1869	38 1/2	88.77	10.01	0.94	0.12	0.02	0.13	84.8	32 3/4
61	UO_2, C	1892	45	90.83	8.97	0.16	0.00	0.00	0.04	87.2	39 1/4
60	UO_2, C	1922	62 3/4	92.17	7.20	0.55	0.00	0.01	0.07	89.3	56

TABLE IX

RESULTS OF CARBON MONOXIDE EQUILIBRIUM PRESSURE DETERMINATIONS FOR THE EQUILIBRIA $UO_2 + 3'UC_2' = 4'UC' + 2CO$

Run	Reactants	Temperature °K	Pressure mm. Hg.	Gas Phase Composition *							CO Equilibrium Pressure, mm. Hg.
				%CO	$\%H_2$	%N	$\%O_2$	%A	$\%CO_2$	%CO corr.	
23	'UC',CO	1761	6 1/4	94.88	4.74	0.06	0.09	0.01	0.23	93.1	5 3/4
45	UO_2,$'UC_2'$	1778	6 1/4	90.57	9.43					87.0	5 1/2
29	'UC',CO	1822	13	93.74	5.42	0.44	0.15	0.02	0.23	91.7	12
40	UO_2,$'UC_2'$	1847	15 1/2	86.88	11.85	0.96	0.06	0.02	0.24	82.3	12 3/4
105	UO_2,$'UC_2'$	1878	21 1/2	89.82	9.88	0.20	0.00	0.00	0.10	85.9	18 1/2
44	UO_2,$'UC_2'$	1914	28 1/2	93.42	6.11	0.20	0.00	0.00	0.27	91.0	26
34	'UC',CO	1911	31 3/4	94.75	4.41	0.52	0.06	0.00	0.26	93.0	29 1/2
57	UO_2,$'UC_2'$	1939	38 3/4	91.31	8.29	0.27	0.00	0.00	0.13	87.9	34
52	'UC',CO	1953	52 1/4	87.83	7.11	3.42	0.18	0.07	0.25	84.9	44 1/4

* The gas phase of run 52 contained 1.14% helium in addition to other gases listed.

consistent with the data of Tables VIII and IX describing the univariant equilibria. An account of these divariant equilibria and all experimental runs not reported as results is presented in Appendix E.

Divariant Equilibria Involving Nitrogen

The results of the equilibrations involving nitrogen are summarized in Table X. The results of runs 9, 50, and 57 are included because the lattice parameters of the monocarbide phases in the residues of these runs were measured.

Lattice Parameter Measurements

The lattice parameters measured for monocarbide rich phases have been tabulated in Table X. Values for which the uncertainty is expressed as $\pm$ 0.001 Angstrom units were calculated from measured values of the diffraction angle, THETA, for the 620 reflections. These values were greater than 80°, and the corresponding precision and accuracy in the calculated values of the lattice parameter is better than $\pm$ 0.001 Angstrom units. Values for measured lattice parameters of uranium dioxide phases are listed in Table XI. The reagent grade uranium dioxide for which the lattice parameter was measured is the dioxide used as a starting material in this study as described on page 71.

TABLE X

SUMMARY OF EQUILIBRATIONS INVOLVING NITROGEN AS A COMPONENT

Run	Charge	Tem. °K	CO Pressure mm. Hg.	N_2 Pressure mm. Hg.	Solid Phases in Residue	Monocarbide Phase Lattice Parameter, Å
101	UO_2 + C	1875	21.66	31.31	UO_2,C,U(C,N)	4.935 ± 0.001
102	UO_2 + C	1878	22.86	63.17	UO_2,C,U(N,C)	4.9214 ± 0.0003
103	UO_2 + C	1878	24.54	15.05	UO_2,C,U(C,N)	4.938 ± 0.001
104	UO_2 + UC_2	1878	19.43	3.13	UO_2,UC_2,U(C,N)	4.953 ± 0.001
105	UO_2 + UC_2	1878	18.47	0.04	UO_2,UC_2,U(C,N)	4.9608 ± 0.0003
57	UO_2 + UC_2	1939	34	0.10	UO_2,UC_2,U(C,N)	4.9616 ± 0.0003
50	UO_2 + UC_2	1892	21	0.01	UO_2,UC_2,U(C,N)	4.9573 ± 0.0006
9	UO_2 + C	1795	4	0.03	UC_2,U(C,N)	4.9582 ± 0.0002

TABLE XI

MEASURED LATTICE PARAMETERS FOR INDICATED URANIUM DIOXIDE PHASES

Phase Source	Lattice Parameter, A
Reagent Grade UO_2	5.4685 ± 0.0001
Residue from Run 7 at 1936°K	5.4707 ± 0.0003
Residue from Run 45 at 1778°K	5.4704 ± 0.0005

ANALYSIS OF RESULTS

Effect of Nitrogen on the Univariant Equilibria

The results of the studies of divariant equilibria among nitrogen, carbon monoxide, uranium dioxide, graphite, uranium dicarbide, and the uranium monocarbide phase indicate that coformation of uranium mononitride occurs in the presence of gaseous nitrogen. This coformation is manifested in the decrease of the lattice parameter of the monocarbide phase with the nitrogen concentration of the gas phase. Consequently, the presence of nitrogen during equilibrations carried out in this study would result in errors in the values determined for carbon monoxide equilibrium pressures for the equilibria of Equation (53). For these equilibria, the equilibrium constant, K_T, is given by

$$K_T = \frac{a_{UC}^{4} \, p_{CO}^{2}}{a_{UC}^{3}} \quad . \tag{54}$$

The effect of coformation of the mononitride is to lower the concentration and, therefore, the activity of the monocarbide. But as the activity of the monocarbide is decreased, the measured equilibrium pressure is increased, according to Equation (54). The objective of this section is to determine the magnitude of errors incurred in this work due to the presence of nitrogen in the gas phase.

In the case of the equilibria of Equation (53), the carbon monoxide equilibrium pressure is very sensitive to changes in the activity of uranium monocarbide. For example, if the monocarbide activity was reduced to 0.95 due to the presence of the mononitride in solid solution, the carbon monoxide equilibrium pressure would

be about ten per cent higher than the value corresponding to unit activity of the monocarbide.

In order to assess the magnitude of these errors using the results shown in Table X, additional data are needed. These data are the lattice parameters of the monocarbide-mononitride solid solutions as a function of composition. Lattice parameters of various solid solutions of uranium monocarbide and uranium mononitride have been measured both by Austin and Gerds[14] and by Williams and Sambell[38]. The results of Austin and Gerds are replotted as Figure 8. The results of Williams and Sambell lie very close to the dotted straight line shown in this figure. The apparent lack of agreement of these results in the region of high uranium monocarbide concentration can be accounted for; it will be desirable to do this in order to establish proper interpretations of these results. The concepts of the ideal solution will be useful in this respect.

The criterion that is most readily invoked in testing for ideal behavior of solid solutions is that the volume change in the formation of an ideal solution is zero.[3] Consequently, the volume of an ideal solution, V^{id}, is related to the volume of its consistuents and their mole fractions by

$$V^{id} = \sum^{i} N_i V_i \qquad (55)$$

where N_i and V_i are the mole fraction and volume respectively of constituent i. Therefore, for a cubic ideal solid solution, a graph of

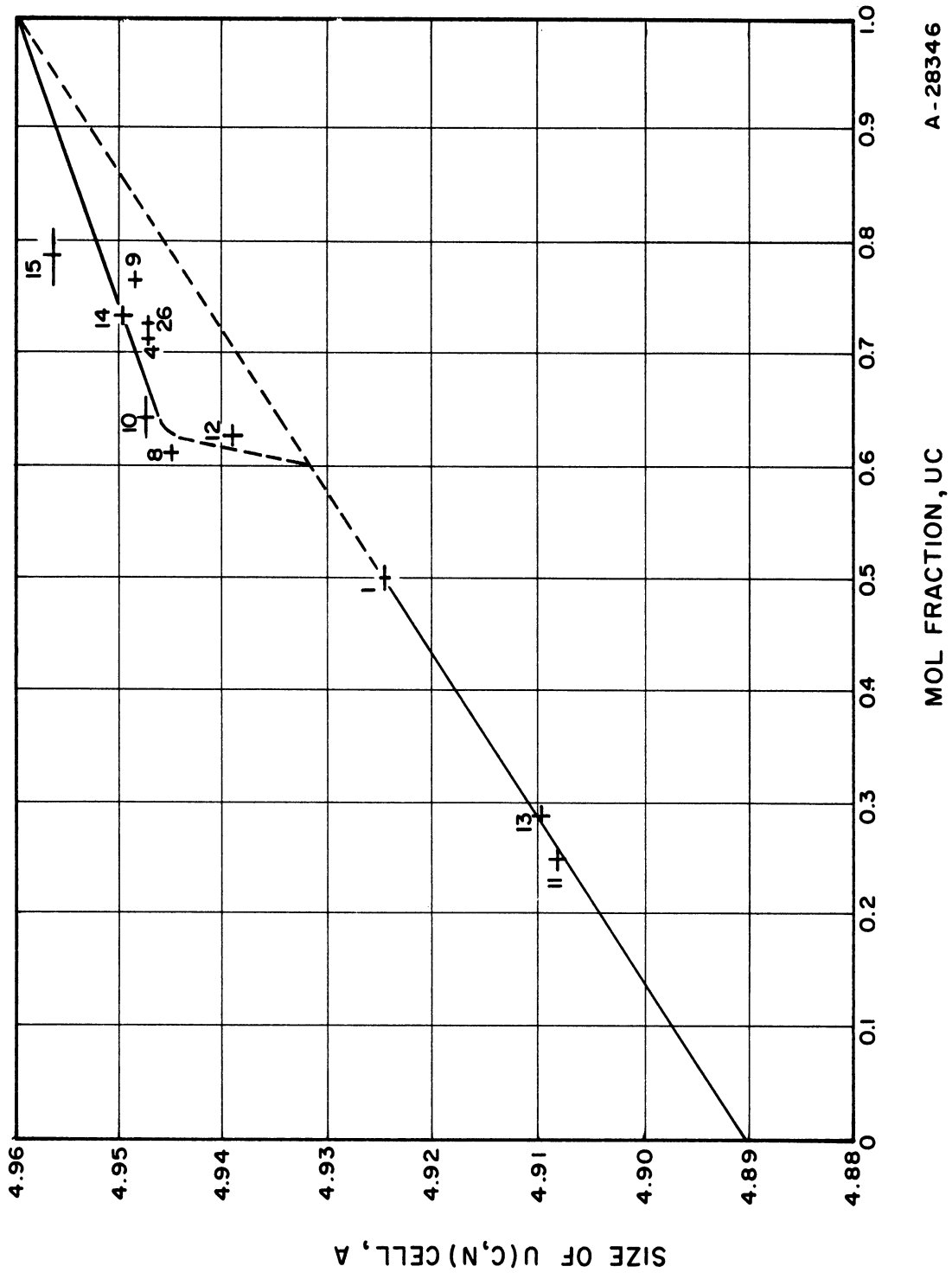

Figure 8. Plot of U(C,N) Cell Size Versus Mole Fraction of UC in Solid Solution.(14)

the cube of the lattice parameter versus composition in mole per cent would be linear. However, in cases where ideal behavior is exhibited in a binary system the difference in the lattice parameters of the two components is small, so that a graph of lattice parameter versus composition in mole per cent is very nearly linear; this is the physical significance of Vegard's law.(39)

In investigations of lattice parameters of TiN - TiC, VN - VC, and NbN - NbC Duwez and Odell found these systems to obey Vegard's law or to exhibit very slight positive deviations from it.(40) Solid solutions of stoichiometric uranium monocarbide and uranium mononitride also would be expected to exhibit ideal or nearly ideal behavior. They would not be expected to exhibit ideal behavior up to a certain concentration and then suddenly begin to behave nonideally.

The solid solutions of uranium monocarbide and uranium mononitride studied by Williams and Sambell were made from the stoichiometric compounds by solid state diffusion.(38) Consequently, their finding nearly linear variation of the lattice parameter with composition is consistent with the experimental results and theoretical considerations that have been mentioned. On the other hand, the monocarbide rich solid solutions investigated by Austin and Gerds were formed by equilibrating with uranium dicarbide at 2073°K.(14) But it has already been mentioned that at 2073°K the composition of the monocarbide phase in equilibrium with uranium dicarbide is about 52 atom per cent carbon in the binary system. Consequently, the monocarbide rich solid solutions equilibrated with uranium dioxide at 2073°K would be expected to contain less than 50 atom per cent uranium, and this could account for the anomalous variation of lattice

parameter with composition reported by Austin and Gerds. As a matter of fact, Williams, Sambell, and Wilkinson have found evidence that the lattice parameter of the monocarbide phase increases with per cent carbon[41], and this finding is consistent with the results of Austin and Gerds.[14] The work of Williams, Sambell, and Wilkinson will be discussed further in the section on estimation of solid phase compositions and activities beginning on page 94 .

In using Figure 8 to determine compositions corresponding to measured values of lattice parameters of monocarbide rich monocarbide-mononitride solid solutions, two things must be kept in mind. First, all the equilibrations made in this work and involving a monocarbide phase also involved a dicarbide phase. Second, some of the equilibrations were made at temperatures considerably below 2073° K, and at these lower temperatures the ability of the monocarbide phase to accommodate excess carbon is considerably less than at 2073° K. Consequently, the manner in which Figure 8 is employed will depend on the equilibration temperature involved, and there will be a small degree of uncertainty involved in the estimated values.

Before using the data of Table X in conjunction with Figure 8, it must be established that the changes in lattice parameter reported in the table are due only to changes in the nitrogen content of the monocarbide phase. If there were other causes, they would have been changes in the carbon or the oxygen content of the monocarbide phase. These possibilities are taken up in the section on estimating compositions and activities of the solid phases. It is demonstrated there that the oxygen content of monocarbide phases involved in these studies

is very small and that variation of carbon content of these phases has a very small influence in these studies. Consequently, the lattice parameter variations reported in Table X are attributable to changes in the nitrogen content of the monocarbide phase.

The data of direct bearing on the question of error are those of runs 104 and 105 because the phases of Equation (53) are involved in the divariant equilibria reached in these runs. Consequently, these data have been used in conjunction with Figure 8 to produce Figure 9. Figure 9 is a graph of composition of the monocarbide phase in equilibrium at 1878° K with carbon monoxide, nitrogen, uranium dioxide and uranium dicarbide or carbon as a function of the partial pressure of the gaseous nitrogen. By using this graph and examining the data of Table IX, the magnitude of errors in the carbon monoxide equilibrium pressures determined for the equilibria of Equation 53 can be assessed.

In order to estimate the nitrogen content of monocarbide phases from the data of nitrogen content in Table IX, the effect of temperature on the equilibria

$$2UC + \frac{1}{2} N_2 = UN(\text{in } UC) + UC_2 \qquad (55)$$

must be considered. The equilibrium constant, K_T', for this reaction is given by

$$K_T' = \frac{a_{UN}}{a^2_{UC}(p_{N_2})^{1/2}} \qquad (56)$$

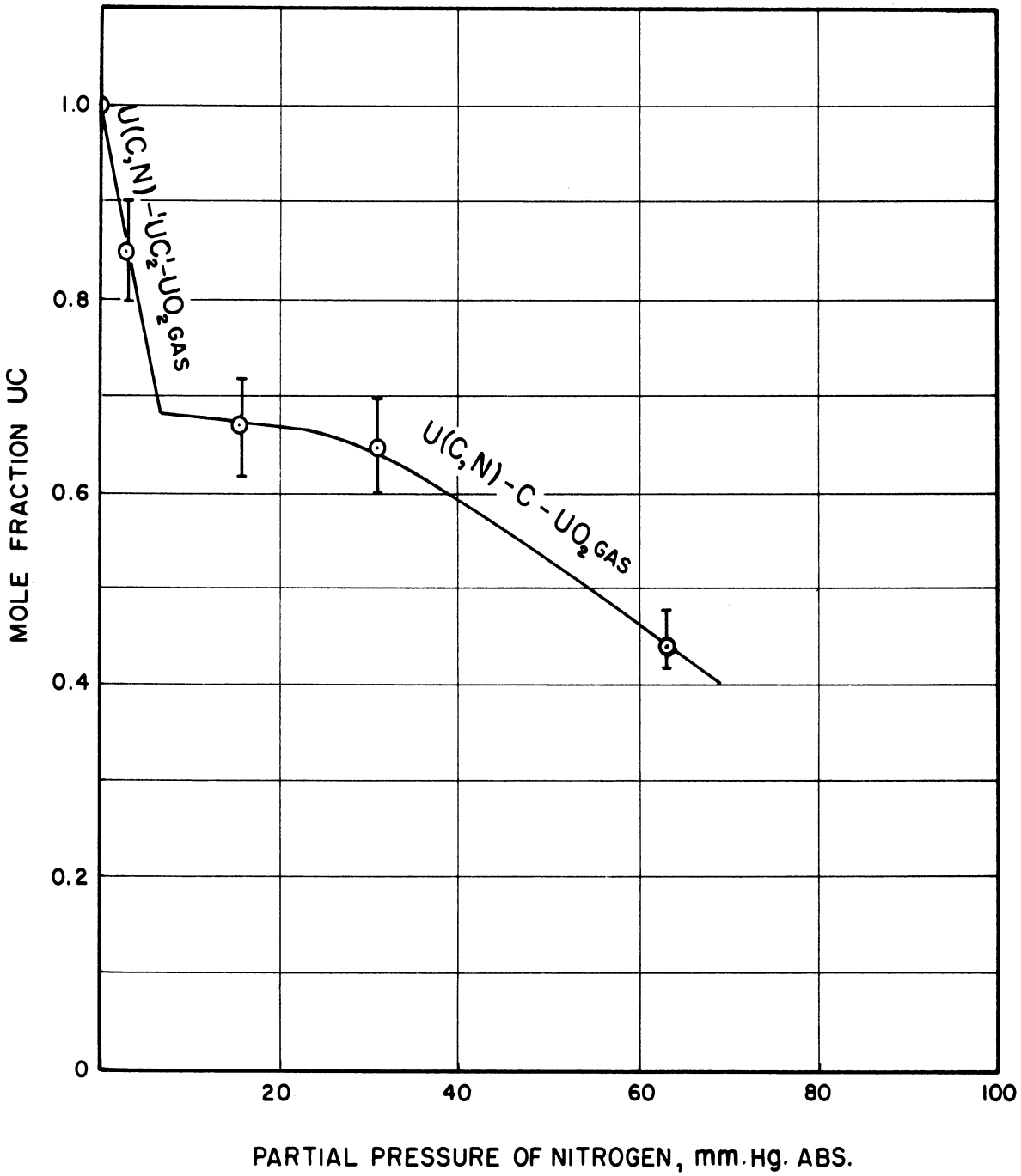

Figure 9. Composition of the U(C,N) Phase Versus the Partial Pressure of Nitrogen at 1878 ± 5 °K in the Equilibria of Runs 101 to 105.

Raising the temperature would favor the formation of nitrogen and uranium monocarbide from the mononitride and the dicarbide. Consequently, K_T' decreases with increasing temperature. This means that for a given nitrogen pressure in the gas phase at equilibrium, the activity of the mononitride would be smaller above 1878° K than at 1878° K.

The nitrogen partial pressures for equilibrations involving

$$UO_2 + 3'UC_2' = 4'UC' + 2CO \qquad (53)$$

and

$$2'UC' + \frac{1}{2} N_2 = UN(\text{in } UC) + 2UC_2 \qquad (55)$$

have been listed in Table XII. Examination of these data for all equilibrations carried out above 1878° K reveals that the nitrogen

TABLE XII

PARTIAL PRESSURES OF NITROGEN IN EQUILIBRIUM WITH URANIUM DICARBIDE AND SOLID SOLUTIONS OF URANIUM MONOCARBIDE AND URANIUM MONONITRIDE

Run	Temperature °K	Total Pressure mm. Hg.	$\%N_2$	Nitrogen Pressure mm. Hg.
23	1761	6 1/4	0.06	0.00375
45	1778	6 1/4	----	-------
29	1822	13	0.44	0.0572
40	1847	15 1/2	0.96	0.1488
105	1878	21 1/2	0.20	0.0430
50	1892	26	0.05	0.0130
44	1914	28 1/2	0.20	0.0570
34	1911	31 3/4	0.52	0.1651
57	1939	38 3/4	0.27	0.1046
52	1953	52 1/4	3.42	1.787

pressures for all runs except run 52 are of the same order of magnitude as for run 105. Hence the activity of the monocarbide phase should be as high or higher than that for run 105.

If run 52 had been carried out at 1878°K, the activity of the monocarbide phase involved would have been about 0.9, according to Figure 8. Since run 52 was carried out at a higher temperature than run 105, the activity of the monocarbide phase could have been greater than 0.9. However, it is conceivable that this activity could have been as low as 0.95, in which case the measured carbon monoxide equilibrium pressure would be about 10 per cent high. Inspection of Figure 11 on page 87 reveals that this is plausible.

The lattice parameter measured for the monocarbide phase of run 57 (see Table X) confirms the conclusions reached regarding runs above 1878°K. However, the value reported for run 50 is somewhat lower than would be expected if nitrogen content was the only factor influencing the monocarbide phase lattice parameter. This will be discussed further in the section on estimation of compositions and activities of the solid phases.

The assessment of nitrogen contamination for runs carried out below 1878°K can be facilitated by utilizing the lattice parameter measured for run 9, reported in Table X. According to Figure 8, this value of lattice parameter corresponds to a mole fraction of uranium monocarbide of about 0.97. Inspection of Table XII reveals that the nitrogen pressures for runs 23 and 29 are of the same order of magnitude as for run 9. Furthermore, inspection of Figure 10 indicates that the pressures measured for runs 40 and 45 are in line with those

measured for runs 23 and 29. Consequently, it is safe to conclude that the error in the carbon monoxide equilibrium pressure for runs 23, 45, 29, and 40 is of the order of less than ten per cent.

In summary, it has been deduced from the above considerations that the error in the carbon monoxide equilibrium pressures measured in runs 23, 45, 29, 40 and 52 is of the order of less than ten per cent.

No appreciable error is considered to have been incurred due to the presence of nitrogen in the equilibria of Equation (52). This contention is based on the findings of Austin and Gerds that the solubility of nitrogen in uranium dicarbide is negligible.[14] However, the data of Table X indicate that when large amounts (greater than 30 per cent) of nitrogen are present in equilibrium in the gas phase, that the monocarbide phase rather than the dicarbide exists in equilibrium with mixtures of uranium dioxide and graphite. This is a result of the lowering of the monocarbide activity.

Carbon Monoxide Equilibrium Pressures as Functions of Temperature

The data of carbon monoxide equilibrium pressures versus temperatures tabulated in Tables VIII and IX are plotted in Figure 10. Based on these data, analytical expressions for the carbon monoxide pressures as functions of temperature were formulated for the equilibria of Equations 52 and 53. These expressions are

$$\log p_{CO} = -\frac{18,000}{T} + 8.23 \qquad (57)$$

and

$$\log p_{CO} = -\frac{16,600}{T} + 7.26 \qquad (58)$$

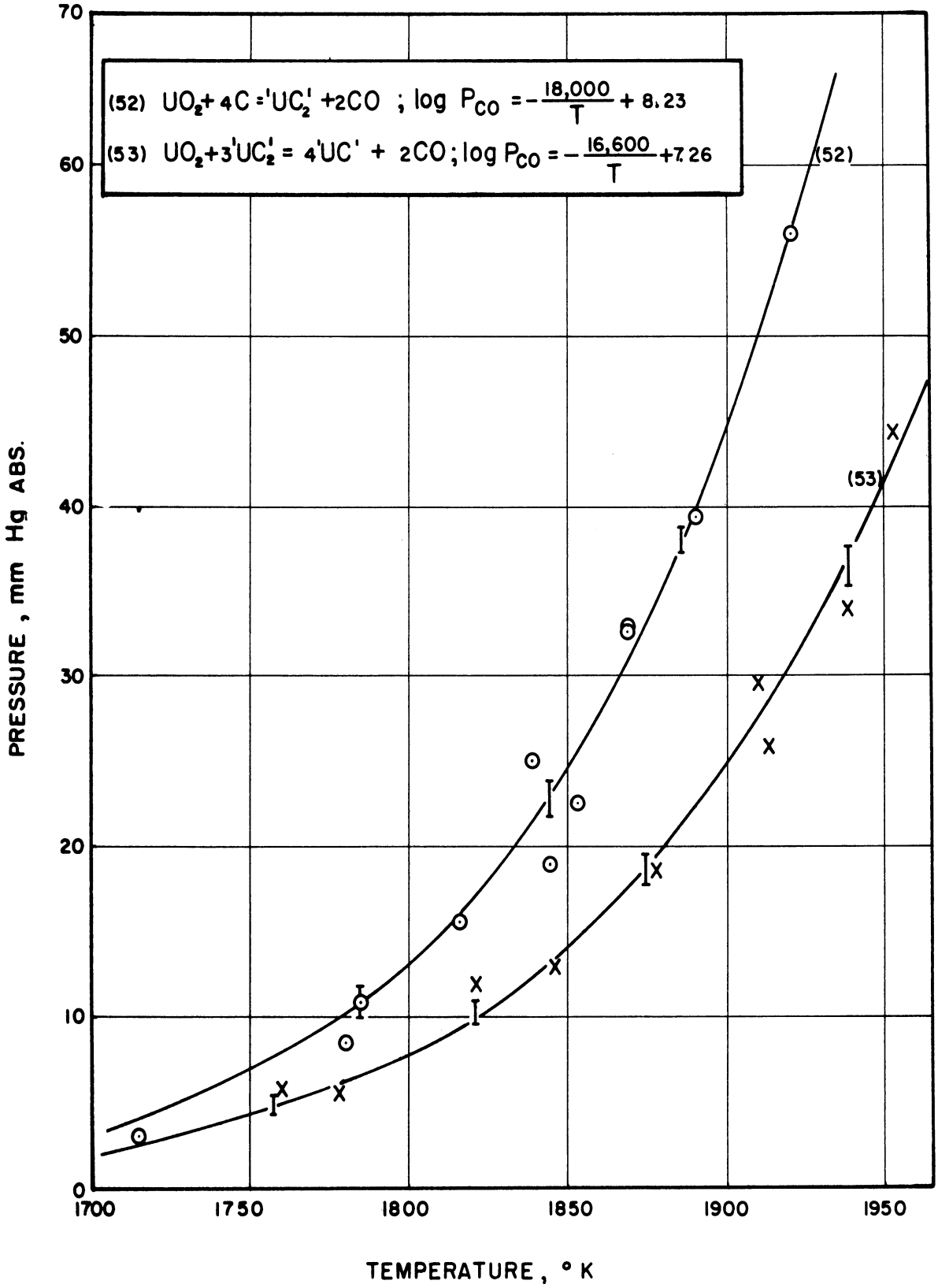

Figure 10. Carbon Monoxide Equilibrium Pressure Versus Absolute Temperature for the Equilibria $UO_2 + 4C = 'UC_2' + 2CO$ and $UO_2 + 3'UC_2' = 4'UC' + 2CO$.

for Equations (52) and (53) respectively. The formulation of these expressions will be described in this section.

The problem of formulating analytical expressions to fit experimental data can be resolved into two parts. The first part consists in finding the correct analytical expression. The second consists in finding the best values of the parameters involved in the expression, that is, in finding the particular member of a predetermined family of curves which best fits the data.

The problem of determining the type of analytical expression to fit the data is relatively straightforward in this case. The basis for this determination is the procedure for fitting free energy data that was outlined in the last section of the introduction.

Consider the equilibria

$$UO_2 + 4C = 'UC_2' + 2CO \,. \qquad (52)$$

For these equilibria at an absolute temperature, T, the standard Gibbs free energy of reaction, ΔG°_T, is related to the carbon monoxide equilibrium pressure at $(T, p_{CO}(T))$, and the activity of uranium dicarbide, $a_{UC_2}(T)$, by

$$\Delta G^\circ_T = - RT\ln K_T = -2.303RT(2\log p_{CO}(T) + \log a_{UC_2}(T)). \qquad (59)$$

Assuming that a_{UC_2} is a constant or varies linearly with temperature, the form of an analytical expression for $\log p_{CO}(T)$ corresponding to a specified form of an analytical expression for ΔG°_T can easily be deduced.

In the introduction it was pointed out that data of ΔG°_T could adequately be fitted to two or three term analytical expressions of the form

$$\Delta G^\circ_T = J + LT \tag{60}$$

or

$$\Delta G^\circ_T = A + BT \log T + CT \tag{44}$$

respectively. Corresponding to these expressions, are the expressions

$$\log p_{CO} = \frac{A}{T} + B \log T + C \tag{61}$$

and

$$\log p_{CO} = \frac{J}{T} + L \tag{62}$$

for Equations (44) and (60) respectively. Consequently, a graph of the experimental data where log p is plotted versus 1/T would dictate the type of expression to be used. If the graph was linear or very nearly linear, an expression of the type of Equation (62) would adequately represent the data. Otherwise, one of the form of Equation (61) would be appropriate.

The data in Table VIII and IX for Equations (52) and (53) were plotted on graphs of log p_{CO} versus 1/T. These graphs are shown in Figure 11. It was concluded from examining these graphs, that both sets of data could be adequately represented by expressions of the form of Equation (62). Consequently, it only remained to determine the best values of the parameters, J and L, and to assess the random error of the experimental determinations by determining standard deviations based on external consistency of the measurements.

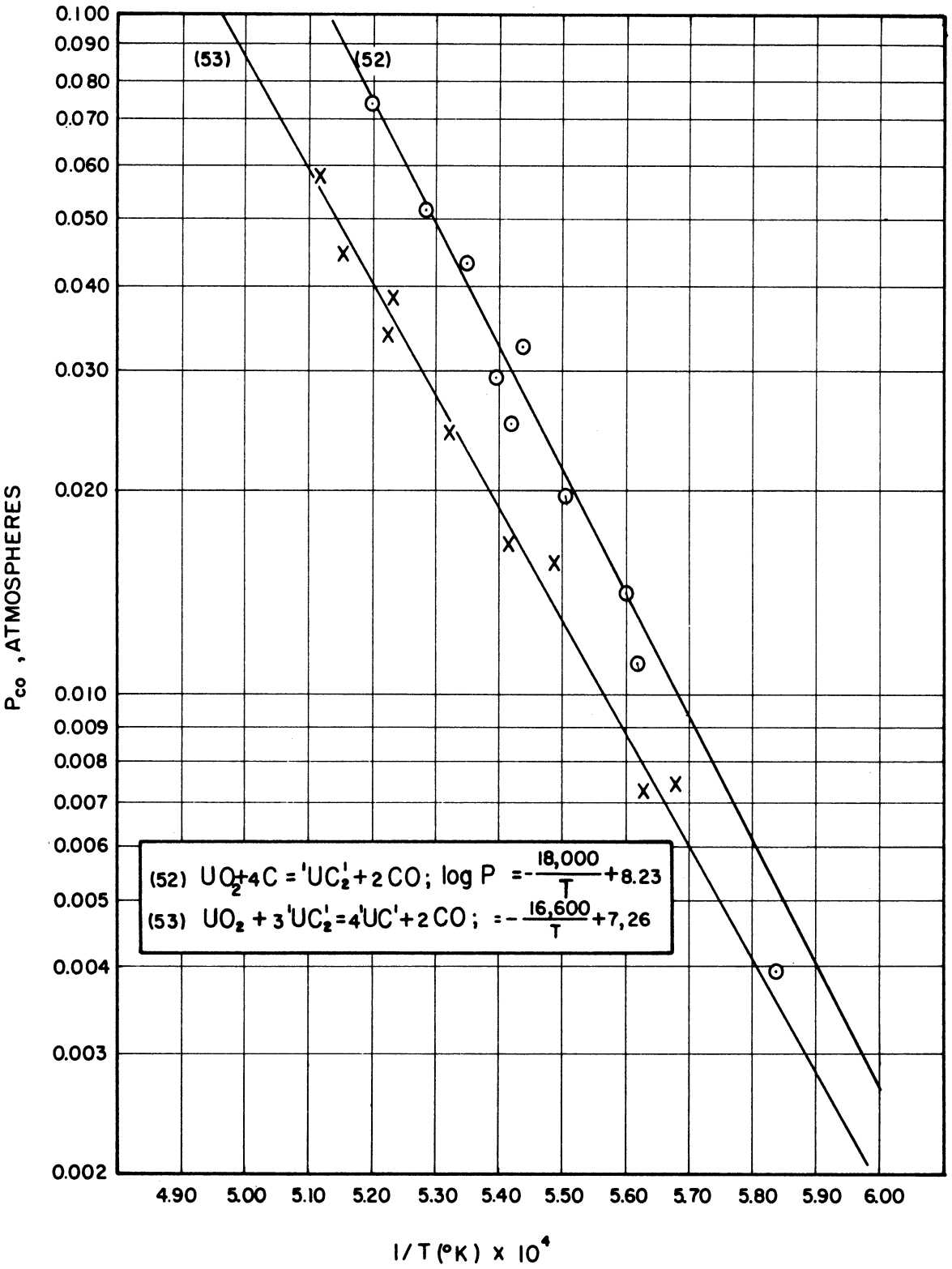

Figure 11. Common Logarithm of Carbon Monoxide Equilibrium Pressure Versus the Reciprocal of the Absolute Temperature for the Equilibria $UO_2 + 4C = 'UC_2' + 2CO$ and $UO_2 + 3'UC_2' = 4'UC' + 2CO$.

Provided that the scatter of the experimental data is random in nature, the best straight lines reporting the data would be those lines for which the sum of the weighted squares of the residuals is a minimum. These lines are determined using the method of least squares.

The results of run 62 plus observed pressure fluctuations in other runs above 1878°K, demonstrated that equilibrium was very closely approached during these runs. Consequently, the scatter of the data around the above 1878°K can be assumed to be random. Furthermore, if the deviations of data at the lower temperatures are systematic, due to the fact that the equilibrium pressures were not quite reached, then the assumption of randomness would lead to a more conservative assessment of the random error. Nearly equal numbers of each equilibria are approached in both directions at the lower temperatures so that very little systematic error would be incurred in the curve fitting operation. In view of these considerations the use of least squares analyses was considered appropriate and desirable.

The precisions of the temperature and the gas pressure measurements were assessed as $\pm$ 6°K and $\pm$ 1/2 millimeters of mercury respectively. These precisions corresponded to precisions of one to ten per cent in the measured pressure, depending on the pressure, and about a third of one per cent in the temperature measurement. Therefore, it was considered reasonable to assume that all of the random errors were made in the pressure measurements. This assumption enabled considerable simplification in the least squares analysis without incurring error in the curve fitting operation.

The question of weight factors was important in the analysis of the results of this study. As was mentioned previously, the precision in measured values of gas pressure was $\pm$ 1/2 millimeters of mercury throughout the range of pressures measured. However, since this precision in the carbon monoxide equilibrium pressure, p_{CO}, is invariant with pressure, the precision in log p_{CO} varies markedly with p_{CO}. This behavior must be taken into account by assigning appropriate weights to the values of log p_{CO}.

The general problem of determining proper weights for data of unequal precision is treated by Scarborough.[37] The criterion is shown by him to be that the weights be inversely proportional to the squares of the probable errors. Using this criterion and the law of propagation of error, the weight factor for the least squares analysis can be derived. A formula expressing the law of propagation of error is derived by Scarborough.[37] This formula is

$$R^2 = \sum^{i} \left(\frac{\partial Q}{\partial q_i}\right)^2 r_i^2 \qquad (63)$$

where Q is the function of the independent quantities, q_i denotes the ith independent quantity, and R and r_i are the probable errors of Q and q_i respectively. Using Equation (63) and the criterion for weights, it is easily shown that

$$w\ (\log p_i) = K\ p_i^2 \qquad (64)$$

where K is a constant of proportionality.

Using the criterion that the sum of the weighted squares of the residuals be a minimum, the weighted normal equations for the

parameters J and L were formulated in the manner of Scarborough.[37] The expression for the sum of the weighted squares of the residuals, V_i, is

$$\sum^{i} w_i V_i^2 = \sum^{i} K p_i^2 (J/T_i + L - \log p_i)^2 \quad . \tag{65}$$

On the basis of Equation (65), the following normal equations were derived:

$$(\sum^{i} p_i^2/T_i^2)\, J + (\sum^{i} p_i^2/T)\, L = \sum^{i} p_i^2 \log p_i/T_i \tag{66}$$

and

$$(\sum^{i} p_i^2/T_i)\, J + (\sum^{i} p_i^2)\, L = \sum^{i} p_i^2 \log p_i \quad . \tag{67}$$

An IBM 704 high speed digital computer was used to calculate the coefficients and solve the normal equations. The calculated coefficients for both equilibria are listed in Table XIII. The computer was also used to calculate the standard deviations of the parameters J and L for each set of equilibria and the standard deviation of computed values of log p_{CO} for various values of p_{CO}. The computer program was written in FORTRAN.

The values of standard deviation were calculated in an analogous fashion to a method presented by Beers.[35] First the standard deviation of log p about the line defined by J and L, $s_{\log p}$, was calculated using the formula

$$s^2_{\log p} = \frac{\sum^{i} (\overline{w_i})(J/T_i + L - \log p_i)^2}{k - 2} \tag{68}$$

where k is the number of sets of measurements (p_i, T_i) and $\overline{w}_i$ is a normalized weight of that measurement such that

$$\sum^{i} \bar{w}_i = \sum^{i} \bar{K}^{-1} p_i^{\,2} = k \quad . \tag{69}$$

Then the standard deviations of the slope and intercept, s_J and s_L, were calculated using an expression analogous to Equation (63) for the propagation of error. This expression is identical to that of Equation (63) except that probable error is replaced by standard deviation. For the standard deviation of the slope, s_J

$$s_J^{\,2} = \sum^{i} \left(\frac{\partial J}{\partial \log p_i}\right)^2 s^2_{\log p} \tag{70}$$

and for that of the intercept, s_L,

$$s_L^{\,2} = \sum^{i} \left(\frac{\partial L}{\partial \log p_i}\right)^2 s^2_{\log p} \quad . \tag{71}$$

By differentiating the normal equations with respect to $\log p_i$, simultaneous equations in $\frac{\partial J}{\partial \log p_i}$ and $\frac{\partial L}{\partial \log p_i}$ were obtained. These equations were solved to obtain the contributions of all k terms of the summations of Equations (70) and (71). Then the summations were carried out and the square root of the sums taken to obtain values of s_J and s_L. These values are listed in Table XIII.

A computed value of $(\log p)_o$ is found by substitution of the desired value of the independent variable $1/T_o$ into Equation (57) or Equation (58). The contribution to the standard deviation

TABLE XIII

VALUES AND STANDARD DEVIATIONS OF THE SLOPES AND INTERCEPTS OF THE LINEAR EXPRESSIONS FOR THE COMMON LOGARITHMS OF THE CO EQUILIBRIUM PRESSURES AS FUNCTIONS OF THE RECIPROCAL OF ABSOLUTE TEMPERATURE

Equilibria	Value and Standard Deviation, s_J, of the of the Slope J	Value and Standard Deviation, s_L, of the of the Slope L
(Eq. 52) UO + 4C = 'UC$_2$' + 2CO	- 17,977 ± 1,519	8,2256 ± 0.8156
(Eq. 53) UO + 3'UC$_2$' = 4'UC' + 2CO	- 16,634 ± 1,218	7.2624 ± 0.6440

in $(\log p)_o$ as a result of the deviation in one of the measured values is given by

$$\frac{\partial(\log p)_o}{\partial \log p_i}(\delta \log p_i) = \left(\frac{\partial L}{\partial \log p_i} + \frac{1}{T_o}\frac{\partial J}{\partial \log p_i}\right)\left(\frac{J}{T_i} + L - \log p_i\right) . \qquad (72)$$

TABLE XIV

STANDARD DEVIATIONS OF COMPUTED VALUES OF THE COMMON LOGARITHM OF THE CO EQUILIBRIUM PRESSURES

Equilibria	Run	Absolute Temperature T_o, degrees Kelvin	Standard Deviation $s_{(\log p)_o}$, of Computed Values of the Common Logarithm of the CO Equilibrium Pressure $(p_{CO})_o$	Corresponding Range of Carbon Monoxide Equilibrium Pressures in Millimeters of Mercury Absolute
$UO_2 + 4C = 'UC_2 + 2CO$	30	1714	± 0.0586	2.4 - 3.1
	42	1780	0.0379	
	41	1786	0.0361	10.0 - 11.7
	12	1817	0.0271	
	49	1845	0.0193	21.8 - 23.8
	39	1839	0.0209	
	11	1853	0.0171	
	62	1869	0.0130	29.8 - 31.6
	62	1869	0.0130	29.8 - 31.6
	61	1892	0.0078	39.1 - 40.6
	60	1922	0.0060	
$UO_2 + 3'UC_2' = 4'UC' + 2CO$	23	1761	0.0478	4.4 - 5.5
	45	1778	0.0425	
	29	1822	0.0295	9.6 - 10.9
	40	1847	0.0228	
	105	1878	0.0159	18.7 - 20.1
	44	1914	0.0121	
	34	1911	0.0121	
	57	1939	0.0139	35.2 - 37.7
	52	1953	0.0160	

The k contributions are squared and summed and then the square root taken to arrive at the value of s_o, the standard deviation of $(\log p)_o$.

Calculated values of s_o are listed in Table XIV. Selected values of s_o are indicated in the graphs of Figure 9.

After the activities of the solid phases involved in the equilibria investigated are assessed, analytical expressions for the standard Gibbs free energies, enthalpies, and entropies of reaction can be formulated. Finally, the equation for propagation of error can be used to evaluate the standard deviations of these quantities. These matters will be taken up in the next two sections of this analysis.

Estimation of Solid Phase Compositions and Activities

It was pointed out in the introduction that the compositions of the uranium dioxide, and the uranium carbide phases might be expected to deviate somewhat from their respective stoichiometric compositions. Furthermore, the possibility of appreciable oxygen substitution for carbon in the monocarbide phase was mentioned. It was considered that the compositions of these phases could be adequately appraised from lattice parameter measurements and binary solubility data, without resorting to chemical analysis. The lattice parameter data obtained in this study and previously determined binary solubility data will be utilized in this section to estimate the compositions and activities of the uranium dioxide, uranium monocarbide, and uranium dicarbide phases involved in the equilibria of Equations (52) and (53).

Values of the lattice parameter of uranium dioxides are listed in Table XV for comparison with the data of Table XI. Utilizing these data, the compositions and activities of the dioxide phases will be assessed.

TABLE XV

REPORTED VALUES FOR URANIUM DIOXIDE LATTICE PARAMETERS

Compound	Parameter, Å	Investigators
UO_2	5.4691 ± 0.0005	Rundle (7)
UO_2	5.4682	Swanson and Fuyat(42)
UO_2	5.468 ± 0.001	Hering and Perio (6)
$UO_{2.35}$	5.427 ± 0.001	Hering and Perio (6)

The values listed in Table XV are quite consistent with one another and with the value determined for the reagent grade dioxide used in this study, listed in Table XI. The two values of the dioxide lattice parameters reported by Hering and Perio represent the limits of values measured for a range of uranium to oxygen atom ratios. They found that the lattice parameter of this phase varies linearly with the uranium-oxygen atom ratio within the range studied. Utilizing this relationship, the lattice parameters measured for the dioxide phase of runs 7 and 45 correspond to a compound formula of $UO_{1.99}$ provided that a small linear extrapolation to oxygen-uranium ratios less than two is valid. The temperatures of runs 7 and 45 represent

extreme values of the range studied. Consequently, it is concluded that the composition of the dioxide phase is invariant at $UO_{1.99} \pm 0.01$ in the range studied. Moreover, the corresponding activity of the dioxide phases is essentially unity since $UO_{1.99}$ consists of 99.7 mole per cent UO_2.

Values reported for the lattice parameter of uranium monocarbide are listed in Table XVI. By comparing these values with the values measured for monocarbide phases involved in this study, reported in Table X, the compositions and activities of these phases will be assessed.

TABLE XVI

REPORTED VALUES FOR URANIUM MONOCARBIDE LATTICE PARAMETERS

Parameter, Å	Investigator
4.961 ± 0.001	Rundle (7)
4.9598 ± 0.0003	Austin and Gerds (14)
4.9605 ± 0.0004	Williams and Sambell (38)
4.9614 ± 0.0005	Wilson (43)

Three factors can affect the value of the lattice parameter of the monocarbide phase. First, solid solution formation with the mononitride lowers the lattice parameter as described earlier in this section. Second, solid solution formation with the monoxide lowers the lattice parameter as mentioned in the introduction. Third, evidence has been cited to indicate that the lattice parameter increases with the carbon content of the monocarbide phase.[41] All three of these

factors must be considered in attempting to evaluate composition of monocarbide phases from lattice parameter data.

The effects of the small amounts of nitrogen that were present in the equilibrium studies involving the monocarbide phase have already been assessed. It was concluded that the mononitride contents of the equilibrium monocarbide phases were less than five mole per cent.

The question of whether uranium monoxide solution in the monocarbide phase is significant in this work can be resolved by the results of the studies of the effect of nitrogen. The value of the lattice parameter of the monocarbide phase approaches the value for pure monocarbide as the nitrogen pressure approaches zero. This is apparent by comparing Figure 9 with the values listed in Table XVI.

The values in Table XVI have a range of only 0.0016 angstrom units. Furthermore, the value of the lattice parameter of the monocarbide phase of run 105 falls in the middle of this range. The lattice parameter of uranium monoxide has been estimated by Rundle to be 4.93 ± 0.01 angstrom units.[7] This estimate is consistent with experimental results of Vaughan, Melton, and Gerds.[8] Consequently, it is concluded that the monoxide content of the phase is of the order of three per cent or less because the presence of more than two per cent of the monoxide phase would be expected to lower the phase parameter by about 0.001 angstrom unit, assuming the lattice parameters of the monocarbide-monoxide solid solutions to be in accord with Vegard's law.

The results of Williams and co-workers[41] indicate that the lattice parameter of uranium monocarbide decreases with the carbon content of that phase from 4.9600 ± 0.0005 Å at 50.3 atomic per cent down to 4.9520 ± 0.0002 Å at some undetermined carbon content less than 50.3 atomic per cent. The experiments of these workers indicate that carbide rich alloys of uranium and uranium monocarbide formed by arc melting in a helium atmosphere contain a monocarbide phase deficient in carbon. Unfortunately, these workers did not determine the carbon content of the monocarbide phase, but merely the over-all carbon content of the alloys. Nevertheless, their results are useful in this analysis.

The monocarbide phases involved in these studies would be expected to be carbon rich because they are in equilibrium with uranium dicarbide. Consequently, these monocarbides would be expected to contain 50 atom per cent carbon or more. As mentioned in the introduction, the carbon solubility in uranium monocarbide increases with temperature so that the solubility limit at 2073°K is about 52 atomic per cent carbon. At 1873°K this solubility limit is less than 51 atomic per cent. Therefore, at temperatures below 1873, the lattice parameter of oxygen and nitrogen free monocarbide saturated with carbon would be expected to be about 4.960 angstrom units. Due to additional carbon solubility at temperatures above 1873°K, the lattice parameter of this saturated uranium monocarbide would be expected to be greater than 4.960. The value of 4.9616 angstroms reported in Table X for run 57 is indicative of increasing carbon solubility with temperature. However, the value of 4.9573 angstrom

units reported for run 50 would then be indicative of carbon replacement by nitrogen or oxygen.

In view of the fact that the nitrogen content of the gas phase for run 50 was relatively low, the low value of the lattice parameter cannot be attributed to the presence of nitrogen. However, it is possible that the low value was due to depletion of uranium dicarbide so that the phase was only in equilibrium with uranium dioxide and carbon monoxide. Thus the low value would have been due to the presence of oxygen. As a matter of fact, the amount of uranium dicarbide indicated by X-ray diffraction to have been present was quite small. In view of these considerations the carbon monoxide equilibrium pressure measured in run 50 was rejected.

Based on the foregoing considerations it is concluded that the activity of the monocarbide phases probably was reduced slightly below unity by one or more of the following causes: (1) carbon in excess of the stoichiometric amount, (2) uranium monoxide in solid solution, or (3) uranium mononitride in solid solution. It is considered that the activity was not reduced below 0.9 but could have been reduced to 0.95. Consequently, the activity of the monocarbide phases throughout the region investigated will be taken as 0.95 ± 0.05.

No lattice parameters were reported for the uranium dicarbide phase because data are not available to interpret such values. However, some assessment of the activity of this phase can be made. As was mentioned earlier, the solubility of nitrogen in the dicarbide phase is very small. However, this phase has a tendency to accommodate uranium in excess of stoichiometry as was mentioned in the introduction. In view of this consideration, the activity of the dicarbide phase was taken as 0.95 ± 0.05 throughout the region investigated. This procedure

does not reflect the increasing uranium accommodation with temperature, but this omission does not affect appreciably the calculated values of the thermodynamic functions reported in the next section.

Determination of Thermodynamic Functions

Analytical expressions for the common logarithms of the carbon monoxide equilibrium pressures as functions of temperature have been formulated, and the activities of the solid phases involved in the equilibria have been assessed. Therefore, analytical expressions for Gibbs free energies of reaction can readily be formulated for the chemical reactions of Equations (52) and (53).

Starting with the general expression for the standard Gibbs free energy of reaction, ΔG_T°,

$$\Delta G_T^\circ = - RT \ln K_T, \tag{32}$$

an expression of the form

$$\Delta G_T^\circ = - 9.15J - 4.574T(2L - 0.223) \tag{73}$$

was derived for both equilibria. In Equation (73), J and L are the slope and intercept of the appropriate straight line defining the relationship between the common logarithm of the carbon monoxide equilibrium pressure and the absolute temperature. The expression was described on the basis that the equilibrium constants for the equilibria of Equations (52) and (53), K_T^{52} and K_T^{53} could be expressed as follows:

$$K_T^{52} = p_{CO}^{\ 2} a_{UC_2} = 0.95 \, p_{CO}^{\ 2} \tag{74}$$

and

$$K_T^{53} = \frac{p_{CO}^2 \, a_{UC}^4}{a_{UC_2}^3} = 0.95 \, p_{CO}^2 \quad . \tag{75}$$

Thus expressions for the standard Gibbs free energies of reaction, $\Delta G_T^\circ(52)$ and $\Delta G_T^\circ(53)$, for the equilibria of Equations (52) and (53) respectively were found to be

$$\Delta G_T^\circ(52) = 164{,}500 - 74.23 \, T \tag{76}$$

and

$$\Delta G_T^\circ(53) = 152{,}200 - 65.42 \, T \quad . \tag{77}$$

In Equations (76) and (77), the free energy charge is that which occurs as a result of the reaction of one gram mole of uranium dioxide. In these expressions, the constant terms and the coefficient of the absolute temperature, T, represent the mean values of the standard enthalpies and entropies of reaction respectively, over the temperature range investigated.

Utilizing the expression for propagation of error

$$R^2 = \sum^{i} \left(\frac{\partial Q}{\partial q_i}\right)^2 r_i^2 \tag{63}$$

the standard deviations of values of ΔG_T° computed from Equations (76) and (77) can be calculated. This was done using

$$\Delta G_T^\circ = - RT \ln K_T \tag{32}$$

and the expressions of Equations (74) and (75) for the equilibrium constants. It was decided to express the uncertainty in the free energies as two standard deviations. Two standard deviations of the activity values were taken to be $\pm$ 0.05, which is the value predicted in previous sections as the maximum uncertainty in the activities. On this basis, values of two standard deviations in ΔG_T° were calculated at selected values of the absolute temperature for

both reactions investigated. These values are listed in Table XVII. The uncertainty in activity values corresponds to uncertainties in the free energies of reaction of about 200 and 1,000 calories in the expressions of Equations (76) and (77) respectively.

The expressions for the standard Gibbs free energy of reaction can be used to evaluate similar expressions for other reactions of interest. In combining various free energy expressions in the remainder of this section, the law of propagation of error (Equation 63) will be used to calculate the uncertainties of the resulting expressions. In those calculations, the uncertainties of the expressions of Equations (72) and (73) will be taken as $\pm$ 1,200 calories and $\pm$ 1,500 calories respectively. For the reactions

$$UO_2 + 3C \rightarrow UC + 2CO \qquad (78)$$

and

$$UC + C \rightarrow UC_2 \qquad (79)$$

the standard Gibbs free energies of reaction,

$\Delta G_T^\circ(78)$ and $\Delta G_T^\circ(79)$ were calculated as:

$$\Delta G_T^\circ(78) = 161,400 - 72.03\ T \pm 900 \text{ cal.} \qquad (80)$$

and

$$\Delta G_T^\circ(79) = 3,100 - 2.20\ T \pm 1,350 \text{ cal.} \qquad (81)$$

Utilizing expressions for the standard Gibbs free energies of formation of carbon monoxide and uranium dioxide, along with Equations (76) and (80), expressions can be determined for the free energies of formation

TABLE XVII

CALCULATED VALUES OF TWICE THE STANDARD DEVIATION OF THE GIBBS FREE ENERGY OF REACTION FOR THE REACTIONS $UC_2 + 4C \rightarrow UC_2 + 2CO$ AND $UO_2 + 3UC_2 \rightarrow 4UC + 2CO$ AT SELECTED VALUES OF THE ABSOLUTE TEMPERATURE

Temperature, °K	Gibbs Free Energy of Reaction	
	$UO_2 + 4C \rightarrow UC_2 + 2CO$	$UO_2 + 3UC_2 \rightarrow 4UC + 2CO$
1714	37,300 ± 1,800	
1786	31,900 ± 1,200	
1845	27,500 ± 700	
1869	25,800 ± 500	
1892	24,100 ± 300	
1761		37,000 ± 1,800
1822		33,000 ± 1,400
1878		29,300 ± 1,100
1939		25,400 ± 1,100

of uranium monocarbide and uranium dicarbide. For the reaction

$$2C + O_2 \rightarrow 2CO \qquad (82)$$

Kubaschewski and Evans[12] list the free energy of formation as

$$\Delta G^\circ_T(82) = -53,400 - 41.90T \pm 2,000 \text{ cal. } (298\text{-}2,500\,^\circ K) \qquad (83)$$

For the reaction

$$U(\alpha, \beta, \gamma, l) + O_2(g) = UO_2 \ (5) \qquad (84)$$

Coughlin[44] expresses the free energy of formation as

$$\Delta G^{\circ}_{T}(84) = -258{,}650 + 40.64T \pm 600 \text{ cal } (298\text{-}1{,}500^{\circ}K). \quad (85)$$

Since the expression of Equation (85) gives values of the free energy of formation of uranium dioxide within 600 calories of the experimentally determined values below 1500°K, it is considered sound to use the expression at temperatures up to 2000°K to give values accurate to 1,000 calories.

Utilizing Equations (76), (80), (83), and (85), expressions were calculated for the standard Gibbs free energies of formation of uranium monocarbide and uranium dicarbide. For the reactions

$$U(l) + C \rightarrow UC \quad (86)$$

and

$$U(l) + 2C \rightarrow UC_2 \quad (87)$$

the calculated free energies of formation are

$$\Delta G^{\circ}_{T}(86) = -43{,}850 + 10.51T \pm 2{,}400 \text{ cal} \quad (88)$$

and

$$\Delta G^{\circ}_{T}(87) = -40{,}750 + 8.31T \pm 2{,}400 \text{ cal.} \quad (89)$$

It will now be desirable to compare the expressions of Equations (88) and (89) with the expressions

$$\Delta G^{\circ}_{T}(86G) = -25{,}200 + 3.6T \ (1723\text{-}1823^{\circ}K) \quad (90)$$

and

$$\Delta G^{\circ}_{T}(87G) = -32{,}610 + 3.6T \ (2001\text{-}2071^{\circ}K) \quad (91)$$

recently reported by Grieveson[45]. Grieveson obtained Equation (91) by measuring the effusion of uranium vapor from a graphite Knudsen cell containing solid uranium dicarbide. He obtained Equation (90) by equilibr ting monocarbide-dicarbide mixtures with gold-uranium alloy beads, measuring the effusion of gold vapor from a graphite Knudsen cell, and integrating the Gibbs-Duhem equation to obtain the activity of solid uranium in equilibrium with the carbide mixture. Using these data, Equation (91), and the free energy change for melting of uranium, Equation (90) was obtained.

The linear expressions of Grieveson (Equations 90 and 91) have been plotted in Figure 12 along with the expressions formulated in this work (Equations 88 and 89). The agreement of the two expressions for the free energy of formation of uranium dicarbide is fairly good. However, the expressions for the free energy of formation of uranium monocarbide yield values that differ by over 5,000 calories between 1700 and 1900°K. It is noteworthy that Grieveson's results indicate that the free energy of reaction for

$$UC + C = UC_2 \qquad (79)$$

is -7,410 calories throughout the temperature range of 1700 to 1900°K. Based on this figure, it would be necessary to reduce the activity of the monocarbide to about 0.13 to equilibrate the monocarbide and graphite with uranium dicarbide. However, according to the expression for the free energy of the reaction written as Equation (81), the activity of the monocarbide in equilibrium with graphite and uranium dicarbide at 1875°K would be 0.76. This value is more in line with the results of

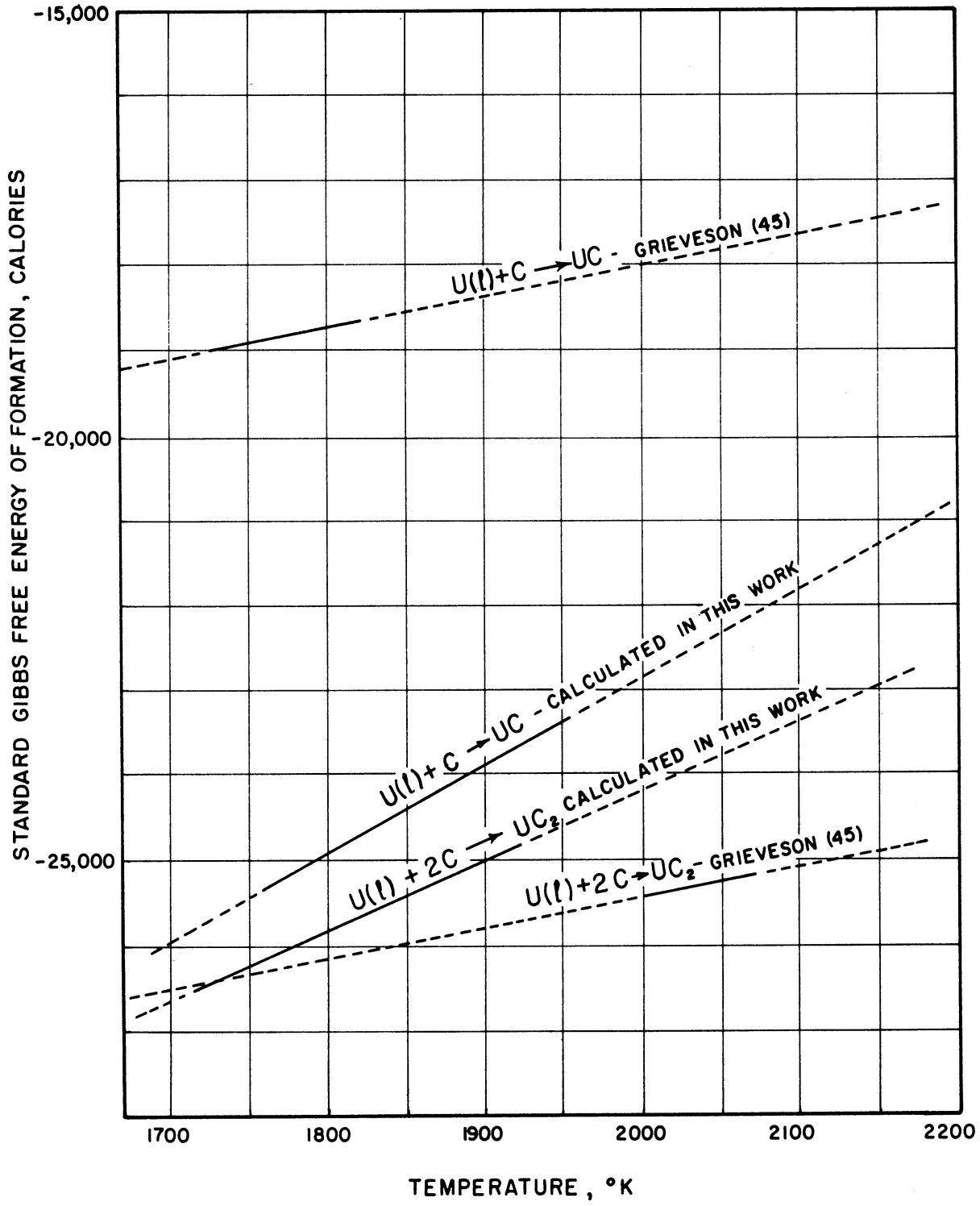

Figure 12. Standard Gibbs Free Energies of Formation of Uranium Monocarbide and Uranium Dicarbide as Functions of Temperature.

TABLE XVIII

SUMMARY OF CALCULATIONS MADE TO DETERMINE THE FREE ENERGY OF FORMATION OF URANIUM MONONITRIDE AT 1878° K

Run	a_{UC}	a_{UN}	p_{N_2} (atm)	$K_{1878}(92)$	$K_{1878}(93)$	$\Delta G°_{1878}(92)$	$\Delta G°_{1878}(93)$
101	0.65±0.05	0.35±0.05	0.0412±0.002	2.65±0.44		-3,635±619	
102	0.45±0.05	0.55±0.05	0.0831±0.002	2.84±0.41		-3,894±538	
103	0.67±0.05	0.33±0.05	0.0198±0.002	3.49±0.61		-4,663±652	
104	0.85±0.05	0.15±0.05	0.0041±0.001		3.08±1.16		-4197±1405

Run	$\Delta G°_{1878}$ for $U(\ell) + \frac{1}{2} N_2 \rightarrow UN$
101	-27,800 ± 2,500
102	-28,000 ± 2,500
103	-28,800 ± 2,500
104	-27,300 ± 4,400

NOTE: For $U(\ell) + C = UC$; $\Delta G_{1878} = -24,150 \pm 2,400$ cal.

For $U(\ell) + UC_2 \rightarrow 2UC$; $\Delta G_{1878} = -23,130 \pm 4,150$ cal.

runs 101 to 104, shown in Tables X and XVIII and Figure 9.

Finally, the data of Table X were used to evaluate the free energy of formation of uranium mononitride at 1878°K. This was accomplished by determining the free energy of reaction for

$$UC + \frac{1}{2} N_2 \rightarrow UN + C \qquad (92)$$

and

$$2UC + \frac{1}{2} N_2 \rightarrow UN + UC_2 \qquad (93)$$

utilizing the relations:

$$\Delta G^\circ_{1878}(92) = -RT \ln \left(\frac{a_{UN}}{a_{UC}\, p_{N_2}^{1/2}}\right) \qquad (94)$$

and

$$\Delta G^\circ_{1878}(93) = -RT \ln \left(\frac{a_{UN}\, a_{UC_2}}{a_{UC}^2\, p_{N_2}^{1/2}}\right) . \qquad (95)$$

In using Equations (94) and (95), the activity was taken to be the mole fraction. Estimated uncertainties in the various measured quantities were used in Equation (63) to calculate the propagation of error in the free energies of reaction. The value determined for the free energy of formation of the mononitride from nitrogen gas and liquid uranium at 1878°K was -28,200 $\pm$ 2,500 cal. The determination of this figure is summarized in Table XVIII. The final figure is the average of the values from runs 101, 102, and 103.

Analysis of Errors

Measures taken to eliminate systematic errors and to assess random errors have already been described. In this section, the order

of magnitude of uncorrected systematic errors will be estimated; and the size of the observed random errors will be compared with the expected precision of the measurements involved.

The precision that could have been attained in this study was limited by the precision with which pressure and temperature could be measured. These precisions were assessed earlier as $\pm$ 1/2 millimeter of mercury for the manometer and $\pm$ 6°K for the optical pyrometer. Examination of Figure 9 reveals that most of the measured coordinates lie within these values of the fitted curve. The discrepancies are attributed partly to slow reaction rates at temperatures below about 1850°K, and it is also believed that some of the temperature measurements have been as much as 10°K in error.

The calculated precision in the free energy values based on precisions of $\pm$ 1/2 millimeter of mercury and $\pm$ 6°K were about $\pm$ 720 calories at 1750°K and $\pm$ 120 calories at 1925°K, the increase in precision being due almost entirely to the increase in pressure between 1750 and 1925°K. The calculated standard deviation of the free energy values due to random errors in pressure only were calculated to be about 100 calories larger than these values. Consequently, it is concluded that the values of the standard deviations of the experimental data based on external consistency are in line with what would be expected from the precision of the measuring instruments employed. This conclusion is based in part on the fact that additional measurements were required to determine the carbon monoxide equilibrium pressure from the measured value of the total gas pressure and the analysis of the gas sample. However, the expected reduction of

precision due to these determinations is small as indicated in Appendix B.

The two major sources of systematic error in this work are errors in temperature measurement and errors in the estimated effect of thermal diffusion of hydrogen. The order of magnitude of the former has been estimated in the section of the Introduction on temperature measurement and in Appendix A. From the considerations made in this estimation, it is concluded that the effective emissivity of the hot source is at least 0.95. For this effective emissivity the observed temperature at 2000°K would be 8 1/2°K low.(47)

The only conclusion that can be reached with regard to thermal diffusion is that the order of magnitude of the systematic errors incurred in estimating it are small. Examination of Tables VIII and IX reveals that the correction for thermal diffusion is only one part in twenty if the hydrogen content in the gas phase is ten per cent. Assuming that the error in this correction is half the correction itself, the error would amount to one part in forty. Utilizing the relation

$$\Delta G^{\circ}_{T} = -RT \ln K_{T} \qquad (32)$$

the corresponding error in ΔG°_{T} is about $\pm$ 200 calories at 1900°K.

One item of internal inconsistency should be mentioned. This involves the values of carbon monoxide pressures reported in Table X for runs 101 to 104. Using Equations (58) and (80) and the measured activity values, the calculated values of carbon monoxide

equilibrium pressures for these equilibrations are 27 1/4, 32 3/4, 27 and 23 1/2 millimeters of mercury for runs 101, 102, 103 and 104 respectively. The two most likely reasons for these discrepancies seem to be that equilibrium was not reached or that the gas analyses were in error. The reactants were maintained at temperature for only about 20 minutes after the pressure stopped changing, and it is possible that this was insufficient time. The reason for suspecting the gas analysis is that the relative sensitivities for the carbon monoxide standard of the two peaks used to analyze carbon monoxide and nitrogen were inconsistent with previous observations. This was attributed to nitrogen, and the sensitivities were corrected on that basis. Had this correction not been made, the carbon monoxide pressures determined would have been higher.

The primary purpose of runs 101 to 104 was to assess the effect of nitrogen on the composition of the monocarbide phase, and the results of runs 101 to 104 are considered satisfactory for this purpose.

Interpretations of the Observed Phase Equilibria

In this section the compatibility of the observed phase equilibria with previous observations of the carbon-oxygen uranium system will be discussed. Also, the observed phase relations will be utilized to predict phase relations outside of the range of pressure, temperature and composition studied in this investigation.

The univariant equilibria observed in the carbon-oxygen-uranium system is analogous to that observed by Boericke[20] for the

carbon-oxygen-chromium system as described in the introduction beginning on page 27. These phase relations among the carbides and oxides of uranium are similar to those predicted in the Introduction on page 13 except for the fact that the presence of uranium sesquicarbide was not observed in this study.

Mallett, Gerds, and Vaughn[46] and Wilson[43] have reported that it is necessary to subject mixtures of uranium monocarbide and uranium dicarbide to stress to cause the sesquicarbide to form. No attempt was made in this study to stress the solid phases involved. Consequently, the equilibria

$$UO_2 + 3'UC_2' = 4'UC' + 2CO \qquad (53)$$

can be considered as quasi-stable even though it appears plausible that the equilibria

$$UO_2 + 7UC_2 = 4U_2C_3 + 2CO \qquad (11)$$

and

$$UO_2 + 3U_2C_3 = 7UC + 2CO \qquad (12)$$

may be stable univariant equilibria in the system carbon-oxygen-uranium.

The data of the common logarithm of the carbon monoxide equilibrium pressure versus the reciprocal of the absolute temperature for Equations (52) and (53) indicate the existence of an invariant equilibrium among the five phases involved in these equilibria. The temperature and pressure of this equilibrium predicted by extrapolating the linear relations in log p_{CO} and 1/T are 1445°K and 0.045 millimeters of mercury absolute. Associated with this invariant equilibrium are

five univariant equilibria among the five possible sets of four of the five phases: uranium dioxide, graphite, uranium dicarbide, uranium monocarbide, and carbon monoxide. Two possible arrangements of the curves of pressure versus temperature for these equilibria consistent with requirements of the Phase Rule are sketched in Figure 13.

From the observations made in this study, certain features of the carbon-nitrogen-oxygen-uranium phase diagram can be predicted. These features involve four phase equilibria among uranium dioxide, graphite, uranium dicarbide, solid solutions of uranium monocarbide and uranium mononitride and a gas phase of nitrogen and carbon monoxide. Since four components are involved, these four phase equilibria are divariant. The nature of these divariant equilibria is shown in Figure 14, which is a three dimensional graph qualitatively relating pressure, temperature and composition of the gas phase. The divariant equilibria appear as surfaces. These surfaces have a common intersection which is a space curve representing the univariant equilibria among the five phases in question. One of the termini of this curve is the invariant equilibrium among the five phases in the ternary system carbon-oxygen-uranium. This terminus lies on the face of the graph for which the per cent nitrogen in the gas phase is zero. This face is the p-T diagram for the carbon-oxygen-uranium system.

In order to verify the predictions that have been made and to quantitatively establish the related portions of the phase diagrams, it would, of course, be necessary to carry out equilibrations of the type executed in runs 101 to 105.

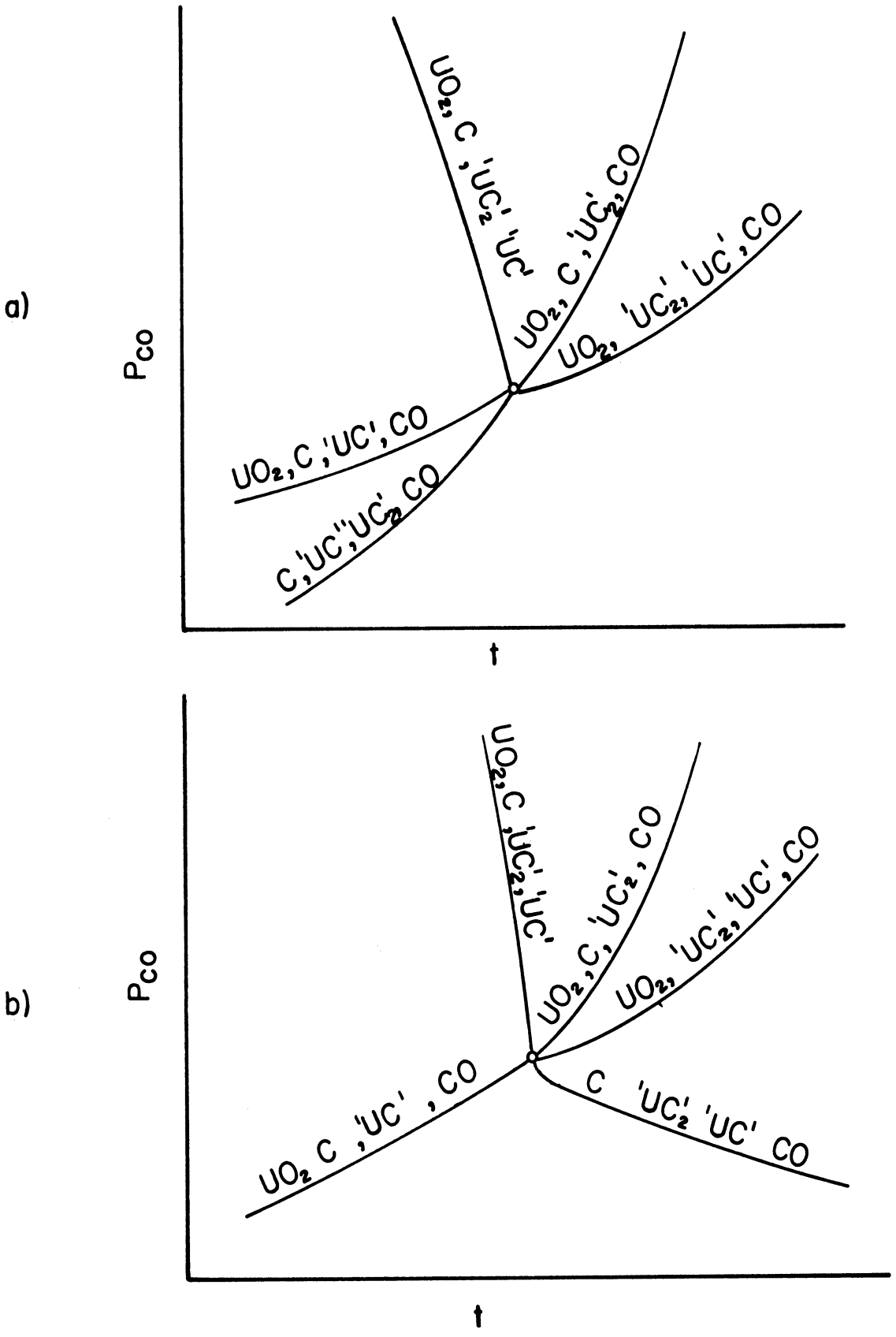

Figure 13. Two Possible Configurations of Curves of Equilibrium Pressure Versus Temperature for the Five Sets of Four Phase Equilibrium Among UO_2, 'C(gr)', 'UC_2', 'UC' and CO.

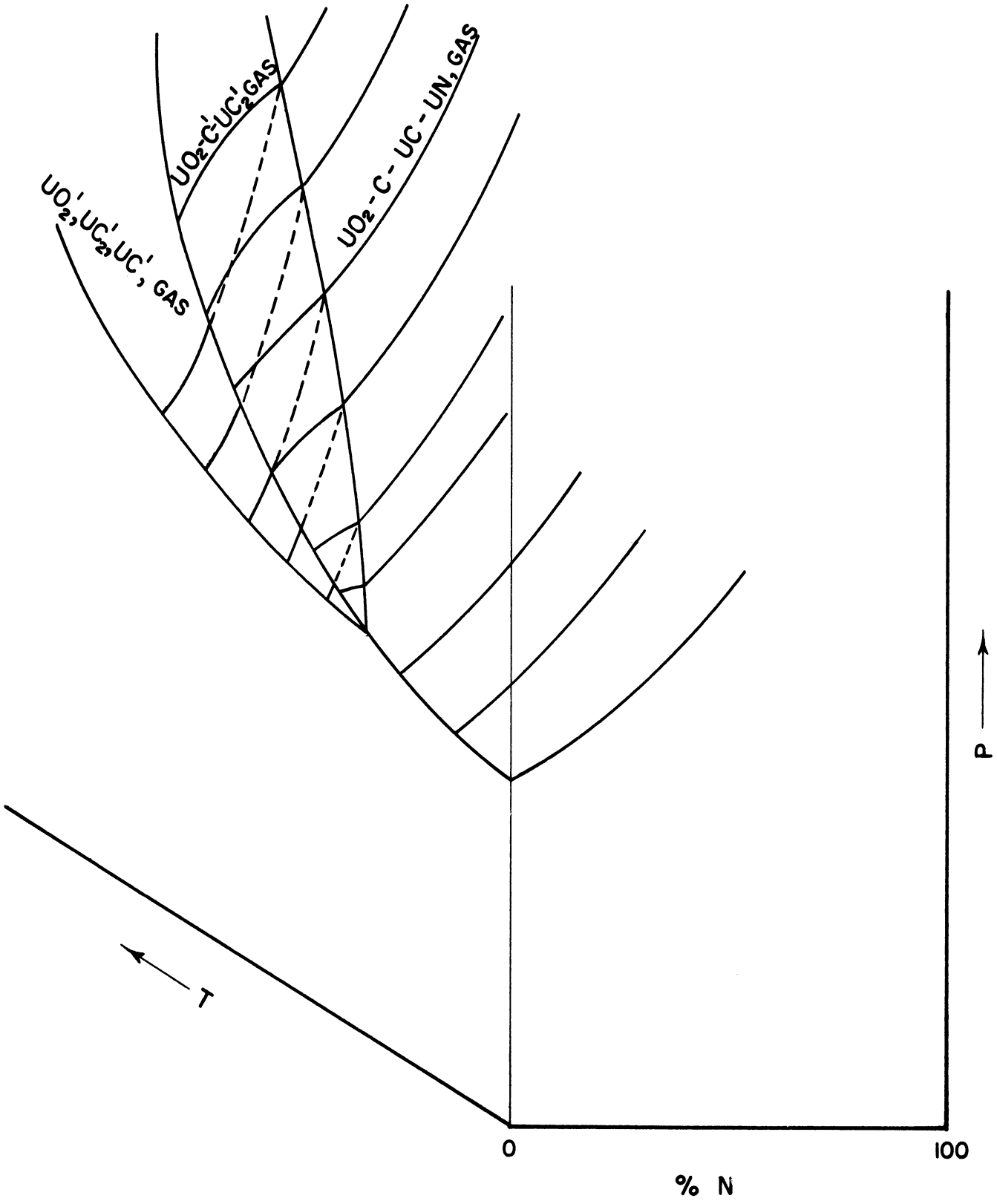

Figure 14. Composition of the Gas Phase Involved in Various Equilibria in the System Carbon-Nitrogen-Oxygen-Uranium as Functions of Temperature and Pressure.

The type of experimental system used in this work appears to be suitable for equilibrations involving nitrogen because demixing of nitrogen and carbon monoxide due to thermal diffusion should be rather slight. The mass of these two molecules is identical and the volume is nearly identical. However, it would be desirable to carry out experiments to measure the extent of thermal diffusion in the binary system carbon monoxide-nitrogen.

CONCLUSIONS

As results of the experimental work carried out for this thesis, phase equilibria in the carbon-oxygen-uranium system have been described and expressions for Gibbs free energies of reaction have been determined. In addition to these quantitative results, a number of conclusions can be drawn from the observations of the investigation. These conclusions are as follows:

1. Uranium monocarbide can be formed under vacuum in the solid state from a mixture containing three gram atoms of carbon per gram mole of uranium dioxide. The carbon monoxide pressure must be maintained below the equilibrium pressure for Equation (53), and appreciable rates of reactions can be attained by using finely divided and well-mixed powders and reacting at temperatures above 1850°K. If the charge is compacted at room temperature, the monocarbide formed will be sintered but porous. Crushing, recompacting, and reheating may be necessary to expedite the complete consumption of the reactants.

2. Uranium mononitride will coform with uranium monocarbide at temperatures between 1770 and 1970°K if nitrogen is present in the gas phase and the conditions for the formation of uranium monocarbide are satisfied. The mole fraction of uranium mononitride in the monocarbide-mononitride phase will depend on the nitrogen pressure, the carbon monoxide pressure and the absolute temperature.

3. Uranium dicarbide can be formed under vacuum in the solid state from a mixture containing four gram atoms of carbon per gram mole

of uranium dioxide. The carbon monoxide pressure must be maintained below the equilibrium pressure for Equation (52), and the nitrogen pressure must be maintained below a critical level, which was not determined in this investigation. Appreciable rates of reaction can be attained by using finely divided and well-mixed powders and reacting at temperatures above 1850°K.

4. A systematic investigation of carbide-oxide-nitride equilibria in the system carbon-nitrogen-oxygen-uranium would supplement the knowledge of the chemistry of nuclear fuels. Such an investigation could enable the determination of the free energy of formation of uranium mononitride as a function of temperature.

APPENDIX A

CALIBRATION OF THE OPTICAL PYROMETER

The subject of corrections to temperatures observed with the disappearing filament type optical pyrometer is taken up in this section. It was pointed out in the introduction that corrections to observed temperatures are of three types: namely, corrections for the effective emissivity of the radiating object being less than unity, corrections for absorption of light between the object and the pyrometer, and corrections to the temperature scale readings of the instrument. The determination of these corrections is described below.

Instrument Calibration

On completion of the experimental program the optical pyrometer was shipped to the High Temperature Measurements Laboratory of the National Bureau of Standards in Washington, D.C. At that laboratory, the pyrometer lamp filament current was measured as a function of the temperature of a perfect radiator (black body) . The temperature of the perfect radiator was measured with a high precision pyrometer of the laboratory. Pertinent portions of these calibration data are reproduced in Table A-I. The laboratory reported that the maximum uncertainties in the temperature values reported decrease from about $\pm$ 8 degrees at 1450°F to about $\pm$ 6 degrees at 1950°F and then increase to about $\pm$ 15 degrees at 5100°F.

The completion of the calibration consists in observing the temperature scale reading of the pyrometer as a function of the lamp current. This is accomplished with an ammeter in the lamp circuit by

adjusting the lamp current to the various desired values and then moving the potentiometer slide wire contact to balance the pyrometer galvanometer.

TABLE A-I

CORRESPONDING VALUES OF THE LAMP CURRENT AND TEMPERATURE WHEN SIGHTING ON A BLACK BODY FOR L. AND N. PYROMETER #1157073 WITH LAMP F-246

Current (ma., abs.)	Low Range Degrees F*	High Range Degrees F*
42.00	1816	2442
45.00	1893	2568
48.00	1967	2691
51.00	2038	2812
54.00	2106	2930
57.00	2173	3048

* In this table °F is defined as 9/5 x Degrees C (Int. 1948) + 32.

The arrangement of the various components of the electrical circuit of the pyrometer is shown in Figure A-1. The circuit consists of four flashlight batteries for providing filament current, a rheostat for adjusting the illumination, and a potentiometer slide wire with standard cell and galvanometer for accurately measuring lamp current and thus measuring black body temperature. The filament current is manually adjusted by rotating R_1 to obtain a brightness match between the filament and the source. The rheostat contact and the potentiometer contact, P, are connected through a frictional clutch so that when the

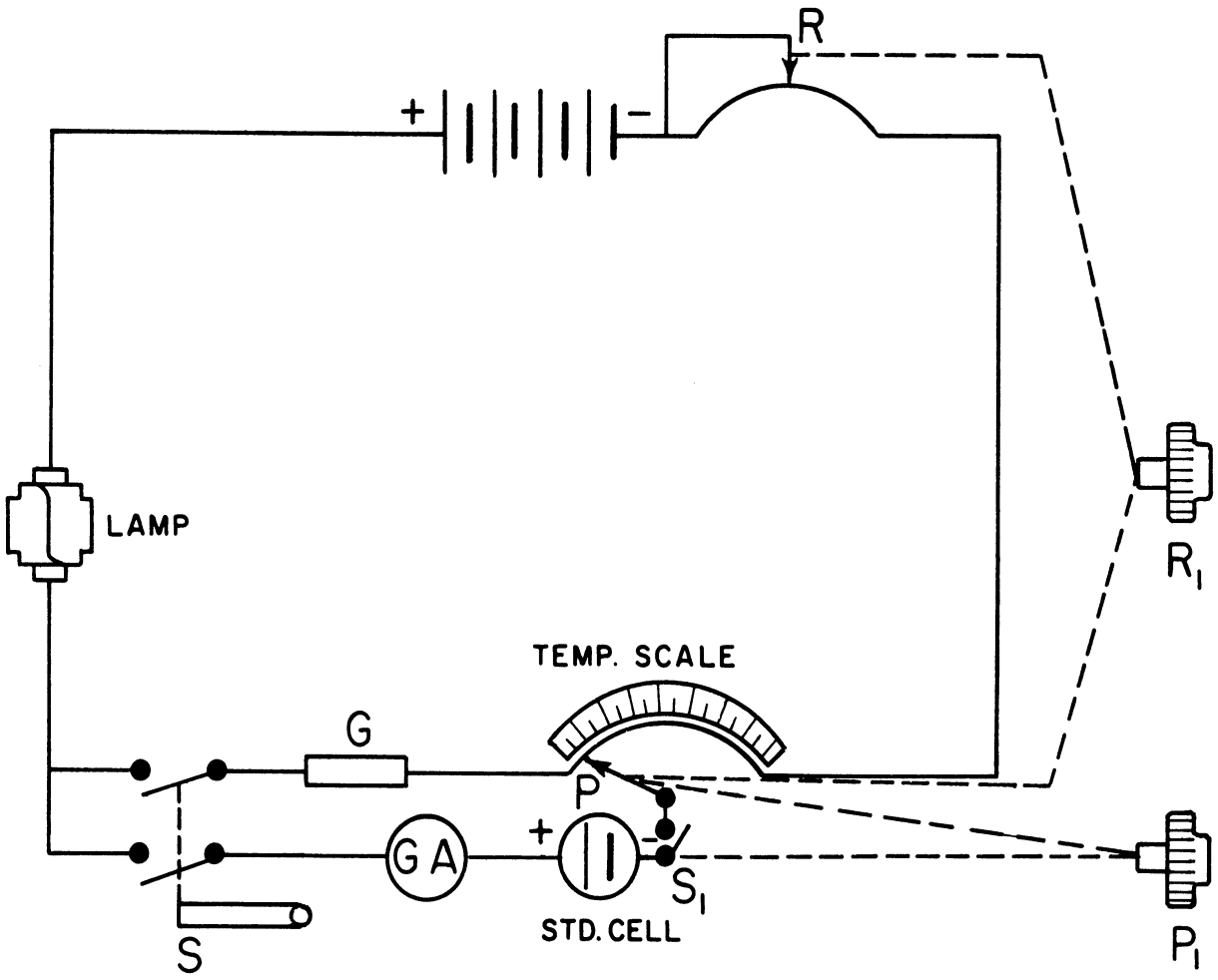

Figure A-1. Optical Pyrometer Circuit Diagram.

current is adjusted by moving R_1, the potentiometer contact is also moved to maintain an approximate balance. Consequently, when the standard cell circuit is closed by pressing the potentiometer knob, P_1, only a minor adjustment is needed to zero the galvanometer. Knob P_1 moves only the potentiometer contact P.

The calibration of the temperature scale was not carried out by the laboratory at the Bureau of Standards because they were not able to properly balance the potentiometer. They attributed this to malfunctioning of the galvanometer. However, on receipt of the pyrometer from Washington, the malfunctioning was found to be due to the fact that the rheostat slide wire was being turned by the potentiometer knob, P_1. Consequently, the galvanometer could be balanced at only one value of the lamp current. On close examination of the pyrometer it was found that the temperature scale drum bearing was frozen to the shaft of the rheostat knob, P_1, so that independent movement of the potentiometer drum could not be achieved. This was corrected by regreasing the bearing. This corrective action restored the pyrometer to working order.

The pyrometer was then compared with another pyrometer, with which it had been previously compared just before shipment to the Bureau of Standards for calibration. The results of these comparisons indicate that no significant change in the operation of the pyrometer took place between the time of the end of the experimentation and the time of receipt after calibration. The seizure of the drum bearing may have been due to temperature changes during shipment of the pyrometer; the pyrometer was sent to the Bureau of

Standards in January. At any rate, the malfunctioning definitely developed after shipment.

After repairing the pyrometer, its temperature scale was calibrated. For this purpose, a Weston milliammeter was inserted in the lamp circuit. This ammeter was borrowed from the Standards Laboratory of the Department of Electrical Engineering of the University of Michigan. A recent test indicated this instrument to be accurate to a quarter of a per cent of the full scale reading.

The scale calibration was effected by adjusting the lamp rheostat to obtain desired values of the lamp current, zeroing the galvanometer and reading the temperature scale. The results of the calibration are listed in Table A-II. Based on these results it was concluded that no correction should be applied to the low range temperatures and that a correction of + 10°F (+ 6°K) should be applied to the high range temperature measured in the experimental work of the thesis.

TABLE A-II

CORRESPONDING VALUES OF LAMP CURRENT, BLACK BODY TEMPERATURE, AND INDICATED TEMPERATURE FOR L. AND N. PYROMETER NO. 1157073 WITH LAMP F-246.

Current (m.a. abs.)	Low Range Degrees F		High Range Degrees F	
	True	Indicated	True	Indicated
42.0	1816	1816	2442	2433
45.0	1893	1892	2568	2558
48.0	1967	1966	2691	2681
51	2038	2038	2812	2803
54	2106	2105	2930	2918
57	2173	2175	3048	3042

Absorption Corrections

The media between the crucible and the pyrometer consisted of the gaseous atmosphere of the reaction vessel, the sight glass, the totally reflecting prism, and the air in the room.

The gaseous atmosphere was shown to absorb a negligible amount of light by observing the melting point of copper under conditions approximating the two gas pressure extremes of the experimental studies. There was no difference in the melting points observed under these two conditions. The procedure for the melting point determination is described in the next section.

The correction for absorption by the sight glass and prism was determined by utilizing a tungsten ribbon filament lamp in series with a rheostat across a low voltage power supply. The corrections to various observed temperatures were determined by first measuring the filament temperature by sighting directly upon it and then interposing the prism and sight glass and measuring the temperature again. In this way the difference in observed temperatures due to the presence of the glass was determined. The data obtained were plotted as the corrections to observed temperature as a function of temperature. This graph is shown as Figure A-2.

Corrections for Effective Emissivity of the Crucible Interior

In the introduction it was contended that the effective emissivity of the sample tablet enclosed in the graphite crucible would be higher than 0.95. In order to test the reasoning on which this contention was based the freezing point of copper was measured, with the copper contained in the graphite crucible.

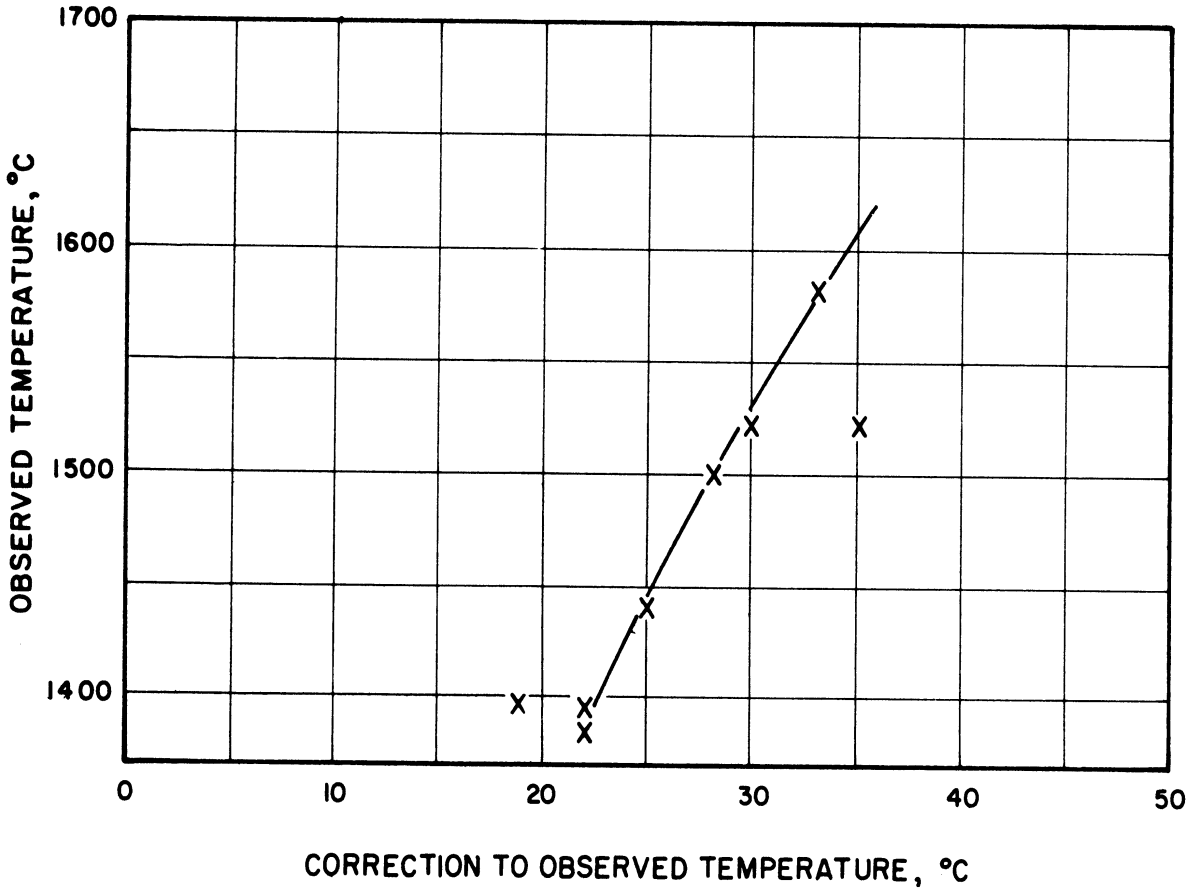

Figure A-2. Observed Temperature Versus Correction to Observed Temperature for Absorption by the Vessel Sight Glass and the Total Reflecting Prism.

In the first type of determination made, about 25 grams of copper was placed in the crucible and heated, with the system at a pressure of two or three millimeters of mercury, to a temperature above the melting point. Then the power input was reduced and the temperature of the metal surface was measured at intervals of 30 or 60 seconds as the metal cooled. The data of temperature versus time are plotted as Figure A-3. The horizontal portion of this graph represents the period during which the copper was freezing and thus evolving latent heat. After applying the corrections for absorption and instrument error to the observed temperature the freezing point was found to be 1343°K. (The correction to the observed temperature for absorption was determined to be + 18 $\pm$ 3°K using the method described in the previous section.)

This experiment was repeated with carbon monoxide in the system at a partial pressure of about 60 millimeters of mercury, and the same apparent freezing point was observed. This established that the absorption of light by carbon monoxide in the system was negligible as mentioned earlier.

The freezing point determined in the method described was 13°K below the secondary standard freezing point of copper of 1356°K.[47] This discrepancy was attributed to the facts that the 0.65 micron spectral emissivity of copper is only 0.15[47] and the crucible walls were about 30°K below the temperature of the freezing copper. The calculated error using 0.15 as the spectral emissivity of liquid copper and assuming the walls to be 30°K below the freezing metal was 19°K. The calculation was made by using the Planck radiation law and the

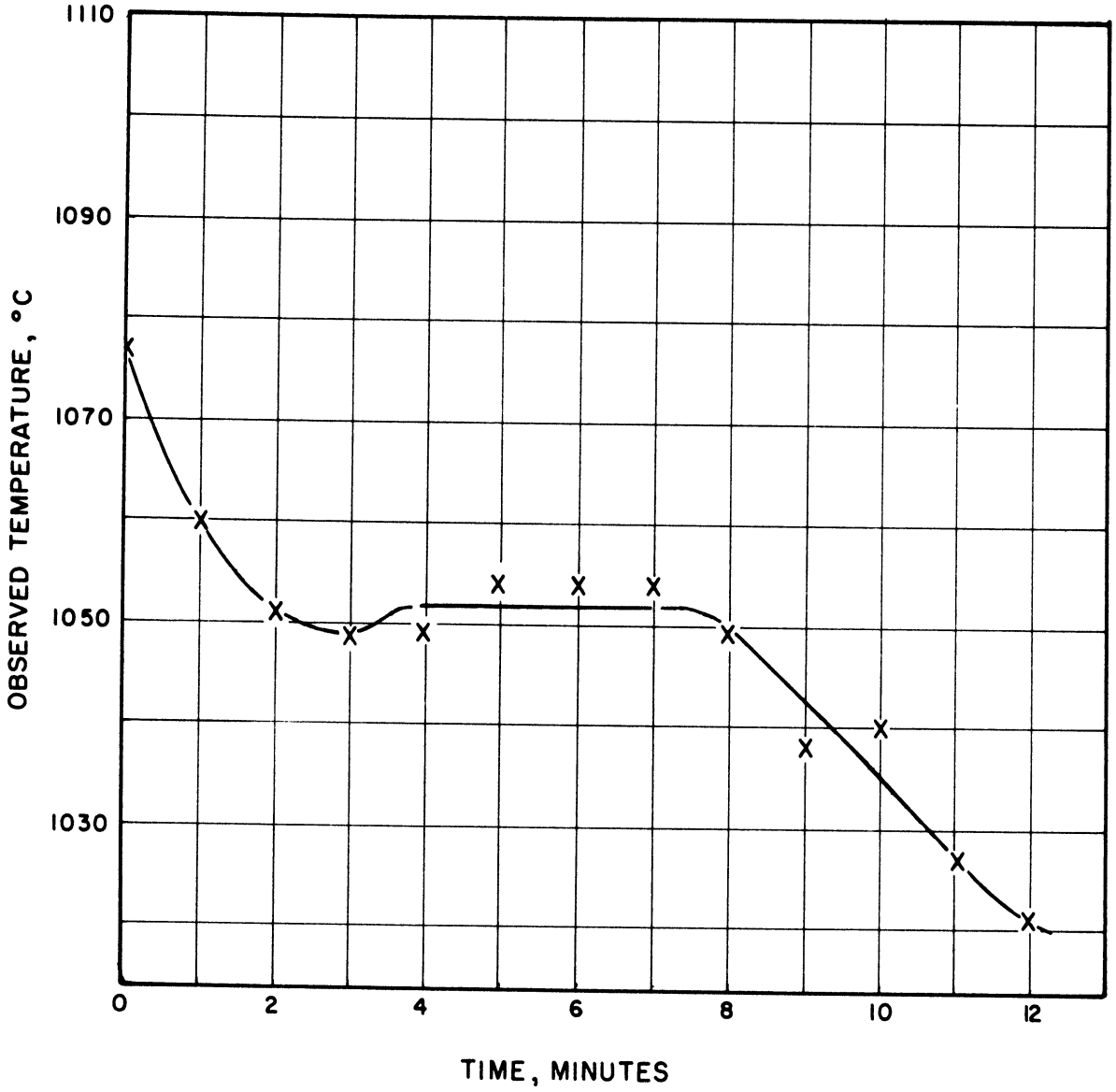

Figure A-3. Observed Temperature Versus Time for Freezing Copper Contained in Graphite Crucible Using L. and N. Optical Pyrometer No. 1157073.

formula for effective emissivity developed on page 39. It was not feasible to reduce the rate of heat abstraction from the copper below the value corresponding to the 30°K temperature difference observed to exist between the crucible walls and the freezing copper.

In order to eliminate most of the errors cited above, the experiment was repeated using a thin graphite cap, which floated atop the molten copper. The cap was fashioned in the shape of a concavo-convex diverging lens so that the concave surface of the cap conformed to the convex upper surface of the copper. The copper did not wet the graphite container, and the stirring action of the electromagnetic field is believed to have accentuated the curvature of the upper surface of the copper. The thickness of the cap was about 1/32 inch.

The data of temperature versus time for the modified copper freezing point determination is shown as Figure A-4. After correcting the observed temperature, the freezing point was determined to be 1353°K.

The system with freezing copper in the graphite crucible does not constitute a source of radiation that is completely identical to the sample tables in the crucible as shown in Figure 4 on page 38. This is true for three reasons: First, the emissivity of the graphite cap is not the same as that of a typical sample tablet, which is somewhat lower than that of the graphite. Second, the fact that the crucible was about one-fourth full of molten copper would tend to contribute to temperature uniformity. Third, the crucible walls were at a lower temperature than the surface sighted upon because heat was flowing out of the freezing copper. However, the difference caused by reason three would tend to offset those due to the first two, and all three differences are

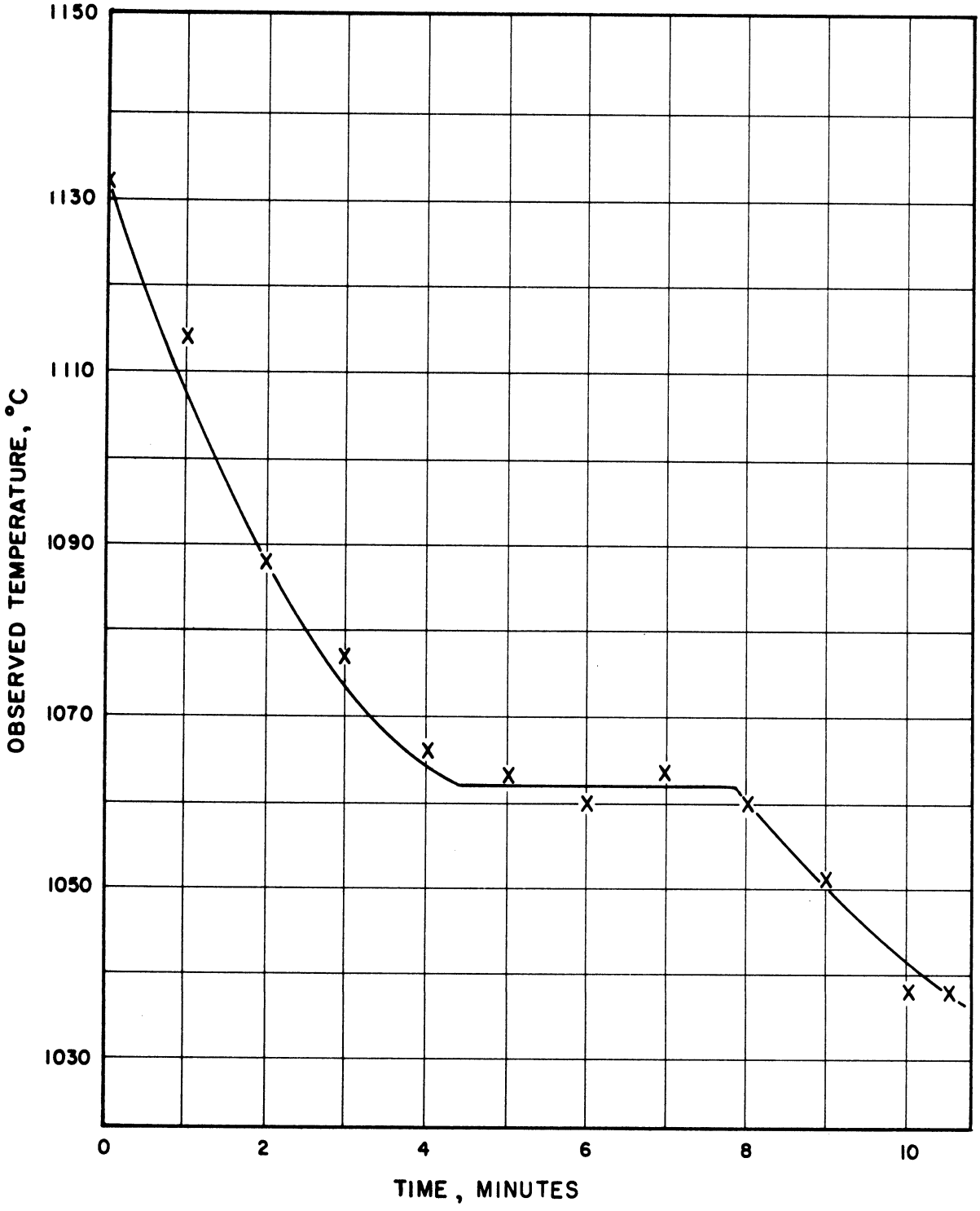

Figure A-4. Observed Temperature Versus Time for Graphite Cap on Freezing Copper in the Graphite Crucible Using L. and N. Pyrometer No. 1157073.

considered small. Consequently, from these considerations and the results of the experiments with freezing copper, it is concluded that the effective emmissivity of the crucible is of the order of 0.98. According to a graph of correction to observed temperatures versus the observed temperature with the 0.65 micron spectral emissivity as a parameter[47], the error incurred in assuming unit emissivity would be 2 or 3°K.

APPENDIX B

ANALYSIS OF GAS SAMPLES

Analyses of gas samples were made using a Consolidated Engineering Corporation Analytical Mass Spectrometer, Model 21-103B. In this instrument, a portion of the gas sample being analyzed is first transferred to a bulb, and the size of the portion is adjusted so that the bulb pressure is of the order of 15 microns. A voltage of about 70 volts is used to ionize the molecules in the bulb. The ions are then accelerated in an electric field into a magnetic field. In the magnetic field the molecules are deflected to follow a circular path, the radius of which is dependent on the mass to charge ratios of the ions. Finally the ions strike a collector, depositing a charge which is amplified and recorded on a photographic chart. The peak height in the chart for a given mass to charge ratio is directly proportional to the abundance of ions having that ratio of mass to charge.

In order to relate peak height and pressure for a given gas, a standard is used. Sensitivity values are determined for any desired mass to charge ratio in the cracking pattern of that gas. The sensitivity is the ratio of peak height to gas pressure. Sensitivity values for all gases involved can then be used to determine the partial pressures of these gases. In this determination the fact that the contribution of a gas to a given peak is proportional to the partial pressure of that gas is utilized.

The gases present in significant amounts in the samples of this investigation were observed to be hydrogen, carbon monoxide, nitrogen, oxygen, argon, and carbon dioxide. For mixtures comprised only of these gases, the analytical procedure is simple because the major peaks for all but carbon monoxide and nitrogen are unique peaks. A unique peak is one that is due solely to the presence of one particular gas. For such cases the partial pressure can be calculated using

$$p_G = \frac{h}{S_G} \qquad \text{(B-1)}$$

Here h is the unique peak height and S_G and p_G are the sensitivity and partial pressure of the gas respectively.

The carbon monoxide and nitrogen contents were determined by solving the simultaneous equations

$$S^{14}_{CO}p_{CO} + S^{14}_{N_2}p_{N_2} = h_{14} \quad , \qquad \text{(B-2)}$$

and

$$S^{28}_{CO}p_{CO} + S^{28}_{N_2}p_{N_2} = h_{28} \quad . \qquad \text{(B-3)}$$

In these equations h_{14} and h_{28} are the peak heights for mass to charge ratios of 14 and 28 respectively, S^i_j represents the sensitivity of gas j for a mass to charge ratio of i, and p_{CO} and p_{N_2} are the partial pressures of carbon monoxide and nitrogen respectively.

A set of six to nine samples was analyzed on the same day, and standard samples were used to determine sensitivities for each gas present. A table of typical values of sensitivities for all peaks involved is shown in Table B-I.

TABLE B-I

TYPICAL SENSITIVITY VALUES FOR GASES DETECTED IN SAMPLES TAKEN FOR DETERMINATION OF CARBON MONOXIDE EQUILIBRIUM PRESSURES

Gas	Mass to Charge Ratio	Sensitivity, Scale Units/ Micron
H_2	2	95
N_2	14	30
CO	14	1.4
N_2	28	200
CO	28	210
O_2	32	175
A	40	250
CO_2	44	225

In a few cases it was necessary to correct gas analyses for small air leaks that occurred between the time of sampling and the time of analysis. These corrections were made whenever the height of the oxygen peak was unusually great. The excessive portion of this height was attributed to leakage, and the nitrogen leakage was taken as four times that for oxygen.

One test was made to evaluate the reproducibility of results determined with the spectrometer. This was done by simultaneously taking two samples of a gas phase. The results of this test is shown in Table B-II.

TABLE B-II

RESULTS OF ANALYSES OF TWO GAS SAMPLES
TAKEN SIMULTANEOUSLY DURING RUN 55

	Sample One	Sample Two
% CO	69.53	70.37
% N_2	14.48	14.86
% H_2	12.37	10.98
% O_2	3.00	3.16
% A	0.19	0.20
% CO_2	0.43	0.43

Some further idea of the reproducibility of the results of the gas analyses can be obtained by examining the gas analyses for the two equilibrations of run 62. These data are shown in Table VIII; the second sample was taken one hour and forty-five minutes after the first. Just after the first sample had been taken, carbon monoxide was added to cause the equilibrium of Equation (52) to be approached by the consumption of carbon monoxide and uranium dicarbide.

APPENDIX C

CORRECTIONS FOR THERMAL DIFFUSION OF HYDROGEN

Thermal diffusion may be defined as the generation of a concentration or activity gradient in a phase due to a temperature gradient. The theory of thermal diffusion in gases is treated by Jost[48] and by Chapman and Cowling[49] and will not be systematically developed in this appendix.

The Nature of Thermal Diffusion Effects in the Experimental System

The degree of concentration difference at steady state in a gas mixture at non-uniform temperature depends on the temperature extremes and the constituents of the mixture. The larger the temperature differences, the larger will be the separation in a given gas mixture. Also, the greater the difference in size and mass of the gaseous molecules, the greater will be the separation.

The gases involved in this study were hydrogen, nitrogen, carbon monoxide, oxygen, argon, and carbon dioxide. The nitrogen and oxygen molecules are quite similar to that of carbon monoxide, and these gases were considered to undergo a negligible amount of separation. Although carbon dioxide and argon have somewhat heavier molecules, the level of concentration of these gases was so small that the error incurred in neglecting their thermal diffusion is insignificant. Consequently, the only significant concentration difference between the cold and hot regions of the gas space in the experimental system would be due to the thermal diffusion of hydrogen. The hydrogen molecules, being the lightest and smallest in

the system, would tend to concentrate in the hot region of the system.

Derivation of the Correction Formula

In deriving the correction formula for computing the hydrogen concentration in the hot zone from the hydrogen concentration in the cold zone, several assumptions were made. While these assumptions are not completely rigorous, they should be adequately valid because the size of the thermal diffusion correction is of the order of five per cent or less of the total measured pressure.

It was first assumed that the gas mixtures could be treated as binary mixtures of hydrogen and carbon monoxide. In nearly every case, these gases comprised over 99 per cent of the gas phase.

Ibbs and Underwood measured demixing of carbon monoxide and hydrogen in a thermal gradient.(50) They found that for mixtures containing less than 25 per cent hydrogen, the separation was directly proportional to the mole fraction of hydrogen in the mixture. However, their work was limited to a hot zone temperature of 373°K. Consequently, a relation between separation and temperature is needed.

The early work in experimental investigations of thermal diffusion was carried out at temperatures of 373°K and below. It was found that separation was proportional to $\log_{10}(T_h/T_c)$ where T_h and T_c are the absolute temperatures of the hot and cold zone respectively. Chapman and Cowling have concluded that this proportionality is generally valid except at low temperatures near the liquification point of one of the gases involved.(49)

In deriving the correction equation, the data of Ibbs and Underwood[50] were utilized, and the separation was assumed to be proportional to $\log_{10}(T_h/T_c)$. The correction equation obtained on this basis was

$$\Delta N_{H_2} = 0.416 \log_{10} (T_h/T_c)(N_{H_2})_{av.} \qquad (C\text{-}1)$$

where N is the mole fraction and $(N_{H_2})_{av.}$ is the mean hydrogen concentration in the system.

In using the correction equation it was further assumed that the mean gas composition in the system was the arithmetic mean of the compositions at the two extreme temperatures. Then the correction could be computed using Equation (C-1) and a simple method of successive approximations. In this method, ΔN_{H_2} was assumed, the corresponding value of $(N_{H_2})_{av.}$ was used to calculate the value of ΔN_{H_2}, and the calculated value compared to the assumed value. This process was repeated until the calculated and assumed values of ΔN_{H_2} became identical.

The calculated value of 100 ΔN_{H_2} was subtracted from the per cent of carbon monoxide in the sample to obtain the percentage of carbon monoxide in the gas phase in the hot region.

APPENDIX D

PRECISION LATTICE PARAMETER DETERMINATIONS

The general problem of precision lattice parameter determination can be resolved into sample preparation, X-ray diffraction techniques, and analysis of results. These subjects will be taken up as they apply to the determination of the lattice parameters of uranium monocarbide and uranium dioxide phases involved in the experimental work.

X-ray Powder Photography

Two types of X-ray cameras was utilized in this work. These were a 114.6 millimeter diameter Debye-Scherrer camera and a 120 millimeter diameter symmetrical back reflection focusing camera. Since the samples were polycrystalline, the choice of techniques was limited to those involving these cameras and the wide angle goniometer used for phase identification. The use of the goniometer was considered to be inferior because of the need for using reference substances to correct for misalignment and the other systematic errors involved.

The choice of the type of radiation to be utilized depends on the technique employed to determine the lattice parameter. The various procedures that can be employed in precision lattice parameter determination of cubic and non-cubic phases are thoroughly treated by Klug and Alexander[51]. The bases for all these techniques is that the precision in the sine of the diffraction angle, θ, increases with the value of θ and that systematic errors in measured values of θ approach zero as θ

approaches ninety degrees. These systematic errors include errors due to film shinkage, displacement of the sample from its proper position, and absorption of X-rays by the sample. The nature of these errors depends on the technique used; this is discussed by Klug and Alexander[51] with respect to the more commonly used methods for precision lattice parameter determination.

All techniques employed utilize diffraction occurring at large values of θ in order to maximize precision. The various techniques can be classified into two types: those that seek to minimize systematic errors and those that seek to correct for systematic errors.

The practice of minimizing systematic errors has been developed to a high degree of perfection by Straumanis. In his method, asymmetric film mounting is employed to eliminate errors due to inaccurate knowledge of the camera radius and to uniform film shrinkage. A very thin sample and the largest possible values of θ are employed to minimize absorption and other errors. An intricate technique is employed to properly position the samples, and a very precise comparator is used to make film measurements. The Straumanis method is discussed in detail by Klug and Alexander[51]. It was not considered feasible in this work because it requires rather intricate techniques and precision equipment that was not available.

The types of methods in which the systematic errors are corrected involve mathematical techniques and the use of a reference substance. The use of mathematical extrapolation techniques is considered superior because no dilution of the sample is required and the method is readily adaptable

to use of high speed computers. The details of the extrapolation techniques employed in this work is described in the section on analysis of X-ray photographs.

With regard to the mathematical extrapolation techniques, the choice of radiation should be made to maximize the number of lines in the high back reflection region (θ greater than 60°) and to obtain lines at very high values of θ (θ greater than 75°). The relative merits of the various types of radiation available were assessed for each phase by using approximate values of the lattice parameter to calculate values of θ for diffraction from the various planes of each phase involved. On this basis, cobalt and copper radiation were selected for the dioxide and monocarbide phases respectively.

In using the Debye-Scherrer camera, the sample was mounted in the camera and carefully centered utilizing a focusing lens and centering devices built into the camera. Then the camera was aligned with respect to the X-ray beam, loaded with film, and the film exposed. Asymmetric film mounting was employed, and the exposure times used were two to four hours. In some cases aluminum foil was used to selectively filter background radiation. The sample was slowly rotated about its axis by means of a small motor and belt drive system. The temperature near the camera was measured at selected times during the exposure.

The symmetrical back reflection focusing camera was aligned, loaded, and exposed in a manner similar to that described for the Debye-Scherrer camera. The sample was oscillated through a very small angle during exposure by means of a small motor and cam system.

Sample Preparation

All samples were crushed to very fine powder by grinding in an agate mortar. Grinding was carried out under trichloroethylene in order to avoid spontaneous ignition of the powder. The samples for the Debye-Scherrer camera were loaded into thin glass capillary tubes of 0.3 millimeter diameter. A standard hollow brass sample holder contained the sample in the capillary tube. The sample was installed by packing clay into both ends of the holder, piercing the clay with a fine wire, inserting the capillary tube, breaking it off at the desired length, and then carefully packing the clay to hold the sample in place.

Powder for exposure in the back reflection focusing camera was mixed with a small amount of vacuum grease to form a paste. This paste was then applied into a specially made sample holder. The holder was made by cementing together two pieces of exposed and developed X-ray film. One of these pieces had a rectangular hole cut from it to accommodate the sample. While the cement set, the sample holder was maintained in a curved position by wiring it to a piece of cylindrical pipe having nearly the same diameter as that of the camera. The sample holder was held in the camera by means of four small screws.

Analysis of X-ray Photographs

After assigning Miller indices to the diffraction lines on the film, the value of the diffraction angle, θ, corresponding to the various diffracting planes was measured directly by means of a film comparator. This comparator utilized a millimeter scale with a vernier device so that film distances could be measured with an ultimate precision of

$\pm$ 0.025 millimeters. This precision corresponded to $\pm$ 0.0125 degrees in θ for the films exposed in the Debye-Scherrer cameras and about $\pm$ 0.005 degrees in films exposed in the symmetrical back reflection focusing camera.

The basis for the mathematical extrapolation techniques is that functions of θ can be found with which the systematic errors in θ vary linearly. This enables linear extrapolation of calculated values of the lattice parameter, a_o, to the value of the function corresponding to θ equal to 90°, where the systematic error is zero. Such a function, applicable for both the Debye-Scherrer and the symmetrical back reflection focusing camera, is the function, $\phi \tan \phi$, where ϕ is the complement of the diffraction angle, θ. This function varies linearly with the lattice parameter for values of ϕ less than 30° according to Klug and Alexander.[51]

A computer program was written in SAP to calculate the co-ordinates ($\phi \tan \phi$, a_o) corresponding to each measured value of film distance, to determine the best straight line through the experimental points by the method of least squares, and to calculate the standard deviation of the points from the line. In this manner, systematic errors in θ were minimized, and assessment of the random errors was made. A flow sheet for the program is shown in Figure D-1. Except for input and output instructions, the flow sheet shows all the necessary instructions in the FORTRAN language. The input data to the program consists of the number, N, of measured values of film diameters, N values each of the measured film diameters, D(I), the N corresponding

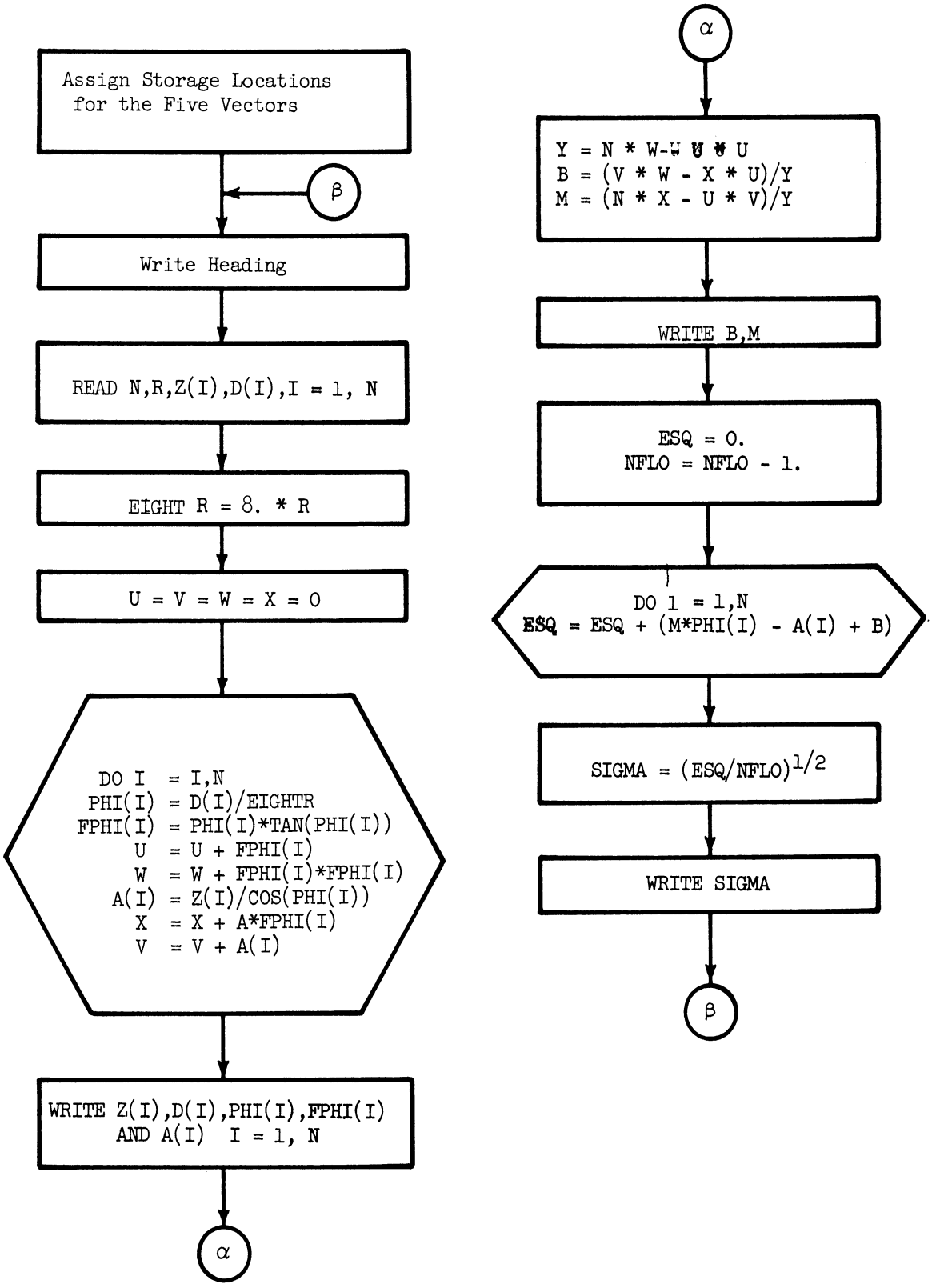

Figure D-1. Flowsheet for Determination of the Lattice Parameter of a Cubic Phase Utilizing Extrapolation Against PHItanPHI.

values of the function, Z(I), and the value of the camera radius, R. The function Z(I) is related to the wave length, λ, of the characteristic radiation employed and the Miller indices of the diffracting planes $(hkl)_I$ by

$$Z(I) = \frac{\lambda\sqrt{h_I^2 + k_I^2 + l_I^2}}{2} \quad . \tag{D-1}$$

Values of Z(I) were taken from tables prepared by the North American Philips Company[52], after indexing the lines.

The N values of $\phi(I)$ are calculated using

$$\phi(I) = \frac{D(I)}{8R} \tag{D-2}$$

This formula is applicable only to the symmetrical back reflection camera. However, for the Debye-Scherrer camera,

$$\phi(I) = \frac{D(I)}{4R} \tag{D-3}$$

so that the program can be used to process data obtained with a Debye-Scherrer camera by introducing half the value of the Debye-Scherrer camera radius as R. Input values of camera radii for the Debye-Scherrer camera were corrected for film shrinkage and inaccurate knowledge of the camera radius by utilizing asymmetric film mounting.

The N values of the lattice parameter, A(I), are calculated using

$$A(I) = \frac{Z(I)}{\cos \phi(I)} \tag{D-4}$$

This formula is nothing more than the rearranged Bragg equation

$$\lambda = 2\, d_{(hkl)_I} \sin \theta(I) \tag{D-5}$$

with the substitution

$$d_{(hkl)_I} = \frac{A(I)}{\sqrt{h_I^2 + k_I^2 + l_I^2}} \qquad \text{(D-6)}$$

where $d_{(hkl)_I}$ is the interplanar spacing of planes with the Miller indices $(hkl)_I$.

The slope, M, and intercept, B, of the best straight line through the experimental points ($\phi(I)$TAN $\phi(I)$, A(I)) is determined by solving the simultaneous normal equations

$$\Sigma A(I) = BN + M \Sigma \phi(I)\text{TAN } \phi(I) \qquad \text{(D-7)}$$

and $$\Sigma A(I)\phi(I)\text{TAN } \phi(I) = B \Sigma \phi(I)\text{TAN } \phi(I) + M \Sigma(\phi(I)\text{TAN } \phi(I)^2 \; . \qquad \text{(D-8)}$$

Finally the standard deviation of the experimentally determined values of the lattice parameter A(I) is determined using

$$\sigma = \left(\frac{\Sigma (M\phi(I)\text{TAN } \phi(I) + B - A(I))^2}{N-1}\right)^{1/2} \; . \qquad \text{(D-9)}$$

No weight factor was used in the least squares analyses even though the precision in the sine of θ increases with θ. Instead lines which were very clear and for which θ was in excess of 70° were measured two or more times depending on line quality and position.

As examples of the results obtained, Figures D-2 and D-3 are plotted to show the lattice parameter determinations for the reagent grade uranium dioxide and the monocarbide phase from run 105 respectively. The measured and calculated data for these determinations are summarized in Tables D-1 and D-II respectively.

In order to assess the consistency of lattice parameters determined using both types of cameras, the lattice parameter of the reagent

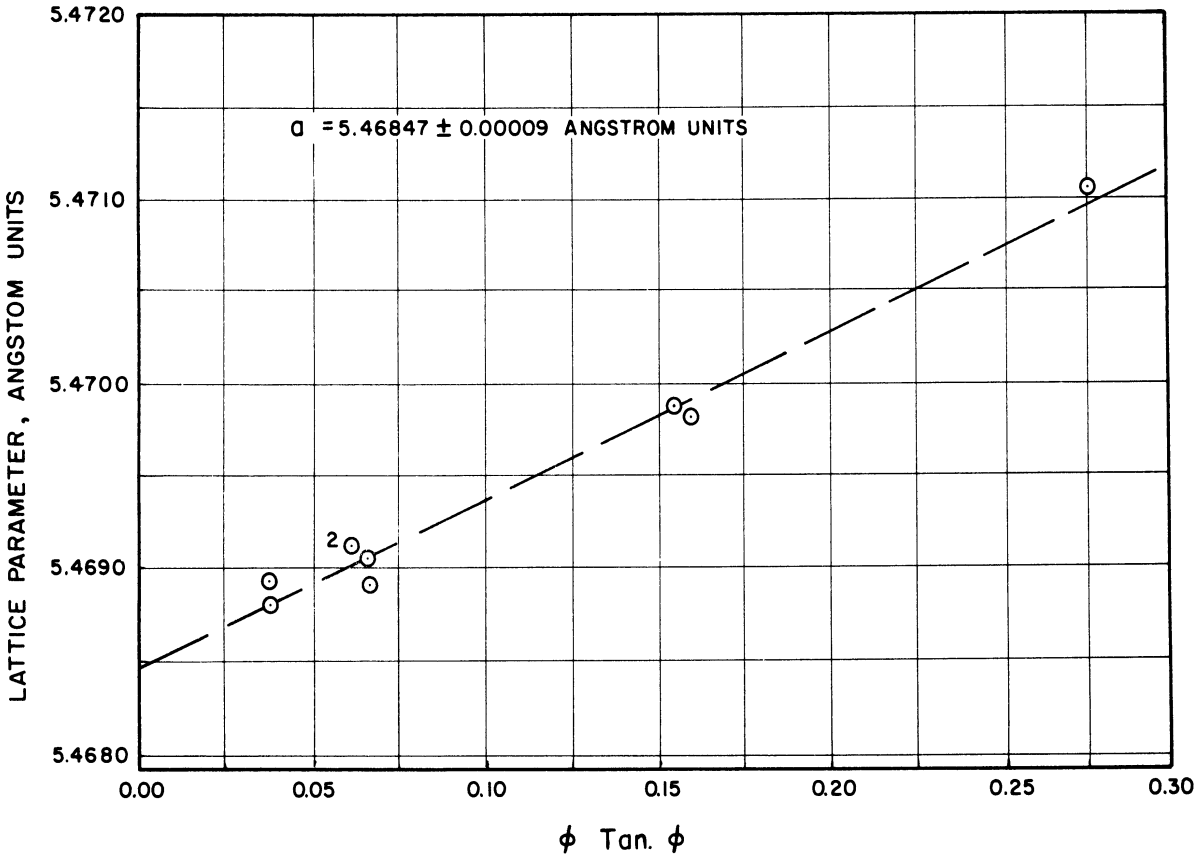

Figure D-2. Determination of the Lattice Parameter of Reagent Grade Uranium Dioxide by Extrapolation Against PHItanPHI, with the Exposure Made in the Symmetrical Back Reflection Focusing Camera.

TABLE D-I

SUMMARY OF MEASURED AND CALCULATED DATA FOR THE DETERMINATION OF THE LATTICE PARAMETER OF REAGENT GRADE URANIUM DIOXIDE BY EXTRAPOLATION AGAINST ϕ tan ϕ

Target: Co Camera: Focusing Radius (R): 6.01 cm Number of Lines (N): 9 Temperature: 24 $\pm$ 3° C

I	$(hkl)_I$	Spectrum	Z(l)	D(I)	ϕ(I)	ϕ(I) tan ϕ(I)	Δ(I)
1	600	K_{α_1}	5.36670	9.305 cm	0.19353	0.03793	5.46880
2	600	K_{α_1}	5.36670	9.310	0.19364	0.03797	5.46891
3	531	K_{α_2}	5.30315	11.875	0.24698	0.06227	5.46911
4	531	K_{α_2}	5.30315	11.875	0.24698	0.06227	5.46911
5	531	K_{α_1}	5.29164	12.275	0.25530	0.06663	5.46891
6	531	K_{α_1}	5.29164	12.280	0.25541	0.06669	5.46905
7	440	K_{α_2}	5.07078	18.480	0.38436	0.15546	5.46987
8	440	K_{α_1}	5.05977	18.735	0.38966	0.16002	5.46980
9	531	K_{β}	4.79418	24.170	0.50270	0.27640	5.47104

Intercept (B) : 5.46847 Angstrom units

Slope (M) : 0.00905 Angstrom units

Standard Deviation: $\pm$ 0.00009 Angstrom units.

a_o = 5.4685 $\pm$ 0.0001 Angstrom units.

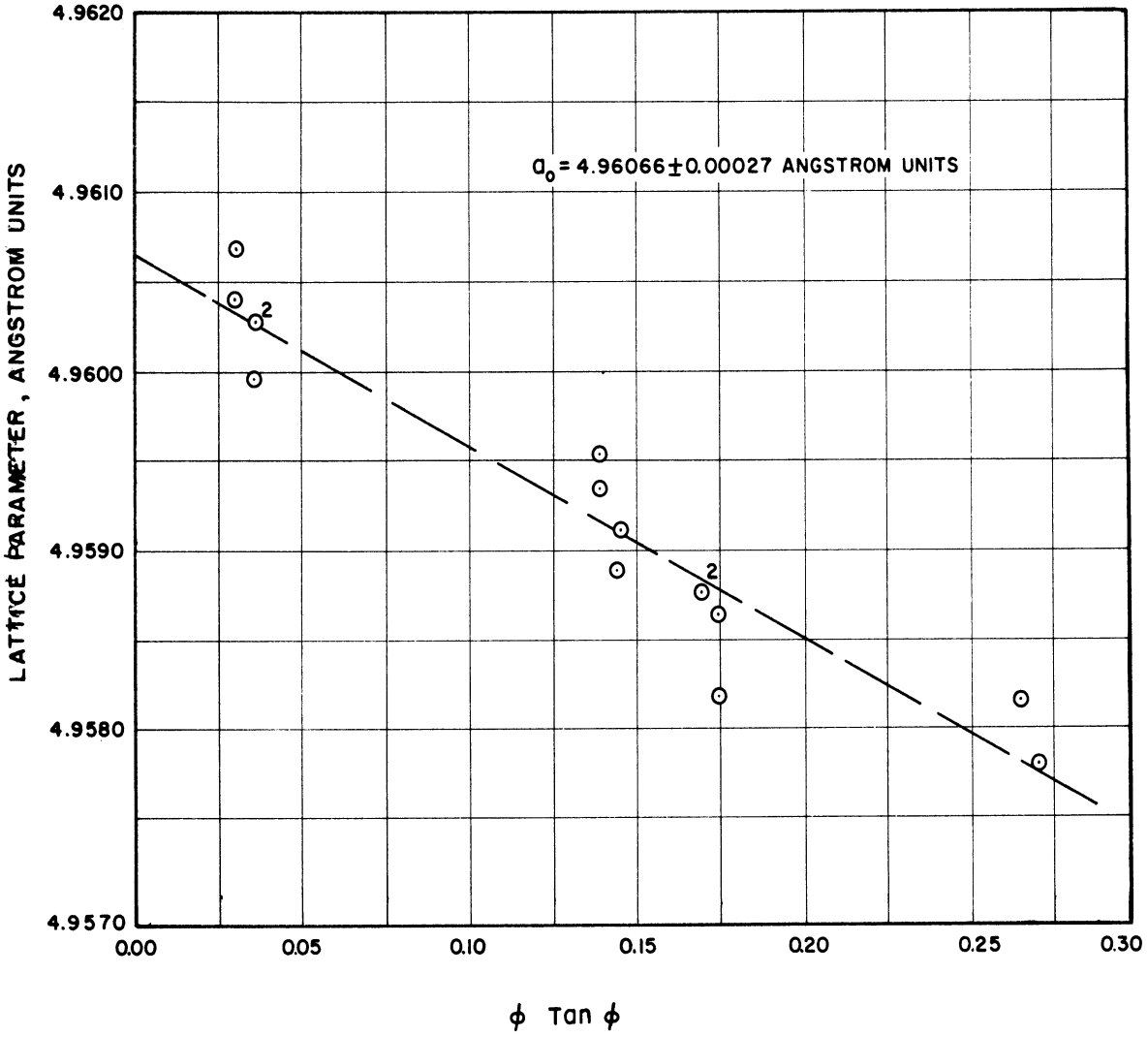

Figure D-3. Determination of the Lattice Parameter of the Uranium Monocarbide Phase of Run 105 by Extrapolation Against PHItanPHI With the Exposure Made in a Debye-Scherrer Camera.

TABLE D-II

SUMMARY OF MEASURED AND CALCULATED DATA FOR THE DETERMINATION OF THE LATTICE PARAMETER OF THE URANIUM MONOCARBIDE PHASE OF RUN 105 BY EXTRAPOLATION AGAINST $\phi \tan \phi$

Target: Cu Camera: Debye-Scherrer Radius (R). 2.860 Number of Lines (N): 15 Temperature: 25 ± 3°C

I	$(hkl)_I$	Spectrum	Z(I)	D(I)	$\phi(I)$	$\phi(I) \tan \phi(I)$	$\Delta(I)$
1	620	K_{α_2}	4.88363	4.03000	0.17616	0.03136	4.96040
2	620	K_{α_2}	4.88363	4.03750	0.17649	0.03148	4.96069
3	620	K_{α_1}	4.87149	4.32750	0.18917	0.03622	4.95997
4	620	K_{α_1}	4.87149	4.33500	0.18949	0.03634	4.96028
5	620	K_{α_1}	4.87149	4.33500	0.18949	0.03634	4.96028
6	600,442	K_{α_2}	4.63302	8.34500	0.36478	0.13930	4.95933
7	600,442	K_{α_2}	4.63302	8.34750	0.36489	0.13939	4.95954
8	600,442	K_{α_1}	4.62150	8.48750	0.37101	0.14433	4.95889
9	600,442	K_{α_1}	4.62150	8.49000	0.37112	0.14442	4.95910
10	531	K_{α_2}	4.56822	9.14000	0.39953	0.16870	4.95875
11	531	K_{α_2}	4.56822	9.14000	0.39953	0.16870	4.95875
12	531	K_{α_1}	4.55686	9.26750	0.40510	0.17372	4.95817
13	531	K_{α_1}	4.55686	9.27250	0.40532	0.17392	4.95863
14	440	K_{α_2}	4.36805	11.29500	0.49286	0.26470	4.95815
15	440	K_{α_1}	4.35719	11.37750	0.49734	0.26998	4.95780

Intercept (B) : 4.96066 Angstrom units.

Slope (M) : -0.01081 Angstrom units.

Standard Deviation: ± 0.00027 Angstrom units.

a_o = 4.9607 ± 0.0003 Angstrom units.

grade uranium dioxide was determined using the Debye-Scherrer camera. Also, the lattice parameter of semiconductor grade silicon was determined using both cameras. These results are presented in Table D-III along with the result obtained for the lattice parameter of the reagent grade uranium dioxide using the symmetrical back reflection focusing camera.

TABLE D-III

COMPARISON OF LATTICE PARAMETER VALUES OBTAINED USING THE DEBYE-SCHERRER AND SYMMETRICAL BACK REFLECTION FOCUSING CAMERAS

Phase	Lattice Parameter, Angstrom Units	
	Debye Camera	Focusing Camera
UO_2 (reagent grade)	5.4693 ± 0.0002	5.4685 ± 0.0001
Si (semiconductor grade)	5.4308 ± 0.0003	5.4304 ± 0.0003

Inspection of Table D-III reveals that parameters determined using the Debye-Scherrer camera are on the order of 0.0005 angstrom units higher than those measured using the focusing camera. While this difference is of interest from the standpoint of parameter determination, it is not sufficiently large to have precluded use of either camera in this study.

In order to assess the accuracy of the cameras, the measured parameters were compared with values reported for silicon of very high purity. These values are listed in Table D-IV. Some of the values listed in Table D-IV were computed for 26°C by Swanson and Fuyat[41] from the reported values. For the computation, a value of the linear

expansion coefficient of 4.15×10^{-6} determined by Straumanis and Aka[56] was used. Temperatures shown in parentheses are the actual temperatures at which the corresponding measurements were made.

TABLE D-IV

VALUES REPORTED FOR THE LATTICE PARAMETERS OF HIGH PURITY SILICON

Year	Investigators	Lattice Parameter	Method
1935	Jette and Foote (53)	5.43077 at 26°C(25°C)	Extrapolation against ϕ tan ϕ.
1935	Straumanis and Ievins (54)	5.4298	Method of Straumanis
1952	Straumanis and Aka (55)	5.43097 at 26°C(25°C)	Method of Straumanis
1953	Swanson and Fuyat (42)	5.4301 at 26°C	Goniometer with Tungsten as Internal Standard

Unless some basis were to exist for preferring either the higher two or the lower two values listed in Table D-VI, it cannot be said which of these is more accurate. No such basis is believed to exist, and the values determined for silicon listed in Table D-III fall in between those listed in Table D-IV.

APPENDIX E

SUMMARY OF EXPERIMENTAL RUNS

TABLE E-I

CONDENSED ACCOUNT OF DESIGNATED RUNS
MADE DURING THE EQUILIBRIUM STUDIES

Run	Temperature	Objective	Results
1	1905°K	to outgas vessel	Some outgassing accomplished.
2	1993°K	to outgas vessel	Rate of gas evolution reduced.
3	1855°K	$UO_2 + 3C \rightarrow UC + 2CO$	CO was evolved but temperature read was that of the crucible lid.
4	1862°K	$UO_2 + 3C \rightleftarrows UC + 2CO$	CO was evolved and then consumed. No gas sample was taken.
5	1844°K	$UO_2 + 3C \rightarrow UC + 2CO$	An equilibrium was reached. No gas sample was taken.
6	1900°K	$UO_2 + 3C \rightarrow UC + 2CO$	Diffractometer trace of solid phases indicated appreciable UC_2 with UC.
7	1940°K	$UO_2 + 4C \rightarrow UC_2 + 2CO$	Reaction as written. Data not used because insufficient time allowed for equilibration.
8	1888°K	$UO_2 + 4C \rightarrow UC_2 + 2CO$	Same as 7.
9	1793°K	$UO_2 + 3C \rightarrow UC + 2CO$	Unsuccessful. All UO_2 consumed. Both UC and UC_2 present in residue. (Final pressure was 4mm Hg).
10	1872°K	$UO_2 + 4C \rightarrow UC_2 + 2CO$	Unsuccessful. Excessive gas evolution attributed to leakage at vessel lid.
11	1853°K	$UO_2 + 4C \rightarrow UC_2 + 2CO$	Successful - See Table VIII.
12	1817°K	$UO_2 + 4C \rightarrow UC_2 + 2CO$	Successful - See Table VIII.
13	1741°K	$UO_2 + 3C \rightarrow UC + 2CO$	Unsuccessful - UO_2, C, UC and UC_2 all present in residue.
14	1772°K	$UO_2 + 3C \rightarrow UC + 2CO$	Same as 13.
15	1922	$UC_2 + 2CO \rightarrow UO_2 + 4C$	Unsuccessful. UC_2 depleted before equilibrium pressure reached.
15a	2000	Outgas modified vessel	Rate of gas evolution reduced to 2-3 mm Hg per hour.
16	1883	$UO_2 + 4C \rightarrow UC_2 + 2CO$	Unsuccessful - Interference due to high oxide content of new graphite insulating powder.

TABLE E-I CONT'D

Run	Temperature	Objective	Results
17	1789	$4UC + 2CO \rightarrow UO_2 + 3UC_2$	Same as 16.
18	1905	$UO_2 + 4C \rightarrow UC_2 + 2CO$	Same as 16.
18a	1877	Outgas modified vessel	Adequate - gas evolution rate low.
19	1886	Equilibrate phases at about 10 mm Hg.	Successful. See Table VII.
20	1766	Equilibrate UO_2, C, and CO at about 8 mm Hg.	Successful. CO equilibrium pressure was 5 3/4 mm Hg.
21	1861	Equilibrate UO_2, C, and CO at about 34 mm Hg.	Successful. CO equilibrium pressure was 34 1/4 mm Hg.
22	1878	Equilibrate UO_2, UC_2, and CO at about 25 mm Hg.	Successful. See Table VII.
23	1761	$4'UC' + 2CO \rightarrow UO_2 + 3'UC_2'$	Successful. See Table IX.
24	1755	$4'UC' + 2CO \rightarrow UO_2 + 3'UC_2'$	Unsuccessful - All 'UC' consumed before equilibrium was reached.
25	1869	$UO_2 + 3\ UC_2' \rightarrow 4UC + 2CO$	Unsuccessful. Failed to take gas sample.
26	1789	$UO_2 + 4C \rightarrow 'UC_2' + 2CO$	Successful. Results overlooked.
27	1861	$UO_2 + 3'UC_2' \rightarrow 4'UC' + 2CO$	Unsuccessful. Excessive CO buildup due to air leakage.
28	1753	$UO_2 + 4C \rightarrow UC_2 + 2CO$	Unsuccessful. Blunder made in determination of barometric pressure.
29	1822	$4'UC' + 2CO \rightarrow UO_2 + 3'UC_2'$	Successful - See Table IX.
30	1714	$UO_2 + 4C \rightarrow 'UC_2' + 2CO$	Successful - See Table VIII.
31	1886	$UO_2 + 3'UC_2' \rightarrow 4'UC' + 2CO$	Unsuccessful - C in charge caused excessive CO pressure - UC content of residue very small.
32	1516	$UO_2 + 3C \rightarrow UC + 2CO$	Unsuccessful. The dicarbide formed.
33	1891	Prepare UC_2	Fair. Some monocarbide formed and unreacted graphite was present.
34	1911	$4UC + 2CO \rightarrow 3'UC_2' + 2CO$	Successful. See Table IX.
35	1866	$UC_2 + 2CO \rightarrow UO_2 + 4C$	Unsuccessful. Run was discontinued prematurely.
36	1883	$UO_2 + 3'UC_2' \rightarrow 4'UC' + 2CO$	Unsuccessful. Residue contained graphite.
37	1911	Prepare C free UC_2	Unsuccessful. Tablets contained appreciable C and UC.

TABLE E-I CONT'D

Run	Temperature	Objective	Results
38	1933	Complete objective of 37	Adequate - UC_2 content of tablets raised to about 80% or higher.
39	1839	$UC_2 + 2CO \rightarrow UC_2 + 4C$	Successful. See Table VIII.
40	1847	$UO_2 + 3UC_2 \rightarrow 4UC + 2CO$	Successful. See Table IX.
41	1786	$UC_2 + 2CO \rightarrow UC_2 + 4C$	Successful. See Table VIII.
42	1780	$UO_2 + 4C \rightarrow UC_2 + 2CO$	Successful. See Table VIII.
43	1874	$UO_2 + 4C \rightarrow UC_2 + 2CO$	Unsuccessful. Generator casualty.
44	1914	$UO_2 + 3UC_2 \rightarrow 4UC + 2CO$	Successful. See Table IX.
45	1778	$UO_2 + 3UC_2 \rightarrow 4UC + 2CO$	Successful. See Table IX
46	1891	$UO_2 + 3UC_2 \rightarrow 4UC + 2CO$	Unsuccessful. See remark for run 31.
47	1916	$UO_2 + 4C \rightarrow UC_2 + 2CO$	Unsuccessful. Result rejected because of systematic error later attributed to reaction between SiC and CO.
48	1897	$UO_2 + 3UC_2 \rightarrow 4UC + 2CO$	Unsuccessful. See remark for run 27.
49	1845	$UO_2 + 4C \rightarrow UC_2 + 2CO$	Successful. See Table VIII.
50	1891	$UO_2 + 3UC_2 \rightarrow 4UC + 2CO$	Unsuccessful. Result rejected for reason cited on page
50a	1993	Outgas vessel	Attempts to outgas were discontinued after observing pressure rise from 1 to 8 mm Hg in 10 min. at 1993°K.
51	1950	$UO_2 + 4C \rightarrow UC_2 + 2CO$	See remark for run 47.
52	1953	$4UC + 2CO \rightarrow UO_2 + 3UC_2$	Successful. See Table IX.
53	1933	$UC_2 + 2CO \rightarrow UO_2 + 4C$	See remark for run 47.
54	1942	$UO_2 + 3UC_2 \rightarrow 4UC + 2CO$	Unsuccessful. See remark for run 31.
55	1889	$UO_2 + 4C \rightarrow UC_2 + 2CO$	Unsuccessful. Excessive pressure rise due to outgassing of a piece of asbestos inserted for positioning inner vessel.
56	1900	$UC_2 + 2CO \rightarrow UO_2 + 4C$	See remark for run 47.
57	1939	$UO_2 + 3UC_2 \rightarrow 4UC + 2CO$	Successful. See Table IX.
58	1942	$UO_2 + 4C \rightarrow UC_2 + 2CO$	See remark for run 47.
59	1938	Assess size of suspected systematic error.	Found spurious decrease in CO pressure of about 2 mm Hg per hour near 70 mm Hg abs. See page
59a	2001	Outgas modified vessel	Reduced rate of gas evolution to about 10 mm per hour at 2000°K and pressures below 5 mm Hg abs.

TABLE E-I CONT'D

Run	Temperature	Objective	Results	
60	1922	$UO_2 + 4C \rightarrow UC_2 + 2CO$	Successful.	See Table VIII.
61	1892	$UO_2 + 4C \rightarrow UC_2 + 2CO$	Successful.	See Table VIII.
62	1869	$UO_2 + 4C \rightleftarrows UC_2 + 2CO$	Successful.	See Table VIII.
101	1875	$UO_2 + 3C \rightleftarrows UC + 2CO$ $UC + \frac{1}{2} N_2 \rightleftarrows UN + C$	Successful.	See Table X.
102	1878	$UO_2 + 3C \rightleftarrows UC + 2CO$ $UC + \frac{1}{2} N_2 \rightleftarrows UN + C$	Successful.	See Table X.
103	1878	$UO_2 + 3C \rightleftarrows UC + 2CO$ $UC + \frac{1}{2} N_2 \rightleftarrows UN + C$	Successful.	See Table X.
104	1878	$UO_2 + 3UC_2 \rightleftarrows 4UC + 2CO$ $2UC + \frac{1}{2} N_2 \rightleftarrows UN + UC_2$	Successful.	See Table X.
105	1878	$UO_2 + 3UC_2 \rightleftarrows 4UC + 2CO$	Successful.	See Tables IX and X.

APPENDIX F

COMPUTER PROGRAM FOR STATISTICAL ANALYSIS

The least squares analysis carried out to analytically represent equilibrium pressures as functions of absolute temperature has been described in the second part of the analysis of results. Also outlined htere is the procedure for determining standard deviations of values of the logarithm of pressure computed from the analytical expressions. The program for carrying out these determinations was written in the FORTRAN language for use with the IBM 704 computer. This program constitutes the remainder of this Appendix.

```
      DIMENSION P(12),T(12),W(12),PL(12),WPL(12),WDT(12),WDT2(12),WPLDT(
     112),PA(12),PB(12),PA2(12),PB2(12),CPL(12),DPL(12),DPL2(12),WN(12),
     2WNDPL2(12),SPO(12),PO(12),PO2(12),RSPO(12),FD(12)
      CALL FTRAP(1)                                                    GMRF53
   20 READ INPUT TAPE 7,30,N,K,(P(I),I=1,N),(T(I),I=1,N)
   30 FORMAT(2I2/(6F12.6))
      S11=0.
      S31=0.
      S33=0.
      S14=0.
      S34=0.
      DO 155 I=1,N
      W(I)=P(I)*P(I)/(P(1)*P(1))
      S33=S33+W(I)
      PL(I)=ELOG (P(I))*.43429448
      WPL(I)=W(I)*PL(I)
      S34=S34+WPL(I)
      WDT(I)=W(I)/T(I)
      S31=S31+WDT(I)
      WDT2(I)=WDT(I)/T(I)
      S11=S11+WDT2(I)
      WPLDT(I)=WPL(I)/T(I)
  155 S14=S14+WPLDT(I)
      WRITE OUTPUT TAPE 6,210,S11,S31,S33,S14,S34,(W(I),I=1,N)
  210 FORMAT ((5E20.8/(6E20.8))
      U=S11/S33-S31/S33
      A=(S14/S31-S34/S33)/U
      B=S34/S33-S31*A/S33
      WRITE OUTPUT TAPE 6,250,A,B
  250 FORMAT (2E60.8)
      S=0.
      DO 270 I=1,N
      CPL(I)=A/T(I)+B
      DPL(I)=CPL(I)-PL(I)
      DPL2(I)=DPL(I)*DPL(I)
      WN(I)=W(I)*FLOATF(N)/S33
      WNDPL2(I)=WN(I)*DPL2(I)
  270 S=S+WNDPL2(I)
      SLOGP=SQRT(S/FLOATF(N-K))
      WRITE OUTPUT TAPE 6,280,SLOGP,(CPL(I),I=1,N)
  280 FORMAT  (E20.8/(6E20.8))
      SPA=0.
      SPB=0.
      DO 300 I=1,N
      FD(I)=1.-4.6051702*DPL(I)
      PA(I)=(WDT(I)*FD(I)/S31-W(I)*FD(I)/S33)/U
      PB(I)=(W(I)*FD(I)-S31*PA(I))/S33
      PA2(I)=PA(I)*PA(I)
      PB2(I)=PB(I)*PB(I)
      SPA=SPA+PA2(I)
  300 SPB=SPB+PB2(I)
      SIGMAA= SLOGP*SQRT (SPA)
      SIGMAB= SLOGP*SQRT (SPB)
      WRITE OUTPUT TAPE 6,310,SIGMAA,SIGMAB
  310 FORMAT (2E60.8)
      J=0
  330 J=J+1
      SPO(J)=0.
      DO 360 I=1,N
      PO(I)=PA(I)/T(J)+PB(I)
      PO2(I)=FD(I)*PO(I)*DPL(I)*DPL(I)
  360 SPO(J)=SPO(J)+PO2(I)
      RSPO(J)=SQRT (SPO(J))
      IF (J-N)  330,365,365
  365 WRITE OUTPUT TAPE 6,370,(RSPO(J),J=1,N)
  370 FORMAT (6E20.8)
      GO TO 20
```

BIBLIOGRAPHY

1. Gibbs, J. W. Transactions of the Connecticut Academy, 3,(1876) 108.

2. Case, L. O. Elements of the Phase Rule. Ann Arbor, Mich.: Edwards Brothers, 1939.

3. Darken, L. A. and Gurry, R. W. Physical Chemistry of Metals. New York: McGraw-Hill Book Company, Inc., 1953.

4. Rough, F. A. and Bauer, A. A. Constitutional Diagrams of Uranium and Thorium Alloys, Reading, Massachusetts: Addison-Wesley Publishing Company, Inc., 1958.

5. Hansen, M. Constitution of Binary Alloys. New York: McGraw-Hill Book Company, Inc., 1958.

6. Hering, H. and Perio, P. Bulletin de la Societe Chemique de France, (1952) 351.

7. Rundle, R. A., Baenziger, N. C., Wilson, A. S. and McDonald, R. A. J. Am. Chem. Soc., 70, (1948) 99.

8. Vaughan, D. A., Melton, C. W. and Gerds, A. F. Battelle Memorial Institute Report (BMI), No. 1175, 1957.

9. Brewer, L. Report for the Manhattan Project (MDDC), No. 438C, 1946.

10. Wilhelm, H. A. and Daane, A. H. United States Patent Office, No. 2,448,479, 1948.

11. Heusler, O. Z. Anorg. u Allgem. Chem., 154, (1926) 324.

12. Kubaschewski, O. and Evans, E. L. Metallurgical Thermochemistry, New York: John Wiley and Sons, Inc., 1956.

13. Bockris, J. O'M, White, J. L. and Mackenzie, J. D., Editors, Physico-Chemical Measurements at High Temperatures, Butterworths Scientific Publications, London, 1959.

14. Austin, A. E. and Gerds, A. F. Battelle Memorial Institute Report (BMI), No. 1272, 1958.

15. Seybolt, A. U. and Burke, J. E. Procedures in Experimental Metallurgy, New York: John Wiley and Sons, Inc., 1953.

16. Prescott, C. H., Jr. J. Am. Chem. Soc., 48, (1926) 2534.

17. Prescott, C. H., Jr. and Hincke, W. B. J. Am. Chem. Soc., 49, (1927) 2753.

18. Prescott, C. H., Jr. and Hincke, W. B. J. Am. Chem. Soc., 49, (1927) 2744.

19. Brantley, L. B. and Beckman, A. O. J. Am. Chem. Soc., 52, (1930) 3956.

20. Boericke, F. S. U.S. Bureau of Mines Report of Investigation (RI), No. 3747, 1944.

21. Meerson, G. A. and Lipkes, J. M. Zur. Prikl. Chim. U.S.S.R., 12, (1939) 1759; 18, (1945) 24 and 251.

22. Meerson, G. A. Redkie Metally, 4, (1935) 6.

23. Richardson, F. D. J. Iron Steel Inst., 175, (1953) 33.

24. Wien, W. Wied. Ann, 58, (1896) 662.

25. Planck, M. Ann. Phys. Ch., 4, (1901) 553.

26. Comite intern. poids et measures, proces-verbaux des seance de 1948, 21, 1948.

27. Foote, P. D., Fairchild, C. O. and Harrison, T. R. United States National Bureau of Standards Technical Paper (TP), Number 170, 1921.

28. Haas, G. O. and Jenson, J. T. J. Appl. Phys., 31, (1960) 1231.

29. Ehlert, T. C. and Margrave, J. L. Am. Cer. Soc. J., 41, (1958) 330.

30. Kirchhoff, G. Pogg. Ann., 109, (1860) 275.

31. Wood, W. P. and Cork, J. M. Pyrometry. New York: McGraw-Hill Book Company, Inc., 1927.

32. Lewis, G. N. and Randall, M. (revised by Pitzer, K.S. and Brewer, L.). Thermodynamics. New York: McGraw-Hill Book Company, Inc., 1961

33. Guggenheim, E. A. Thermodynamics. Amsterdam: North-Holland Publishing Company, 1957.

34. Kelley, K. K. U.S. Bureau of Mines Bulletin No. 371, 1934.

35. Beers, Y. Introduction to the Theory of Error. Reading, Massachusetts: Addison-Wesley Publishing Company, Inc., 1957.

36. Deming, W. E. Statistical Adjustment of Data. New York: John Wiley and Sons, Inc., 1943.

37. Scarborough, J. B. Numerical Mathematical Analysis. Fourth Edition, Baltimore: The Johns Hopkins Press, 1958.

38. Williams, J. and Sambell, R. A. J. J. Less Common Metals, 1, (1959) 217.

39. Vegard, L. Z. Physik, 5, (1921) 17.

40. Duwez, P. and Odell, F. J. Electrochem. Soc., 97, (1950) 299.

41. Williams, J., Sambell, R.A.J. and Wilkinson, D. United Kingdom Atomic Energy Authority Research Group Memorandum (AERE-M), Number 625, 1960.

42. Swanson, H. E. and Fuyat, R. K. National Bureau of Standards Circular 539, Vol. II, 1953.

43. Wilson, W. B. J. Am. Ceramic Soc., 43, (1960) 77.

44. Coughlin, J. P. U.S. Bureau of Mines Bulletin No. 542, 1954.

45. Grieveson, P. PhD Thesis, University of London, 1960.

46. Mallett, M. W., Gerds, A. F. and Vaughn, D. A. J. Electrochem. Soc., 98, (1951) 505.

47. Smithells, C. J. Metals Reference Book, Vol. II, London: Butterworths Scientific Publications, 1955.

48. Jost, W. Diffusion in Solids, Liquids and Gases. New York: Academic Press, 1960.

49. Chapman, S. and Cowling, T. G. The Mathematical Theory of Non-Uniform Gases, Cambridge: University Press, 1952.

50. Ibbs, T. L. and Underwood, L. Proc. Roy. Soc. (London), 39, (1926) 234.

51. Klug, H. P. and Alexander, L. E. X-Ray Diffraction Procedures, New York: John Wiley and Sons, Inc., 1954.

52. Parrish, W., Ekstein, M. G. and Irwin, B. W. Data for X-Ray Analysis, Vol. II, Irvington-on-Hudson, N. Y.: Philips Laboratories, Inc., 1953.

53. Jette, E. R. and Foote, F. J. Chem. Phys., 3, (1935) 605.

54. Straumanis, M. and Ievins, A. Z. Phys., 98, (1935) 461.

55. Straumanis, M. and Aka, E. Z. Appl. Phys., 23, (1952) 330.